

Modified cell penetrating peptides for efficient gene transfer *in vitro* and *in vivo*

Gizem Osman

Thesis submitted to the University of Nottingham for the degree of Doctor of Philosophy

September 2016

ABSTRACT

The efficient delivery of DNA is of great importance for therapeutic applications such as gene therapy, gene-editing and cell programming. However, the phospholipid bilayer of the cell membrane acts as an impenetrable barrier to nucleic acids and therefore a gene must be coupled to an intracellular delivery vector for efficient transfection. An optimal gene carrier must be able to deliver DNA to the entire cell population, transfect cells efficiently, be serum-resistant and cause minimal cytotoxicity. The majority of non-viral transfection strategies fall short of meeting these requirements, limiting their therapeutic utility. Cell penetrating peptide (CPP)-based vectors have been extensively used for the intracellular delivery of DNA, however low transfection efficiency has inhibited their clinical adoption. GET peptides (i.e. CPPs functionalised with heperan sulphate glycosaminoglycan (HS GAG) cell targeting ligands) have demonstrated 2 orders of magnitude improved delivery compared to unmodified CPPs. They overcome some of the challenges in non-viral DNA delivery by exhibiting minimal cytotoxicity and superior gene transfer. Additionally, PEGylated GET/DNA NPs were engineered with tuneable physiochemical properties for widespread and efficient transfection in mouse lung models. "Mucus penetrating" PEG GET NPs exhibited enhanced safety profiles and significantly better *in vivo* transfection efficiency compared to polyethylenimine (PEI) complexes. This work presents efficient GET-peptide mediated *in vitro* and *in vivo* transfection of DNA as a novel approach for gene therapy treatment.

ACKNOWLEDGEMENTS

Firstly, I would like to thank my supervisors Dr James E. Dixon and Professor Kevin M. Shakesheff for all their continuous support and guidance over the past three years. I have benefited both academically and technically from their expertise. I would also like to thank the University of Nottingham, School of Pharmacy and the Regenerative Medicine and Cellular Therapies group for making my time at Nottingham so enjoyable and creating a fun and friendly work environment.

In addition, I would like to thank Prof Justin Hanes and Dr Jung Soo Suk (Johns Hopkins University, USA) for welcoming me into their lab for 3-months and providing with the supervision and facilities to complete my work.

I would like to thank the EPSRC for funding my PhD, without this support the work would not be possible

I am truly grateful my family and friends for their continued support. In particular my mum for believing in me and my dad for his words of wisdom. In particular, I would like to express gratitude to my fiancé, Vasilis, for his unconditional support and encouragement.

PUBLICATIONS

DIXON, J. E., OSMAN, G., MORRIS, G. E., MARKIDES, H., ROTHERHAM, M., BAYOUSSEF, Z., EL HAJ, A. J., DENNING, C. & SHAKESHEFF, K. M. 2016. Highly efficient delivery of functional cargoes by the synergistic effect of GAG binding motifs and cell-penetrating peptides. Proceedings of the National Academy of Sciences of the United States of America, 113, E291-E299

ORAL PRESENTATIONS

(2016) CDT Joint Conference, University of Manchester, Manchester, UK

(2016) CDT Cross Cadre Conference, Loughborough University, Loughborough, UK

POSTER PRESENTATIONS

(2015) TERMIS world congress, Boston, US

(2015) International Symposium CPP Paris, Paris, FR

(2014) CDT Joint Conference, University of Nottingham, Nottingham, UK

(2014) Tissue and Cell Engineering Society (TCES), Newcastle, UK

(2014) CDT Cross Cadre Conference, Keele University, Stoke on Trent, UK

(2013) Annual Symposium - Biochemical Determinants of Tissue Regeneration, Macclesfield, Manchester, UK

AWARDS AND ACHIEVEMENTS

(2016) EPSRC Doctoral Prize winner. Awarded £10,000 research fund and two years stipend for postdoctoral research

Project title: **Cystic fibrosis therapy:** Efficient gene editing using GET gene delivery and CRISPR/Cas9 systems

(2016) Best oral presentation. Awarded prize for the best presenter/speaker at CDT Cross Cadre Conference

(2015) Top 25 abstract submission. Shortlisted as top 25 abstract at TERMIS world congress (over 3000 abstract submissions)

LIST OF ABBREVIATIONS

AAV	Aden-associated virus
AF	Antibody mimetic-affibody
ATIII	Antithrombin-III
BALF	Bronchial alveolar lavage fluid
Bmpr1a	Bone morphogenetic protein receptor type 1 A
Bry	Brachyury
CFGTC	Cystic Fibrosis Gene Therapy Consortium
CFTR	Cystic fibrosis transmembrane conductance regulator
CMV	Cytomegalovirus
CPP	Cell penetrating peptide
CR	Charge ratio
CRISPR	Clustered regularly interspaced short palindromic repeats
DLS	Dynamic light scattering
DMEM	Dulbecco's modified Eagle's medium
DMSO	Dimethyl sulfoxide
DNA	Deoxyribonucleic acid
EB	Embryoid body
EDTA	Ethylenediaminetetraacetic acid
EF-1α	Elongation factor 1
EGF	Epidermal growth factor
eGFP	Enhanced green fluorescent protein
FACS	Fluorescence activated cell sorting
FCS	Fetal calf serum
FGF	Fibroblast growth factor
FITC	Fluorescein isothiocyanate
FLK-1	Tyrosine Kinase Receptor
GAG	Glycosaminoglycan
GET	Glycosaminoglycan-binding enhanced transduction
GF	Growth factors
GFP	Green fluorescent proteins

GM	Growth media
HA2	Hemagglutinin protein
HB EGF	Heparin-binding epidermal growth factor
HBSS	Hanks' balanced salt solution
HEPES	4-(2-hydroxyethyl)-1-piperazineethanesulfonic acid
HER2	Human epidermal growth factor receptor 2
hESCs	Human embryonic stem cells
hiPSCs	Human induced pluripotent stem cells
HIV-1	Human immunodeficiency virus
HS	Heparan sulfate
IMDM	Iscove's modified Dulbecco's medium
IPTG	Isopropyl β-D-1-thiogalactopyranoside
LIF	Leukemia inhibitory factor
MEND	Multifunctional envelope-type nano device
MMP	Matrix metalloprotease
MPS	Mononuclear phagocyte system
mRFP	Monomeric red fluorescent protein
MSC	Mesenchymal stem cell
MSD	Mean squared displacement
MTG	Monothioglycerol
NP	Nanoparticle
PBS	Phosphate buffered saline
PBAE	Poly(beta-amino ester)
PDGF	Platelet derived growth factor
PEG	Poly(ethylene glycol)
PEI	Polyethylenimine
PFA	Paraformaldehyde
PNA	Peptides nucleic acid
PTD	Protein transduction domain
RFU	Relative fluorescence units
RLU	Relative light units
SAP	Sweet arrow peptide

SDS-PAGE	Sodium dodecyl sulfate polyacrylamide gel electrophoresis
TAT	Transcription transactivating
TGF-β	Transforming growth factor beta
TF	Tissue factor
TP10	Transportan 10
VEGF	Vascular endothelial growth factor

LIST OF FIGURES

Figure 1.1 Endocytosis vs. direct penetration. A schematic of the different translocation pathways..... 7

Figure 1.2 Three important steps in the transfection of CPP/DNA complexes. (1) Membrane interaction, (2) translocation and (3) intracellular trafficking. . 17

Figure 1.3 GET peptides (i.e. CPPs functionalised with cell surface HS GAG-targeting sequences) have demonstrated enhanced delivery of a variety of cargos. Adapted with permission from (Dixon et al., 2016). 20

Figure 1.4 Intracellular trafficking of CPPs following endocytosis. CPP/DNA complexes that enter cells via endocytosis can undergo degradation by lysosomes unless an endosomal escape strategy is employed for cytosolic release. 28

Figure 2.1 GET-mediated enhanced delivery of monomeric red fluorescent protein (mRFP) to NIH3T3 cells. (A) A schematic of GET peptide and its components. (B) Fluorescence microscopy images of NIH3T3 cells treated with FmRFP, P21 mRFP, mRFP 8R or P21 mRFP 8R proteins (20 μg/mL 12 h). Scale bar, 100 μm. Figure was adapted with permission from (Dixon et al., 2016). 41

Figure 2.2 Schematic of the different types of cell surface HS GAGs; syndecans, glypicans and perlecans..... 45

Figure 2.3 Graph showing NIH3T3, CGR8 and HUES-7 cells treated with mRFP conjugated peptides (20 μg/mL, 20 h). Flow cytometry analysis was used to quantify mean fluorescence intensity of cells. Error bars indicate SD, n = 3. One-way ANOVA with Dunnett's test was used for multiple comparison

of each treatment group with unmodified CPP (mRFP 8R), *P < 0.05, **P < 0.01. 55

Figure 2.4 Efficient delivery of mRFP to cells via modified CPPs shown to promote GET. Bright field (left) and fluorescence (right) microscopy images of NIH3T3, CGR8 and HUES-7 cells treated with P21 mRFP 8R and FGF2B mRFP 8R peptides (20 µg/mL, 20 h). Following treatment cells were washed twice in PBS to remove background fluorescence and imaged live. Scale bar, 100 µm. 56

Figure 2.5. Representative flow cytometry profiles of the expression of HS4C3 versus Brachyury (Bry) expression of stem cells following a 2.8 day mesodermal differentiation. Bry-GFP embryonic stem cells were differentiated as EBs for 2.8 days, disaggregated and treated with (A) HS4C3 mRFP or (B) HS4C3 mRFP 8R peptides (50 µg/mL, 3 h). HS4C3 peptides were conjugated to mRFP to allow quantification of highly (HS^{HIGH}) and lowly (HS^{LOW}) labelled cells. Baldwin *et al* defined HS4C3 highly labelled cells as a subpopulation that expressed increased 3-O-sulfation epitopes and HS4C3 lowly labelled as cells in which 3-O-sulfation epitopes were not up-regulated (Baldwin et al., 2008). 59

Figure 3.1 Schematic of GET transfection peptides P21 LK15 8R and FGF2B LK15 8R. (A) GET peptide structure. HS GAG binding domain (red), amphiphilic region (blue) and CPP (purple). (B) GET peptide and DNA complex formation. Cationic GET peptides form electrostatic interactions with negatively charged phosphate groups of pDNA to form nanoparticles (NPs). 63

Figure 3.2 GET peptides efficiently bind DNA. Optimization of (+/-) charge ratio of 8R, LK15 8R, P21 LK15 8R and FGF2B LK15 8R to pSIN GFP. The

graph shows a decrease in the percentage fluorescence as peptide binds DNA. Error bars indicate SD, n = 3. 79

Figure 3.3 GET peptide/DNA complexes are efficiently taken up by cells. (A) Uptake of GET peptide/FAM-labelled DNA complexes in NIH3T3 cells at CR2, CR3, CR4 and CR5. Cells were treated with P21 LK15 8R/FAM-labelled DNA NPs or FGF2B LK15 8R/FAM-labelled DNA NPs for 2 h and fluorescence intensity was determined by flow cytometry. (B) Brightfield (left) and fluorescence (right) microscopy images showing cells following 2 h incubation with P21 LK15 8R/FAM-labelled DNA/ NPs at CR3. FAM-labelled DNA (green). Cell nuclei stained with Hoechst (blue). Scale bar, 15 µm. Error bars indicate SD, n = 3..... 81

Figure 3.4 Uptake of GET peptide/DNA NPs is inhibited in the presence of endocytosis inhibitors. NIH3T3 cells were treated with P21 LK15 8R/FAM-labelled DNA complexes in the presence of (A) methyl-β-cyclodextrin (0-10 mM) an inhibitor for calveolae independant endocytosis and (B) amiloride (0-5 mM) an inhibitor of Na+/H+ exchange required for macropinocytosis to investigate the mechanism of internalisation. Error bars indicate SD, n = 3. .. 84

Figure 3.5 Representative flow cytometry dot plots showing GFP expression of NIH3T3 cells following transfection with 1 µg pSIN GFP for 6 h. Following transfection, cells were fixed at a 24 h time point. Flow cytometry analysis was used to quantify the percentage of GFP positive cells..... 86

Figure 3.6 Transfection of 1 µg pSIN GFP via P21 LK15 8R and its component peptides in NIH3T3 cells for 24 h. (A) YO-PRO-1 assay was used to demonstrate the DNA condensation ability of peptides at different CRs. (B) Transfection efficiency of 8R, P21, LK15, P21 LK15, LK15 8R and P21 LK15

8R peptides.. Flow cytometry analysis was used to quantify the percentage of GFP positive cells. Error bars indicate SD, n = 3. 87

Figure 3.7 Optimisation of the transfection of pSIN GFP in NIH3T3 cells by P21 LK15 8R peptide at CR2. Transfections were carried out in OptiMEM, OptiMEM + 10% FCS and GM. Cells were transfected for (A) 3 h, (B) 6 h and (C) 24 h. Following transfection, cells were fixed at a 24 h time point. Error bars indicate SD, n = 3. One-way ANOVA with Bonferroni's post-tests; *P < 0.05, **P < 0.01. 88

Figure 3.8 Endosomal escape reagents improve transfection of P21 LK15 8R. NIH3T3 cells were co-treated with P21 LK15 8R/FAM-labelled DNA NPs and 18 μM P21 HA2, 18 μM LK15 HA2 or 100 μM chloroquine for 24 h. Graphs of (A) transfection efficiency and (B) fold increase in transfection. Error bars indicate SD, n = 3. One-way ANOVA with Bonferroni's post-tests; *P < 0.05, **P < 0.01. 91

Figure 3.9 Optimisation of CR for efficient GET-mediated transfection. Transfection of 1 μg pSIN GFP in NIH3T3 cells by LK15 8R, P21 LK15 8R and FGF2B LK15 8R peptides at CR1, CR2, CR3, CR4 and CR5. Cells were transfected for 1 h, 4 h and 24 h. Following transfection, cells were fixed at 24 h time point. Error bars indicate SD, n = 3. One-way ANOVA with Bonferroni's post-tests; *P < 0.05, **P < 0.01. 93

Figure 3.10 Transfection of GET peptides vs. commercial transfection reagents. NIH3T3 cells were transfected with 1 μg pSIN GFP. GET peptides P21 LK15 8R and FGF2B LK15 8R were compared to leading transfection reagents Lipofectamine 2000, Lipofectamine 3000, JetPEI, TransIT-LT1 and FuGENE HD in terms of (A) transfection efficiency and (B) cell viability

(PrestoBlue assay). (C) Bright field (left) and fluorescence (right) microscopy images of transfected cells expressing GFP (green) following 24 h transfection with FGF2B LK15 8R (CR3). Scale bar, 150 µm. Error bars indicate SD, n = 3., One-way ANOVA with Bonferroni's post-test (for transfection efficiency) or One-way ANOVA with Dunnett's test for the comparison of each treatment group with the control (for cell viability), *P < 0.05, **P < 0.01. 95

Figure 3.11 GET peptide transfection of HeLa, MCF-7, HUES-7 fib and NIH3T3 cells. Cells were transfected with 1 µg pSIN GFP using FGF2B LK15 8R (CR3). Error bars indicate SD, n = 3. 97

Figure 3.12 Efficient and scalable transfection of hiPSCs via GET. (A) Transfection efficiency and (B) cell viability (PrestoBlue assay) of hiPSCs treated with FGF2B LK15 8R or Lipofectamine 3000. (C) Fluorescence image of FGF2B LK15 8R transfected hiPSCs expressing GFP (green) and (D) scale-up of transfection. Error bars indicate SD, n = 3. One-way ANOVA with Bonferroni's post-tests; *P < 0.05, **P < 0.01. 98

Figure 3.13 NIH3T3 cells were treated with FGF2B LK15 8R peptide or commercial transfection reagent Lipofectamine 3000 at Day 1 (24 h), Day 2 (48 h) and Day 3 (72 h) over a 3 day serial transfection of pSIN GFP. Transfections were compared in terms of (A) transfection efficiency, (B) cell viability (PrestoBlue assay), (C) cell proliferation/growth and (D) numbers of transfected cells. Error bars indicate SD, n = 3. One-way ANOVA with Bonferroni's post-tests; *P < 0.05, **P < 0.01. 100

Figure 3.14 FGF2B LK15 8R-mediated transfection of multiple genes. Representative flow cytometry dot plots showing RFP and GFP expression of NIH3T3 cells transfected with 1 µg pSIN GFP, 1 µg pSIN RFP or a mixture

0.5 μg pSIN GFP + 0.5 μg pSIN RFP plasmids. Control was untreated cells. 102

Figure 4.1 Schematic of healthy and cystic fibrosis airway sections. 107

Figure 4.2 Schematic of PEGylated GET peptide/DNA complex formation. NonPEGylated and PEGylated peptides were blended at different ratios to control the density of PEG coating on the outer shell of NPs. 117

Figure 4.3 Graph of hydrodynamic size and zeta potential of GET peptide/DNA NPs at 0%, 10%, 20%, 40%, 60%, 80% and 100% PEGylation rates. The hydrodynamic size was measured in ultrapure water and zeta-potentials were measured in 10 mM NaCl at pH 7.0. Error bars indicate SD, n = 3. 118

Figure 4.4 Representative transmission electron micrographs of FGF2B LK15 8R/DNA NPs at 0%, 40% and 60% PEGylation rates. Scale bar, 500 nm on original images and 250 nm on inserts. 119

Figure 4.5 Stability of PEGylated GET peptide/DNA complexes at 10%, 20%, 40%, 60%, 80% and 100% PEGylation rates following 1 h incubation in water or 10% (v/v) BALF in PBS. Error bars indicate SD, n = 3. 122

Figure 4.6 *In vitro* transfection efficiency of PEGylated GET NPs. NIH3T3 cells were transfected with 1 μg reporter gene expressing GFP for 24 h. Flow cytometry analysis was used to quantify the percentage of GFP positive cells. Error bars indicate SD, n = 3. 123

Figure 4.7 Multiple particle tracking of PEGylated GET NPs in *ex vivo* CF sputum samples. (A) Distribution of particle log MSD at a timescale of 1 s. (B) Representative trajectories of particles. Dot plots of (C) ensemble-median MSD and (D) percentage mucus penetrating particles (MSD ≥ 1 μm^2). Error

bars indicate SD, n = 5-6 patient samples. One-way ANOVA with Bonferroni's post-tests; *P < 0.05, ** P < 0.01. 126

Figure 4.8 *In vivo* distribution of PEGylated GET peptide complexes in healthy mouse lung models. Cy5-labelled DNA was complexed with FGF2B LK15 8R at CR3. (A) Representative images of NP distribution in large airways and lung parenchyma following intratracheal administration of the respective NPs (red). Cell nuclei were stained with DAPI (blue). (B and C) Image-based quantification of (B) coverage of NPs in large airways and (C) distribution of NPs in the lung parenchyma. Tissues were harvested 30 min following intratracheal administration of NPs. Error bars indicate SD, n = 3 mice/group. Two-tailed Student's t-test, *P < 0.05, **P < 0.01..... 128

Figure 4.9 *In vivo* mouse lung transgene expression of luciferase activity following PEGylated GET/DNA NP administration. Error bars indicate SD, n = 3 mice/group. One-way ANOVA with Bonferroni's post-tests; *P < 0.05, **P < 0.01. 130

Figure 4.10 Safety profile of lungs treated with PEGylated GET NPs 24 h post administration. (A) Cell counts from BALF of treated lungs (n = 3 mice/group) and (B) representative images of lung sections stained with hematoxylin and eosin (n = 1 mouse/group). AW, airway, arrow indicates cellular infiltrate. Scale bar, 100 µm. Error bars indicate SD. One-way ANOVA with Bonferroni's post-tests; *P < 0.05, **P < 0.01. 132

Figure 5.1 Future work plan: translation of GET technology for precision CF gene therapy. 139

Figure 6.1 Plasmid map of pSIN GFP IRES PURO (Addgene). 153

Figure 6.2 Plasmid map of pSIN mRFP NSR IRES PURO (Addgene). 154

Figure 6.3 NIH3T3 cells were transfected with 0.1, 0.2, 0.35, 0.5 and 1 µg of pSIN GFP by FGF2B LK15 8R (CR3) for 24 h. Flow cytometry analysis was used to quantify the percentage of GFP positive cells. Error bars indicate SD, n = 3. 155

LIST OF TABLES

Table 1.1 The mechanism of CPP uptake can be influenced by CPP type, CPP concentration, cargo and cell type. 8

Table 1.2 The advantages and disadvantages of widely used alternative non-viral transfection strategies. 16

Table 1.3 A summary of the most promising CPPs for gene transfer *in vitro* and *in vivo*. 34

Table 2.1 Naturally derived growth factors (GFs), chemokines, cytokines and extracellular matrix (ECM) components that are known to interact with cell surface HS ligands.. 42

Table 3.1 Amino acid sequences of 8R, P21, P21 HA2, P21 8R, LK15, LK15 HA2, P21 LK15, LK15 8R, P21 LK15 8R and FGF2B LK15 8R peptides..... 65

Table 3.2 GET peptide/DNA CRs. GET peptide was added to 1 μg of DNA at increasing (+/-) CRs..... 68

Table 3.3 Characterisation of GET peptide/DNA NP hydrodynamic size, polydispersity index and zeta potential..... 78

Table 6.1 Amino acid sequences of the recombinant proteins. 141

Table 6.2 Amino acid sequences of the HS4C3 antibody-derived recombinant proteins. 152

TABLE OF CONTENTS

ABSTRACT i
ACKNOWLEDGEMENTS ii
PUBLICATIONS iii
ORAL PRESENTATIONS iii
POSTER PRESENTATIONS iii
AWARDS AND ACHIEVEMENTS iv
LIST OF ABBREVIATIONS v
LIST OF FIGURES viii
LIST OF TABLES xvi
TABLE OF CONTENTS xvii
CHAPTER 1 Cell penetrating peptides: recent advances in their use for gene transfer 1
1.1 Introduction 1
1.1.1 CPPs definition and classification 3
1.1.2 Mechanism of uptake 5
1.2 CPP transfection reagents 11
1.2.1 Membrane interaction 18
1.2.2 Translocation 21
1.2.3 Intracellular trafficking 24
1.3 Strategies for *in vivo* DNA delivery 29
1.4 Summary 32
1.5 Aims of the project 36
CHAPTER 2 Glycosaminoglycan-binding enhanced transduction (GET) 38
2.1 Introduction 38
2.2 Aims of the project 46
2.3 Materials and methods 47

2.3.1 Preparation of recombinant proteins 47

2.3.2 Bradford assay 48

2.3.3 Cell culture of NIH3T3, CGR-8 and HUES7 cells 49

2.3.4 Protein delivery to cells 50

2.3.5 Maintenance and differentiation of Bry-GFP ES cells, generation of EBs 50

2.3.6 Flow cytometry analysis 51

2.3.7 Microscopy 52

2.3.8 Statistical analysis 52

2.4 Results and discussion 53

2.4.1 Glycosaminoglycan-binding enhanced transduction (GET) 53

2.4.2 GET-mediated cell type specific targeting of the pre-hemangioblast cell 57

2.5 Summary 60

CHAPTER 3 GET peptides for efficient gene transfer 62

3.1 Introduction 62

3.2 Aims of the project 64

3.3 Materials and methods 65

3.3.1 Peptide synthesis 65

3.3.2 Cell culture 66

3.3.3 Preparation of DNA 67

3.3.4 DNA complexation assay 67

3.3.5 Characterisation of GET peptide/DNA complexes 69

3.3.6 Cellular uptake assay 69

3.3.7 Endocytosis inhibitors assay 70

3.3.8 *In vitro* transfection 71

3.3.9 Cell viability assay 73

3.3.10 Endosomal escape reagents 74

3.3.11 Flow cytometry analysis 74

3.3.12 Microscopy 75

3.3.13 Statistical analysis 75

3.4 Results and discussion 77

3.4.1 GET peptide/DNA NP formation 77

3.4.2 DNA delivery 80

3.4.3 NPs are taken up by macropinocytosis 82

3.4.4 Serum-resistant transfection 85

3.4.5 Endosomal escape 89

3.4.6 Optimal CR for transfection – adding excess peptide improves transfection efficiency 92

3.4.7 GET vs. commercial transfection reagents 94

3.4.8 Efficient gene transfer of difficult-to-transfect cell types 96

3.4.9 Sustained delivery and expression of DNA 99

3.4.10 Multiple plasmid delivery 101

3.5 Summary 103

CHAPTER 4 PEGylated GET peptides for inhaled lung gene therapy 104

4.1 Introduction 104

4.2 Aims of the project 108

4.3 Materials and methods 109

4.3.1 Peptide synthesis 109

4.3.2 Preparation of DNA 109

4.3.3 Formation of PEGylated GET/DNA NPs 109

4.3.4 Characterisation of PEGylated NPs 110

4.3.5 *In vitro* transfection 111

4.3.6 Multiple particle tracking 111

4.3.7 Animal studies 112

4.3.8 Statistical analysis 114

4.4 Results and discussion 115

4.4.1 PEGylated GET peptide NP formation 115

4.4.2 Stability of NPs in biological fluid 120

4.4.3 *Ex vivo* NP tracking in CF patient sputum samples 124

4.4.4 Biodistribution of NPs in lung model 127

4.4.5 *In vivo* transfection 129

4.4.6 *In vivo* safety 131

4.5 Summary 133

CHAPTER 5 Conclusions and future work 135

CHAPTER 6 Appendix 141

CHAPTER 7 References 156

CHAPTER 1 Cell penetrating peptides: recent advances in their use for gene transfer

1.1 Introduction

Gene therapy is the therapeutic delivery of nucleic acids to treat or correct genetic diseases. Progress in genetic research has led to the identification of target genes and the development of powerful gene-editing techniques such as the clustered regularly interspaced short palindromic repeats (CRISPR) system (Gaj et al., 2013). To fully utilise their therapeutic potential, efficient DNA delivery must be facilitated *in vitro* and *in vivo* by safe and non-cytotoxic vectors. Many technologies including microinjection, electroporation, polymeric agents, lipid agents and viral vectors have demonstrated gene delivery in culture and animal models. However, thus far no system has the ability to meet all the requirements of an optimal gene carrier in:

- **Highly efficient transfection *in vitro* and *in vivo***
- **Minimal toxicity**
- **Serum-resistance/colloidal stability**
- **Broad cell/tissue spectrum**
- **Safety (low risk of immunogenicity and insertional mutagenesis)**
- **Facile manufacture/manipulation/synthesis**
- **Low cost**

Since their discovery ~25 years ago, cell penetrating peptides (CPPs) have been developed as non-viral delivery tools and show great promise in overcoming the

challenges in efficacious gene delivery. CPPs can non-covalently bind DNA, specifically deliver to target cells/tissues and effectively escape endosomal entrapment for efficient transfection *in vitro* and *in vivo*. This reviews focuses on the modifications made to CPPs to improve their gene transfer activity and their incorporation into multifunctional gene carriers.

1.1.1 CPPs definition and classification

CPPs, also referred to as protein transduction domains (PTDs), are short peptides (~5-30 amino acids) that are defined by their ability to translocate cell membranes and mediate intracellular delivery of hydrophilic molecules. These peptides have been conjugated to a diversity of cargos such as nucleic acids, magnetic nanoparticles, transcription factors and fluorescent molecules for use in a broad spectrum of applications ranging from cell-labelling to stem cell differentiation (Fonseca et al., 2009, Foerg and Merkle, 2008).

The first discovered CPP was transcription transactivating (TAT) protein which was derived from human immunodeficiency virus (HIV-1) (Green and Loewenstein, 1988, Vives et al., 1997). TAT protein was capable of efficient cell penetration and nuclear localisation. Vives *et al* demonstrated that translocation across the cellular membrane could be facilitated by a short truncated sequence (RKKRRQRRR) within the protein. Moreover, when conjugated to cargo the truncated peptide could facilitate cellular uptake of cargo/macromolecules. Soon after, the first examples of CPPs for *in vivo* delivery of proteins and peptide nucleic acids (PNAs) were presented by Schwarze *et al* and Pooga *et al*, respectively (Pooga et al., 1998, Schwarze et al., 1999). Schwarze *et al* reported widespread delivery of protein conjugated to TAT in mice. Markedly, the TAT-protein conjugate was able to overcome the blood-brain barrier following intraperitoneal injection whereas protein was not detected in the brain tissue of mice treated with protein alone (Schwarze et al., 1999). The mechanism by which TAT was able to improve uptake and cross the blood brain barrier was not investigated.

At present, there is a prevalence of identified CPPs including synthetic arginine-rich peptides with sequences that are bio-mimetic of TAT and amphipathic peptides that utilise alpha-helical conformations for cellular penetration. Many reports group CPPs according to different criteria the most common classifications being by their origin, hydrophilicity/hydrophobicity or peptide sequence.

1.1.2 Mechanism of uptake

There is evidence that both endocytosis and direct translocation account for the penetration properties of CPPs (Figure 1.1). The exact mechanism(s) by which CPPs are internalised are not fully understood and contradictory findings are often reported due to the varying physiochemical properties of CPPs as well as the use of experimental methods that differ (Palm-Apergi et al., 2012, Madani et al., 2011). For example, earlier studies reported that TAT uptake occurred through direct penetration and did not involve endocytic pathways (Vives et al., 1997). When the mechanism was re-evaluated by Richard *et al* in 2003 it was found that methods in cell fixation could prevent accurate measurement of uptake by fluorescence-activated cell sorting (FACS) and microscopy (Richard et al., 2003, Kaplan et al., 2005). As endocytosis is an energy dependent process and direct penetration is an energy independent process, CPP internalisation can be studied at 37 °C (endocytosis and direct penetration) and 4 °C (direct penetration). In addition, CPP uptake can be assessed by confocal microscopy or in the presence of endocytosis inhibitors (Jiao et al., 2009). The mechanism of uptake can be influenced by CPP type, CPP concentration, cargo and cell type as summarised in Table 1.1 .Furthermore, multiple pathways could exist for a single CPP and occur simultaneously.

It is generally accepted that endocytosis at least strongly contributes to the cellular uptake of cationic CPPs such as TAT and octa-arginine (8R). During endocytosis, the positively charged peptide forms electrostatic interactions with negatively charged phospholipids and proteoglycans on the cell surface. This triggers the cytoskeleton of the cell membrane to rearrange itself to encapsulate

the CPP/cargo and form an endocytic vesicle known as an endosome. CPP/cargo that remain trapped in endosomes eventually undergo degradation in late endosomes or lysosomes (Tjelle et al., 1996). There are several suggested pathways for endocytosis including macropinocytosis, clathrin-mediated endocytosis, cavaeolae-mediated endocytosis and cavaeolae/clathrin independent endocytosis. Strategies have been developed to facilitate the cytosolic release of CPP/cargo following internalisation, despite this endosomal entrapment remains a challenge for endocytosis-mediated delivery vectors.

Not all CPPs require endocytic pathways. Cells treated with high CPP concentrations and/or amphipathic peptides, such as CADY, have demonstrated internalisation through direct penetration (Crombez et al., 2008). Direct penetration is a non-endocytic mechanism of translocation that is facilitated by destabilisation of the membrane and formation of a transitory structure or pore (Giraldo et al., 2014). There are several suggested pathways for direct penetration including the inverted micelle, toroidal pore, barrel stave pore and carpet model. The clear advantage of this mechanism of uptake is that peptides bypass endosomal entrapment for direct cytosolic delivery. A recent review summarised four key steps that govern direct penetration as 1) the affinity of CPPs for the membrane, 2) structural changes of CPPs at the membrane surface (adoption of secondary structures, peptide folding or aggregation), 3) the membrane-activity of the CPP (such as ability of the peptide to induce lipid reorganisation) and 4) insertion of CPPs into the lipid bilayer (Di Pisa et al., 2015).

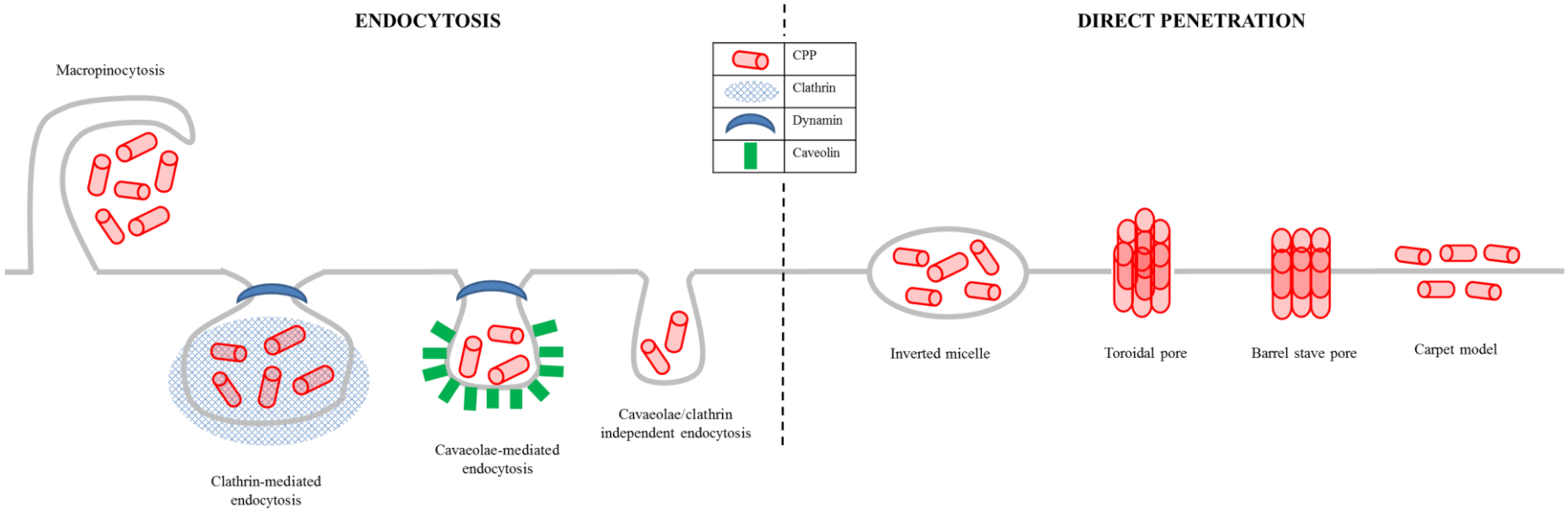


Figure 1.1 Endocytosis vs. direct penetration. A schematic of the different translocation pathways.

Table 1.1 The mechanism of CPP uptake can be influenced by CPP type, CPP concentration, cargo and cell type.

Factor	Effect on uptake
CPP type	CPP sequence, length and conformation can affect their internalisation. CPPs containing a large number of positively charged arginine residues, such as TAT, have been shown to enter cells via endocytosis (Duchardt et al., 2007). On the other hand some amphipathic CPPs, such as CADY and transportan 10 (TP10), can utilise hydrophobic alpha helical structures for direct penetration (Crombez et al., 2008, Deshayes et al., 2011). In addition, it has been shown that the number of arginine residues in poly-arginine CPPs can affect their cellular uptake and localisation. Futaki *et al* tested 4R to 16R lengths of polyarginines and found that 8R demonstrated the most efficient internalisation (Futaki et al., 2007, Futaki et al., 2001). Furthermore, Elmquist *et al* showed that scrambling CPP, pVEC, could inhibit its efficient translocation across the cell membrane (Elmquist et al., 2006).
Concentration	CPP concentration can affect the mechanism of CPP uptake (high CPP concentrations favour direct penetration). Duchardt *et al* investigated the effect of concentration on the uptake of 9R and TAT. At concentrations of $\geq$ 10 μM the distribution of CPPs appeared to be strongly cytoplasmic compared to at low

	concentrations. Furthermore, uptake of the CPPs did not increase linearly with concentration, indicating that concentration affects the route of internalisation (Duchardt et al., 2007).
Cargo	Cargo type and size can alter the CPP uptake mechanism. Tunnemann *et al* reported that TAT exhibited a cargo dependent mode of uptake. TAT conjugated to large cargos appeared to be trapped in endosomes whereas when attached to small cargoes delivery appeared to be cytoplasmic (Tunnemann et al., 2006, Ma et al., 2011). Also, CPPs conjugated to cargos have demonstrated different patterns of distribution and efficiency of uptake compared to CPPs alone (Maiolo et al., 2005). Furthermore, it has been reported that cargo types can affect the mechanism of internalisation. Fischer *et al* have shown that CPPs labelled with different fluorophores demonstrated different uptake efficiency, distribution and cytotoxicity (Fischer et al., 2002).
Cell type	Membrane lipid composition and charge vary between different cell types and can affect the uptake mechanism. For example, Jiao *et al* studied the endocytosis and/or translocation of CPPs in glycosaminoglycan (GAG)-deficient CHO (pgsA-745) cells and wild type CHO (K1) cells. It was observed that the membrane components of

	the different cell types strongly affected the mechanism of uptake (Jiao et al., 2009).

1.2 CPP transfection reagents

Transfection, the process by which foreign nucleic acids are introduced into a cell, requires gene carriers to overcome many biological obstacles from interaction with the cell membrane to intracellular trafficking of genetic material (Kim and Eberwine, 2010). An 'optimal' gene carrier must be able to demonstrate high transfection efficiency and minimal cytotoxicity in a broad cell spectrum including difficult-to-transfect cell types such as stem cells and primary cells (Seo et al., 2013). For *in vivo* application gene carriers must also retain stability in biological fluids and have minimal safety concerns. In addition, for clinical translation gene carriers must also be facile to manufacture, good manufacturing practice (GMP) scalable and cost-effective. The ability of viruses to penetrate the cell membrane and target the nucleus of cells has led to them being exploited as highly efficacious delivery vehicles for gene therapy. Despite boasting high efficiency of transfection, the use of viral vectors has safety issues inhibiting their clinical adoption. These include the increased risk of causing insertional mutagenesis and/or cell mediated immune responses (Matsubara et al., 2014). Furthermore, many viral vectors are restricted with respect to scale-up and by their cargo carrying capacity (Kotterman and Schaffer, 2014).

As non-viral technologies are edging closer to meeting the requirements of an 'optimal' gene transfer system, they are becoming attractive replacements of viral vectors. Cationic lipids and polymers are able to non-covalently bind DNA through electrostatic interactions, transport genetic cargo across the cell membrane and facilitate endosomal release of DNA via fusogenic lipids or the

proton sponge affect (a process by which polymers become protonated in the acidic environment of the endosomes, promoting osmotic swelling and eventual rupture of the vesicle), respectively. However, instability in biological fluids has restricted their efficacy *in vivo* (Duran et al., 2011, Breunig et al., 2007). Furthermore, control of the physiochemical characteristics of polymer based gene carriers during synthesis and modification steps can be challenging.

Alternative transfection systems such as electroporation have been widely adopted, particularly in the transfection of primary cells and in cell reprograming (Lambricht et al., 2016). Electroporation utilises controlled electric pulses that facilitate cell permeabilisation for direct nuclear delivery of one or several genes. The major disadvantage of this technique is that it can cause high levels of cytotoxicity due to the applied electrical fields causing permanent permeabilisation of the membrane (Yarmush et al., 2014). In addition, it requires labour intensive optimisation of many parameters including voltage, pulse duration and number of cycles. Another physical gene transfer method is microinjection for delivering genes to cells via glass micropipettes. Microinjection requires technical skill and is not convenient in the transfection of large numbers of cells (Becattini et al., 2014). However, there have been recent developments in similar approaches that utilise biodegradable silicon nanoneedles for direct cytosolic gene delivery to large cell numbers *in vitro* and *in vivo* (> 90% transfection efficiency in mouse models) (Chiappini et al., 2015). Table 1.2 summarises the advantages and disadvantages of widely used alternative non-viral transfection strategies.

There are several advantages of CPP-based transfection systems in that they are simple to prepare, they can complex high molecular weight DNA and they exhibit minimal cytotoxicity. Furthermore, peptides are versatile and can easily be modified for cell type specificity, enhanced cytosolic release or be incorporated into multi-functional gene carriers.

CPPs are capable of condensing DNA through electrostatic interactions between the positively charged amines of the peptide and the negatively charged phosphate groups of the DNA. An important step in gene transfer is the release of DNA from the CPP to facilitate gene expression. The dissociation of DNA from the gene carrier is most likely to occur in endosomes/lysosomes where a drop in pH can cause conformational changes of the peptide (Yin et al., 2014). One of the major challenges of *in vivo* gene delivery is low gene expression due to the premature release of DNA in the reducing extracellular environment of organs such as the liver (Kwok et al., 2003). Another important step in CPP-mediated transfection is the transport of DNA across the nuclear membrane. During mitosis, the nuclear membrane disassembles allowing nuclear entry of exogenous genes. Non-dividing cell types that do not regularly undergo mitosis cannot be transfected easily and their gene expression can be several orders of magnitude lower than that of proliferative cells (Dean et al., 2005). Nuclear localisation signal (NLS) sequences can be incorporated into CPP/DNA complexes to enhance DNA nuclear translocation (Lam and Dean, 2010). NLS peptides are short amino acid sequences that were originally derived from proteins that were able to target the nucleus of cells. When incorporated into

CPP vectors they have been shown to increase gene expression *in vitro* and *in vivo* (Huang et al., 2015).

The mechanism of uptake can impact genetic cargo delivery and intracellular handling. Whereas direct penetration results in cytosolic delivery of DNA, endocytosis causes sequestration of CPP/cargo in the endosomes. Endosomal entrapment restricts the localisation, activity and bioavailability of DNA. Furthermore, genes that remain trapped will eventually undergo degradation by hydrolytic enzymes in late endosomes/lysosomes. Many approaches have been proposed to facilitate endosomal release of trapped CPP/cargo such as pH buffering agents that respond to the acidic environment of endosomes, photochemical internalisation reagents which utilise photogenerated radical oxygen species for membrane disruption and membrane active agents including fusogenic peptides (Ohtsuki et al., 2015, Lo and Wang, 2008). Genetic cargo that successfully escapes endosomes can go on to reach their nuclear target, however the low efficiency of existing endosomal escape strategies has limited CPP-mediated transfection efficiency.

It is clear that there are many biological obstacles which need to be overcome for successful CPP-mediated transfection (Figure 1.2). This reviews focuses on the modifications of CPPs to improve their gene transfer activity by improving their:

- **Membrane interaction (Section 1.2.1):** active targeting of the cell membrane for enhanced membrane association and/or cell type specific delivery.

- **Translocation (Section 1.2.2):** efficient transmembrane transport by membrane active CPPs such as amphipathic peptides.
- **Intracellular trafficking (Section 1.2.3):** endosomal escape strategies for enhancing the cytoplasmic delivery of genetic cargos.

Table 1.2 The advantages and disadvantages of widely used alternative non-viral transfection strategies.

Transfection strategy	Advantages	Disadvantages	References
Electroporation	• Broad cell spectrum (including non-dividing cells) • High efficiency	• Requires optimisation • Challenging *in vivo* (difficulty of access with electrodes) • High toxicity	(Yarmush et al., 2014, Lambricht et al., 2016)
Microinjection	• Broad cell spectrum (including non-dividing cells) • High efficiency	• Labour intensive (one cell at a time) • Technically challenging • Challenging *in vivo*	(Becattini et al., 2014, Wong et al., 2014)
Polymers (such as polyethylenimine (PEI) and poly-beta-amino ester (PBAE))	• Biocompatible • Biodegradable • Mediates endosomal escape via the "proton sponge" effect	• Lack of control during synthesis results in non-uniform physio-chemical characteristics • High toxicity	(Lv et al., 2006, Park et al., 2006)
Lipid-based agents (such as cationic lipids and liposomes)	• Biocompatible • Easy to produce • Mediates endosomal escape via fusogenic lipids	• Majority are not suitable for *in vivo* (due to poor stability in biological fluids) • High toxicity	(Allen and Cullis, 2013)

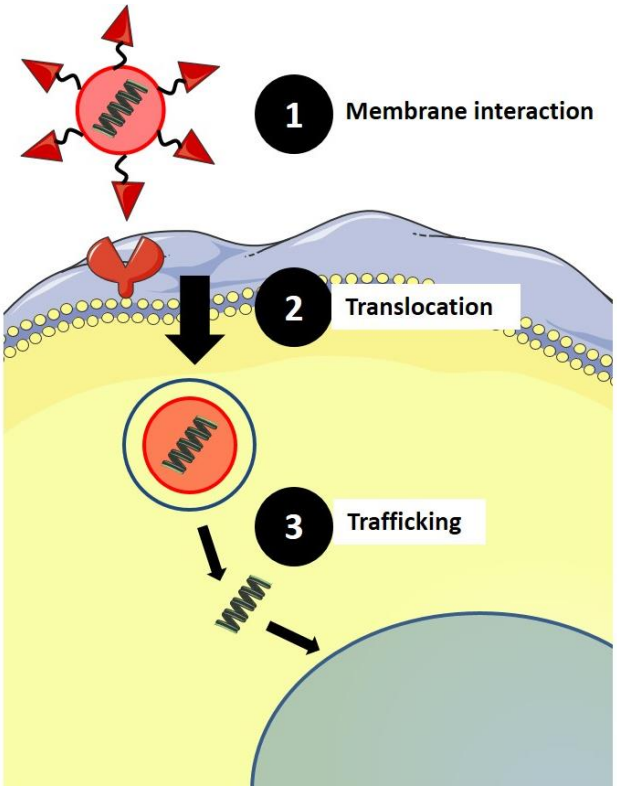


Figure 1.2 Three important steps in the transfection of CPP/DNA complexes. (1) Membrane interaction, (2) translocation and (3) intracellular trafficking.

1.2.1 Membrane interaction

The majority of CPPs non-selectively deliver DNA to cells, however they can be functionalised for powerful approaches such as cell type specific gene therapy of target cells or tissues (Copolovici et al., 2014). Furthermore, conjugation of a cell surface binding ligand to a CPP can enhance its cell surface concentration, membrane association and in turn, improve its efficiency of translocation. CPPs can easily be modified to include cell targeting sequences, this has been a popular approach for the CPP-mediated delivery of anti-cancer drugs to cancer cells or tumour sites (Raucher and Ryu, 2015). Nonetheless, this approach has been underutilised and often overlooked in gene therapy. In one recent expert review, lack of cell targeting was highlighted as an 'inherent weakness' of CPP's in the transfection of nucleic acids (Lehto et al., 2012).

Some attempts have been made to design cell targeting CPPs for gene delivery. An approach by Swiecicki *et al* was to conjugate TAT-Mu to a human epidermal growth factor receptor 2 (HER2) antibody mimetic-affibody (AF) for the targeting and transfection of breast cancer cells expressing HER2+ (Swiecicki et al., 2015). The resulting CPP, termed TMAF, was tested in culture and in animal models. TMAF demonstrated enhanced transfection efficiency in the breast cancer cell line compared to other cell lines. In xenograft mouse models TMAF demonstrated efficient DNA uptake and high reporter gene levels. Furthermore, TMAF nanoparticles (NPs) demonstrated significant tumour specific knockdown of tissue factor (TF). However, the complexes were administered by intratumoral injection and it is not clear whether specificity would be retained following systemic delivery.

We have described glycosaminoglycan (GAG)-binding enhanced transduction (GET) peptides for improved membrane association and highly efficient delivery of cargo into cells (Dixon et al., 2016). Multifunctional peptides comprising of a cell surface heparan sulfate (HS) GAG binding domain (P21) fused to CPP (8R) enhanced intracellular delivery of a self-reporting cargo (monomeric red fluorescent protein (mRFP)) in difficult-to-transduce cell types including mesenchymal stem cells (MSCs), human embryonic stem cells (hESCs) and human induced pluripotent stem cells (hiPSCs) by up to two orders of magnitude compared to unmodified CPP (8R). The same synergistic increase in uptake was observed when P21 was fused to a panel of CPPs other than 8R including TAT, 8K and 8RQ. The GET-system has been utilised for highly efficient delivery of a diverse range of cargos including enzymes, proteins, antibodies, transcription factors, magnetic nanoparticles and nucleic acids for a wide variety of applications from the delivery of NANOG for promoting self-renewal of pluripotency to the differentiation of stem cells (Figure 1.3) (Eltaher et al., 2016, Dixon et al., 2016). Importantly, this included the efficient transfection of plasmid DNA comparable to commercial transfection reagent Lipofectamine 2000. GET-peptides have the potential to overcome challenges in poor delivery efficiency of CPP-based gene carriers that have thus far inhibited their clinical application. In addition to P21 there are over 100 identified GAG-binding sequences (Linhardt, 2009). Further investigation is needed to identify whether HS GAG targeting sequences other than P21 can be conjugated to CPPs for synergistically enhanced delivery of DNA.

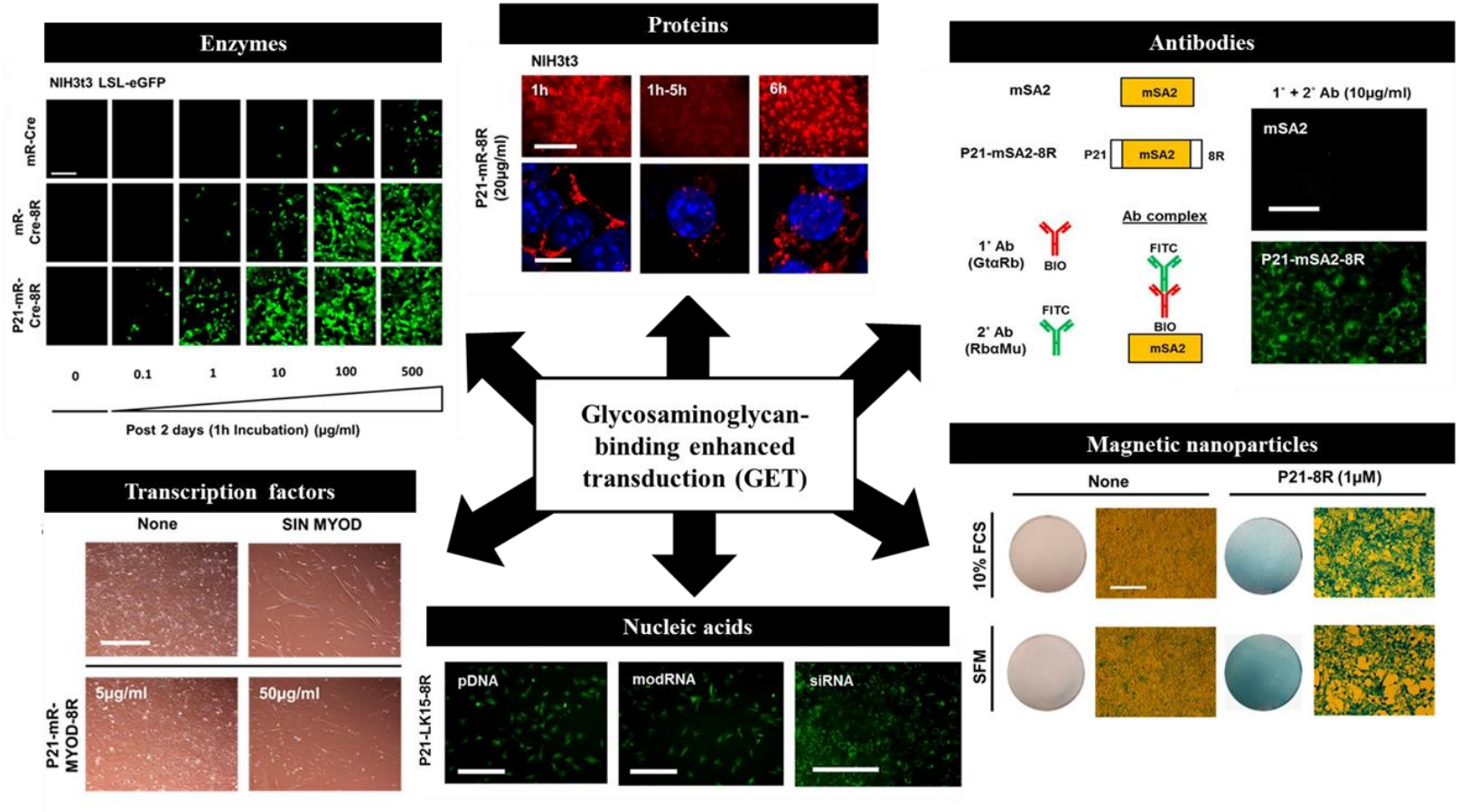


Figure 1.3 GET peptides (i.e. CPPs functionalised with cell surface HS GAG-targeting sequences) have demonstrated enhanced delivery of a variety of cargos. Adapted with permission from (Dixon et al., 2016).

1.2.2 Translocation

In order to achieve maximal delivery of DNA, CPP gene carriers can be designed for improved membrane activity and to increase direct penetration vs. endocytosis to improve their cytosolic availability (Swiecicki et al., 2015).

1.2.2.1 Amphipathic peptides

Amphipathic peptides have demonstrated the ability to bind DNA, translocate across the cellular membrane and in some cases induce endosomal escape (Giraldo et al., 2014). The amphipathic alpha-helical structure plays a role in the interaction of the CPP with the cellular membrane and phospholipid rearrangement during the cell penetration process. The amphipathic helices are composed of alternating hydrophilic and hydrophobic residues. The hydrophobic face can insert into the membrane resulting in thinning of the chain region, increased internal membrane tension and eventual destabilisation of the membrane through transient membrane perturbation (Li et al., 2004, Pujals et al., 2007). The mechanism of action can vary depending on the CPP (primary amphipathic or secondary amphipathic) and the target membrane lipid composition. Proposed models include formation of a barrel stave pore or toroidal pore in which the peptide forms a transmembrane ion channel or a channel composed of both peptide and phospholipids, respectively (Sato and Felix, 2006).

GALA is an amphipathic CPP that undergoes conformational change when pH is reduced from 7 to 5, corresponding to pH changes in early endosomes (pH

6.0-6.5) to lysosomes (pH 4.5-5.5) (Sorkin and von Zastrow, 2002). GALA was able to induce membrane disruption at low pH and also, promote DNA unpacking (Simoes et al., 1999a). Due to its negative charge, GALA could not effectively condense DNA. Therefore, the peptide was coupled with DNA binding gene carriers such as cationic polymers and liposomes (Simoes et al., 1999b, Simoes et al., 1998). Wyman *et al* have described substitution of the glutamic acid residues in GALA with lysine residues to form a cationic amphipathic peptide termed KALA (Wyman et al., 1997). KALA was able efficiently bind, deliver and transfect DNA; eliminating the need for it to be coupled to an alternative gene carrier for transfection.

More recently, Saleh *et al* have described conjugation of amphipathic peptide, LK15, to TAT significantly improved transfection of DNA in HT29 and HT1080 cultured cells (Saleh et al., 2010). TAT LK15 demonstrated superior DNA complexation and membrane penetration compared to TAT alone. However, TAT and TAT LK15/DNA NPs were not able to penetrate tumour spheroid models. This study demonstrates multifunctional peptides can improve efficiency of delivery of DNA. A similar approach was taken by Luan *et al,* whom combined an amphiphilic antimicrobial peptide (AMP), a CPP (TAT), a steryl moiety and a cysteine chain for the transfection of a reporter gene (pGL3) (Luan et al., 2015). The fusion of all four functional peptides resulted in high transfection efficiency comparable to Lipofectamine 2000 in 293T and NIH3T3 cells.

1.2.2.2 Cationic peptides

Cationic CPPs usually contain arginine-rich sequences. Their positive charge facilitates strong interactions with phospholipids and proteoglycans mediating their internalisation. Positive charge is necessary for their translocation, with some studies now investigating whether supercharged peptides and proteins can be utilised for enhanced transfection. Super-positively charged proteins have been shown to complex DNA, interact with the cell membrane and successfully transfect a variety of cell lines (some of which were resistant to transfection by cationic lipids) (Lawrence et al., 2007). Through surface mutagenesis, green fluorescent proteins (GFPs) with net charge ranging from -30 to +48 were generated (Lawrence et al., 2007). McNughton *et al* demonstrated that the supercharged proteins were able to interact with the cell membrane similarly to cationic CPPs and enter cells in a charge dependant manner. The +36 GFP protein was able to complex siRNA and transfect a variety of cell lines without cytotoxicity. However, for successful transfection of DNA +36 GFP had to be fused to an endosomolytic peptide and treatment at high concentrations was needed (McNaughton et al., 2009). Interestingly, the enhanced delivery of Cy3-labelled siRNA by +36 GFP was not observed with synthetic cationic CPPs of similar charge. These results indicate that it is not only the positive charge of CPPs that contributes to their efficient DNA delivery.

1.2.3 Intracellular trafficking

It is well documented that endosomal escape strategies can significantly improve the efficiency of CPP-mediated gene transfer (Shiraishi and Nielsen, 2006). Inability to release DNA from the endosomes leads to degradation of CPP/DNA complexes (Figure 1.4). To reduce the risk of degradation, lysosomotropic agents can be co-delivered with CPP/DNA complexes. Lysosomotropic agents are substances that accumulate in lysosomes and can act to cause lysosomal lysis (Giraldo et al., 2014). Examples are weak bases such as chloroquine and chlorpromazine that are protonated in the acidic environment of endosomes/lysosomes and cause osmotic swelling that eventually leads to rupture of the vesicle. The application of the majority of endosomal escape reagents is restricted by high toxicity at effective doses (Xie et al., 2011). It would be preferable to design peptides that are directly conjugated to lysosomotropic agents to minimise cytotoxic off target effects.

1.2.3.1 Fusogenic peptides

Fusogenic peptides have endosome disruptive properties that have led to their exploitation as endosomal escape reagents. One such example is the influenza virus derived endosomal escape peptide hemagglutinin protein (HA2). HA2 peptide is a pH-sensitive fusogenic peptide made up of 20 amino acid residues. It was reported that co-treatment of reporter cells with dTAT-HA2 peptide and TAT-Cre increased recombination, with no reported cytotoxicity (Wadia et al., 2004). Interestingly, Wadia *et al* found that HA2 peptide alone had little to no effect unless it was fused to delivery peptide TAT.

1.2.3.2 pH inducible amines

Histidine residues can be conjugated to CPPs to induce cytosolic release following endocytosis. In the acidic environment of the late endosomes the imidazole group in histidine is protonated, leading to osmotic swelling and endosome disruption. Lo *et al* fused 10 histidine's (10H) to TAT to promote endosomal release of trapped cargo (Lo and Wang, 2008). Furthermore, two cysteine residues were added to TAT 10H for improved transfection through formation of disulphide bonds that stabilise the CPP/DNA complexes. The disulphide bonds can be reduced in the endosomes, facilitating unpacking of the DNA. C-5H-TAT-5H-C peptide transfected cells efficiently in human and rat glioma cell lines (Lo and Wang, 2008). Furthermore, complexes were administered by stereotactical injection for gene delivery into the nervous system of rats. Transfection efficiency was compared with polyethylenimine (PEI) in the brain and spinal cord. Results were mixed, C-5H-TAT-5H-C demonstrated 5 fold lower transfection efficiency than PEI complexes in the brain and comparable transfection efficiency in the spinal cord. However, the safety prolife of C-5H-TAT-5H-C was significantly better than PEI.

1.2.3.3 Stearylated CPPs

The modification of CPPs to incorporate a stearic acid moiety has been shown to improve DNA transfection. However, the mechanism by which stearylation improves transfection is unclear and the level of success appears to be varied between different CPPs (Pan et al., 2016). Lehto *et al* compared N-stearylated

9R and $(RxR)_4$ CPPs for DNA transfection (Lehto et al., 2010). Stearylation significantly increased transfection levels at all tested charge ratios (CRs) and stearylated $(RxR)_4$ peptides were more efficient than stearylated 9R peptides. Furthermore, chloroquine treatment of stearyl 9R had more of pronounced effect in increasing expression of luciferase compared to stearyl $(RxR)_4$, indicating that endosomal entrapment was a greater problem for 9R/DNA complexes. Despite demonstrating promising results, Lipofectamine 2000 transfection efficiency was significantly higher than all the tested CPPs and stearyl $(RxR)_4$ transfection was inhibited in serum conditions (limiting its suitability for *in vivo* applications). Similarly, DNA delivery by N-stearylated 8R CPPs with NLS sequences were tested by Wang *et al* (Wang et al., 2011). The stearyl group increased membrane penetration and transfection efficiency at high CRs, however transfection efficiency was lower than with PEI complexes. Modified CPPs with a steric acid moiety have also been utilised for *in vivo* transfections. Stearylated amphipathic CPP, TP10, demonstrated non-toxic and dose dependent gene delivery following intramuscular and intradermal administration in mice (Lehto et al., 2011).

Andaloussi *et al* reported a stearyl TP10 peptide with chloroquine analogue moieties covalently incorporated to facilitate endosomal release (Andaloussi et al., 2011). This approach led to trafficking of the peptide/chloroquine moieties to the endosomes resulting in minimised effective dose and localised activity of the chloroquine analogues. The CPP, termed PepFect 6, was able to form NPs with siRNA and efficiently transfect various cells (including primary cells) in serum conditions. Furthermore, following systemic delivery to mice, efficient

knockdown was achieved without toxicity. PepFect 6 also demonstrated efficient transfection of DNA (Parn et al., 2013)

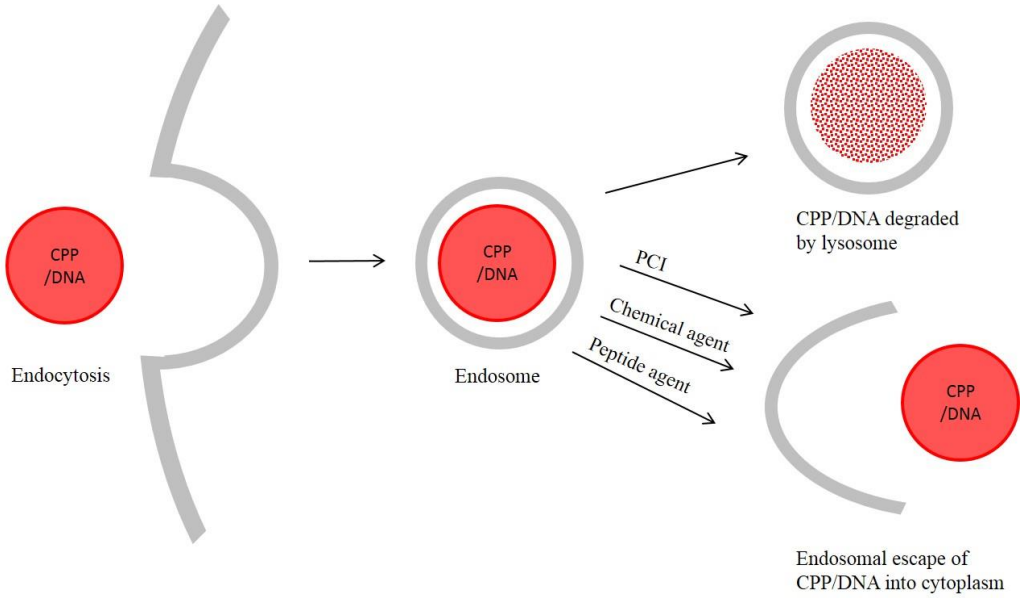


Figure 1.4 Intracellular trafficking of CPPs following endocytosis. CPP/DNA complexes that enter cells via endocytosis can undergo degradation by lysosomes unless an endosomal escape strategy is employed for cytosolic release.

1.3 Strategies for *in vivo* DNA delivery

In vivo gene delivery is a huge challenge for even the most promising *in vitro* gene carriers, hindering their clinical translation. A major scientific goal is the development of NPs are that able to navigate biological barriers for widespread and efficient transfection of target cells/tissues. The main issues inhibiting successful *in vivo* gene therapy of CPP/DNA NPs include:

- **Enzymatic degradation:** Nucleases and proteases in the biological environment can degrade the therapeutic DNA and CPP gene carrier, respectively.
- **Unwanted interaction with biological components:** Interaction of cationic CPPs with biomolecules can lead to aggregation of the complexes and consequently, steric entrapment within biological matrices. This can lead to to poor bio-distribution and inability of complexes to reach target cells/tissue.
- **Immunogenicity:** CPP/DNA NPs can be cleared rapidly due to phagocytosis by the mononuclear phagocyte system (MPS), reducing their circulation half-life and window of therapeutic utility.

Various strategies can be employed to try to overcome these challenges. CPPs are susceptible to degradation by proteases *in vivo*, however their metabolic stability can be improved by swapping L-peptides to D-peptides. (Pujals et al., 2007, Verdurmen et al., 2011). In addition, the surface of CPP/DNA NPs can be shielded by inert molecules to minimise their interaction with biological components and facilitate their navigation of biological barriers *in vivo*.

However, shielding can mask CPP activity thereby reducing transfection activity of complexes.

CPP/DNA NPs coated with a polyethylene glycol (PEG) have demonstrated enhanced colloidal stability, prolonged circulation time, widespread distribution and decreased toxicity *in vivo*. PEGylation is an effective method of improving the features of NPs however, it can reduce the uptake of CPPs. An ideal gene delivery system would mask CPP activity during administration and restore it at the site of the target tissue. Vieman *et al* employed a strategy to reverse PEGylation to restore CPP, PepFect 14, activity at the tumour site through inclusion of a matrix metalloprotease (MMP) substrate (Veiman et al., 2015). Complexes were administered by injection via the tail vain of mice with induced Neuro2a tumours. MMP2 is over expressed in tumours therefore an MMP2 cleavable linker was introduced between the PEG and CPP. Results demonstrated significantly increased gene expression in the tumour.

In other work, an oligopeptide derived from TAT was coupled to PEI using a PEG linker for DNA delivery in mouse lung models (Kleemann et al., 2005). The PEG moiety shielded the PEI/DNA core from unwanted interactions with biological components and TAT improved the cellular uptake of the particles. TAT PEG PEI complexes demonstrated superior colloidal stability when incubated in bronchial alveolar lavage fluid (BALF). Despite exhibiting low transfection efficiency *in vitro*, TAT PEG PEI NPs demonstrated 6 fold higher gene expression in mouse lungs than PEI complexes. This highlights that *in vitro* transfection efficiency alone is not an accurate predictor of *in vivo* efficacy. TAT

PEG PEI polyplexes demonstrated nontoxic, widespread and enhanced transfection efficiency, illustrating the *in vivo* potential of vectors with multiple functions.

A multifunctional approach was also taken by Kogure *et al* in the design/development of multifunctional envelope-type nano device (MEND) gene carriers (Kogure et al., 2008). MEND consisted of a cationic polymer/DNA core, enveloped by a lipid that was functionalised by targeting ligands, CPPs and PEG groups. Unlike the majority of non-viral delivery vehicles, MEND has displayed *in vitro* siRNA transfection efficiency comparable to adenovirus (Moriguchi et al., 2005). In addition, MEND was functionalised with CPP, 8R, for *in vivo* DNA delivery to the skin of mice. 8R directed cellular uptake of NPs by macropinocytosis and endosomal release was mediated by fusogenic lipids/the polymer core (Moriguchi et al., 2005). Topical application of 8R MEND induced reporter gene expression in hair follicles. Furthermore, bone morphogenetic protein receptor type 1 A (Bmpr1a) gene was delivered to induce hair growth. MEND has also been utilised for the efficient delivery of oligonucleotides, proteins and drugs (Nakamura et al., 2006, Suzuki et al., 2007). More recently, Yamada *et al* have shown that MEND can be used for the targeting and delivery of drugs to mitochondria by functionalisation of the gene carrier with 8R and a mitochondrial targeting signal peptide (Yamada et al., 2012).

1.4 Summary

CPPs meet many of the requirements of an optimal gene carrier system, however their clinical adoption has been inhibited by low efficiency of transfection. Recent reports have demonstrated strategies for improving gene transfer through functionalisation of CPPs to enhance their binding of DNA, stability in biological fluids, effective escape from endosomes and cell targeted delivery (Table 1.3). For example conjugation of endosomal escape peptide HA2 to TAT resulted in non-cytotoxic release of trapped cargo, amphipathic peptides such as KALA have demonstrated enhanced membrane activity and GET peptides functionalised with HS GAG cell targeting ligand have demonstrated 2 orders of magnitude improved intracellular delivery (Saleh et al., 2010, Dixon et al., 2016).

The most promising emerging CPP candidates for gene delivery are:

- **Modified CPPs** for cell targeting and enhanced endosomal release.
- **Multifunctional approaches** that combine CPPs, lipids, polymers and/or targeting ligands.

In vivo transfection presents additional challenges, with performance of CPPs *in vitro* unable to be effectively translated in animal models. PEGylation is an effective method of shielding NPs to increase their circulatory half-life, to prevent unwanted interactions with biological components and to improve their safety profile. However, shielding masks CPP activity thereby reducing the transfection activity of complexes. Many advances are being made in CPP gene therapy including design of “smart” carriers that are responsive to the

extracellular environment for reverse PEGylation at the target site. Future work should focus on the further development of multifunctional strategies to overcome challenges of CPP gene carriers, however, the therapeutic potential of CPP-based transfection agents is clear.

Table 1.3 A summary of the most promising CPPs for gene transfer *in vitro* and *in vivo*.

CPP	Model	Reference
TMAF	Breast cancer cells expressing HER2+ and xenograft mouse models (*in vitro* and *in vivo*)	(Swiecicki et al., 2015)
GET	NIH3T3 cells (*in vitro*)	(Dixon et al., 2016)
TAT LK15	HT29 and HT1080 cells and tumour spheroid model (*in vitro* and 3D model)	(Saleh et al., 2010)
C18-C$(LLKK)_3$C-TAT	293T and NIH3T3 cells (*in vitro*)	(Luan et al., 2015)
C-5H-TAT-5H-C	Glioma cell lines and stereotactical injection to the nervous system of rats (*in vitro* and *in vivo*)	(Lo and Wang, 2008)
Stearyl TP10	Intramuscular and intradermal injection in mice (*in vivo*)	(Lehto et al., 2011)
PepFect 6	BHK-21 cells (*in vitro*)	(Parn et al., 2013)
PepFect 14	Tail vain injection of mice with induced Neuro2a tumours (*in vivo*)	(Veiman et al., 2015)
TAT-PEG-PEI	Mouse lung model (*in vivo*)	(Kleemann et al., 2005)
MEND	Topical application to the skin of mice (*in vivo*)	(Moriguchi et al., 2005)

1.5 Aims of the project

1. GET peptides have demonstrated enhanced intracellular delivery through targetting of cell surface HS-GAGs. The first aim of the project was to investigate whether GET peptides could be modified to target HS motifs that were expressed preferentially by different cell types. CPP (8R) was conjugated to a variety of HS binding peptides and a truncated HS epitope binding antibody for cell type specific targeting and delivery.
2. Upon selection of promising GET peptides, the second aim was to optimise GET-mediated gene transfer of a reporter plasmid *in vitro*. GET technology was compared to commercially available non-viral transfection reagents in terms of efficiency and cytotoxicity.
3. The final aim of the project was to engineer PEGylated GET NPs with desirable physiochemical properties for *in vivo* gene delivery with the aim of demonstrating efficient and widespread transgene expression in healthy mouse lung models.

CHAPTER 2 Glycosaminoglycan-binding enhanced transduction (GET)

2.1 Introduction

In previous work we have shown that the conjugation of CPP (8R) to HS-GAG targeting sequence (P21) increased the intracellular delivery of a reporter protein by two orders of magnitude compared to CPP alone (Figure 2.1) (Dixon et al., 2016). This phenomenon was termed GAG-mediated enhanced transduction (GET). The P21 (KRKKKGKGLGKKRDPCLRKYK) peptide is a HS-GAG targeting sequence derived from heparin-binding epidermal growth factor (HB EGF) growth factor. HB EGF is not unique in containing sequences for HS GAG binding, many growth factors (GFs) that regulate a variety of cellular processes interact with cell surface HS chains to stabilise GF-receptor binding and increase the local concentration of the factor on the cell membrane (Figure 2.2) (Table 2.1) (Mahtouk et al., 2006, Wu et al., 2003). HS chains that regulate these ligand interactions are synthesised in the Golgi apparatus by a three-step process that is modulated by enzymes:

- **Step 1 Chain initiation:** chain initiation forms the link between the core protein and the HS chain through a trisaccharide linker, 3Galβ1-3Galβ1-4Xylβ1-O-(Ser).
- **Step 2 Chain polymerisation:** the chain polymerisation step is initiated by GlcNAc, following which alternating GlcA and GlcNAc glycosyltransferases are added to the chain.

- **Step 3 Chain modification:** the sugar residues undergo modifications leading to structural heterogeneities of the HS chains.

During the chain modification (Step 3), changes in the structure of HS sugars leads to distinct cell surface sulphation patterns of different cell types (Schamhart and Kurth, 1997, Delehedde et al., 1997). Furthermore, modifications of HS chains affect the ability of ligands to interact with them. An example is during neural development when a change in HS chain structure correlates to a change from fibroblast growth factor (FGF)-2 to FGF-1 activity (Brickman et al., 1998). FGF-2 has a high affinity for 2-O-sulphated iduronate, while FGF-1 binding also requires 6-O-sulphated glucosamine (Uniewicz et al., 2010). The unique HS expression profiles of different cell types have been exploited for therapeutic targeting, with particular importance in the study of cancer adhesion and metastasis. HS-targeted inhibition of tumour angiogenesis *in vivo* has been achieved by introducing HS mimetics to block specific GF interactions (Fuster and Esko, 2005, Presta et al., 2003). In addition, antibodies known to target specific HS motifs have been utilised as markers of selective cells. Baldwin *et al* have demonstrated targeting of the pre-hemangioblast cell during mesodermal differentiation using a specific HS-epitope binding antibody (HS4C3) (Baldwin et al., 2008). Blocking HS GAG-binding can inhibit signalling by GFs and cytokines as well as affecting cell migration and attachment (Lipscombe et al., 1998, Coombe, 2008). Therefore, it is possible that non-specific binding could affect cell physiology. Different HS structures and cell types may evoke different biological responses therefore the biological effect must be examined individually for each HS mimetic.

In this study a panel of GF derived HS-binding domains, other than P21, were conjugated to CPP (8R) to investigate whether GET-mediated enhanced delivery could be observed. HS-GAG binding domains from FGF-1, FGF-2, FGF-4, FGF-7, platelet derived growth factor (PDGF) and antithrombin-III (ATIII) were identified from the literature and screened for their uptake efficiency. There are only a limited number of identified HS-GAG binding domains therefore the panel were selected on the basis that they had fully characterised binding sequences (peptide sequences are shown on Appendix Table 6.1).

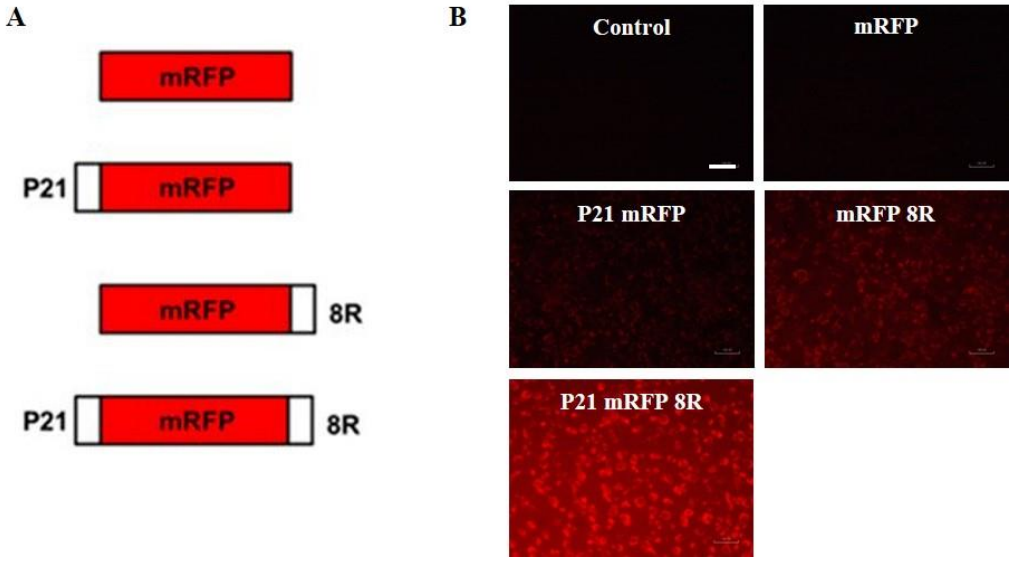


Figure 2.1 GET-mediated enhanced delivery of monomeric red fluorescent protein (mRFP) to NIH3T3 cells. (A) A schematic of GET peptide and its components. (B) Fluorescence microscopy images of NIH3T3 cells treated with FmRFP, P21 mRFP, mRFP 8R or P21 mRFP 8R proteins (20 µg/mL 12 h). Scale bar, 100 µm. Figure was adapted with permission from (Dixon et al., 2016).

Table 2.1 Naturally derived growth factors (GFs), chemokines, cytokines and extracellular matrix (ECM) components that are known to interact with cell surface HS ligands..

HS GAG binding ligands		Biological role	References
Growth factors (GFs)	FGF family	Wound healing, developmental processes and angiogenesis	(Wu et al., 2011, Li et al., 2016)
	EGF family	Stimulates proliferation and differentiation	(Mahtouk et al., 2006)
	PDGF	Angiogenesis and blood vessel formation	(Abramsson et al., 2007)
	TGF-β	Wound healing, proliferation and differentiation	(Demetriou et al., 1996)
	ATIII	Anticoagulation (found in blood plasma)	(Naimy et al., 2008)
	VEGF	Angiogenesis and blood vessel formation	(Teran and Nugent, 2015)
Chemokines	RANTES/CCL5	Secreted by activated T cells to recruit leukocytes	(Oravecz et al., 1997)
	MIP-1α	Recruits leukocytes together with RANTES/CCL5	(Stringer et al., 2002)
	IL8/CXCL8	Induces chemotaxis and phagocytosis	(Gerlza et al., 2014, Belayet et al., 1999)

Cytokines	Interferon γ	Secreted as an immune response against viral infections	(Lortat-Jacob, 2006)
	TNF-α	Cytotoxin (toxic to certain cancer cells)	(Carter et al., 2003)
Morphogens	BMP	Induces formation of bone and cartilage	(Szweras et al., 2002, Rider and Mulloy, 2010)
	Wnt	Regulates paracrine and autocrine cell signalling	(Yamamoto et al., 2013)
	Sonic hedgehog	Plays a role in proliferation and developmental process during embryogenesis	(Ortmann et al., 2015)
	HGF	Stimulates paracrine cellular growth	(Ashikari et al., 1995)
ECM components	Fibronectin	Adhesion, migration and differentiation	(Richardson et al., 2001, Carpentier et al., 2014)
	Thrombospondin	Apoptosis, angiogenesis and immune regulation	(Feitsma et al., 2000)

	Laminin	Differentiation and adhesion. Makes up the basal lamina	(Maruyama et al., 2000)
	Collagen	Plays a role in cell adhesion and proliferation (structural proteins that make up tissues).	(French et al., 1999)
	Vitronectin	Haemostasis and cellular adhesion	(WilkinsPort and McKeownLongo, 1996)

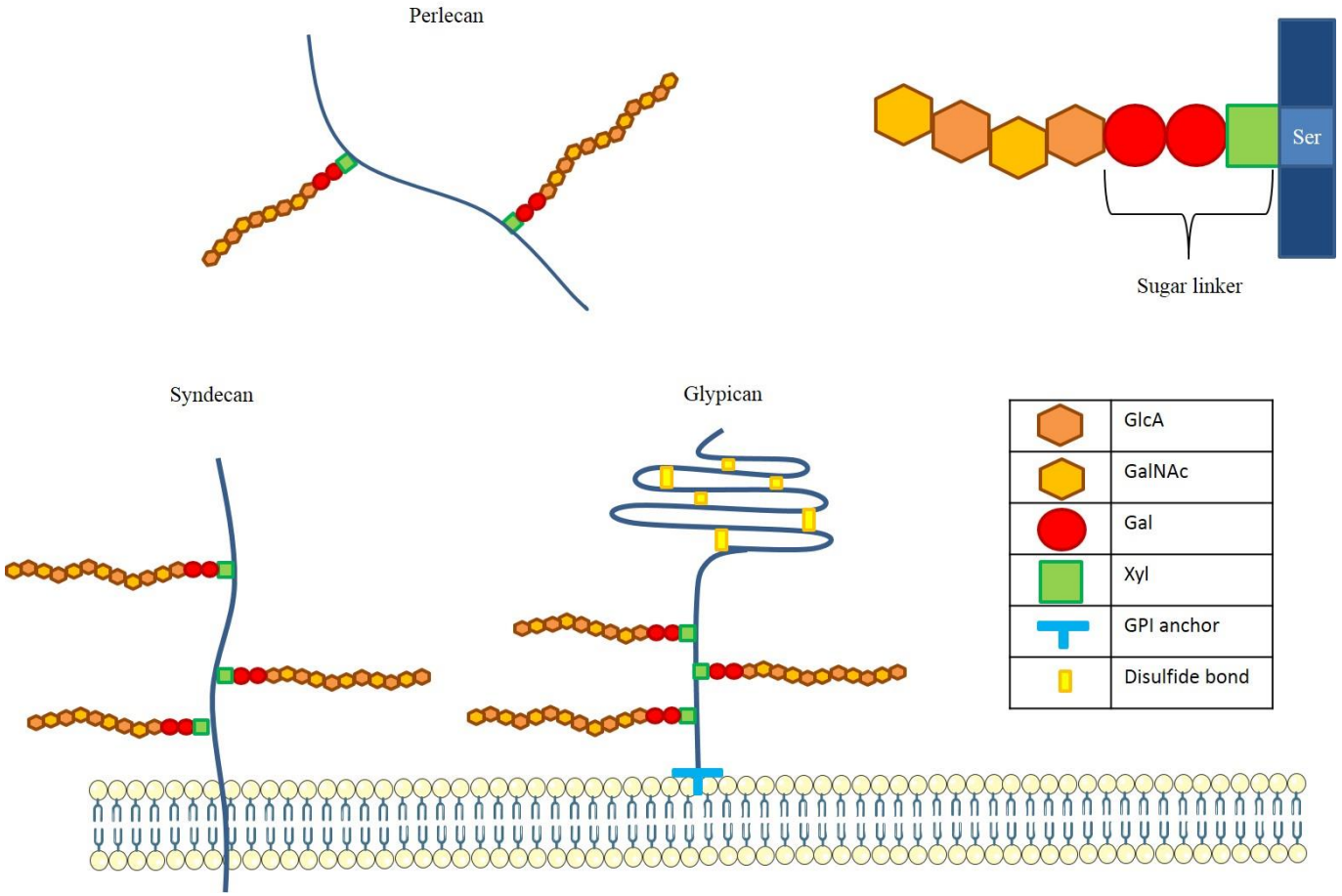


Figure 2.2 Schematic of the different types of cell surface HS GAGs; syndecans, glypicans and perlecans.

2.2 Aims of the project

1. To investigate whether GF derived HS-GAG targeting sequences, other than P21, could be conjugated to a CPP for enhanced delivery into cells. A variety of GF derived HS-GAG binding domains were conjugated to 8R and screened.
2. GET-mediated targeting of specific cell surface HS-epitopes. A truncated HS-binding antibody was conjugated to 8R to investigate whether HS GAG targeting could be utilised for cell type specific delivery. It was hypothesised that HS motifs expressed by selective cell types could be targeted for cell type specific enhanced delivery via GET.

2.3 Materials and methods

2.3.1 Preparation of recombinant proteins

Recombinant proteins were prepared by Dr James E. Dixon as described previously (Dixon et al., 2016). Proteins, mRFP, mRFP 8R, P21 mRFP 8R, FGF1A mRFP, FGF1A mRFP 8R, FGF2A mRFP, FGF2A mRFP 8R, FGF4A mRFP, FGF4A mRFP 8R, FGF7A mRFP, FGF7A mRFP 8R, FGF1B mRFP, FGF1B mRFP 8R, FGF2B mRFP, FGF2B mRFP 8R, FGF4B mRFP, FGF4B mRFP 8R, FGF7B mRFP, FGF7B mRFP 8R, FGF1C mRFP, FGF1C mRFP 8R, FGF2C mRFP, FGF2C mRFP 8R, FGF4C mRFP, FGF4C mRFP 8R, FGF7C mRFP, FGF7C mRFP 8R, ATIII mRFP, ATIII mRFP 8R, PDGF mRFP, PDGF mRFP 8R, VEGF mRFP, VEGF mRFP 8R, HS4C3 mRFP and HS4C3 mRFP 8R (Appendix Table 6.1 and Table 6.2), were cloned as cDNAs into pGEX6-PI vector (Novagen) and expressed in BL21(DE3)pLysS Escherichia coli (E. coli) (Novagen). Briefly, cultures were grown in lysogeny broth (LB) (OD600 nm = 0.4-0.6) while being shaken at 220 rpm at 37˚C and induced using 1 mM isopropyl β-D-1-thiogalactopyranoside (IPTG) for 24 h at 25˚C. The cultures were centrifuged (2000xg, 5 min) and the supernatant was discarded. The bacterial pellet was lysed and sonicated in 1X STE extraction buffer (50 mM Tris, pH 7.5, 150 mM NaCl, 1 mM ethylenediaminetetraacetic acid (EDTA) containing 1mM dithiothreitol (DTT), 0.2 mg/ml lysozyme and 1X protease inhibitor cocktail). Insoluble protein was retrieved using the Rapid GST inclusion body solubilisation and renaturation kit (AKR-110; Cell Biolabs, Inc., San Diego, CA). Recombinant proteins were purified by affinity chromatography using Glutathione-Sepharose resin (GE Healthcare).

PreScissionTM Protease cleavage (GE healthcare) in 1X cleavage buffer (50 mM Tris-HCI pH 7.0, 150 mM NaCl, 1 mM EDTA and 1 mM DTT) was used to remove GST-tags.

Integrity and full length protein expression was confirmed by sodium dodecyl sulfate polyacrylamide gel electrophoresis (SDS-PAGE). 10% polyacrylamide Tris-glycine gels and running buffer were purchased from Invitrogen (Invitrogen). 20 μg of protein samples were mixed 2X lamelli loading buffer (4% SDS, 20% glycerol, 10% 2-mercaptoethanol and 0.004% bromophenol blue). The protein marker/rainbow marker and prepared protein samples were loaded into each lane of the gel. The gel was run at 120V for 1-2 h. Gels were stained in Coomassie dye for 1-2 h and destained with 20% methanol: 10% acetic acid (v/v) for 1-2 h to wash away excess unbound dye. Gel bands were used to determine protein size and to confirm that the GST tag had been cleaved. Fluorescence of the recombinant proteins were confirmed using the TECAN infinite 200PRO multimode reader, the difference in fluorescence intensity measurements between samples was <10%.

2.3.2 Bradford assay

Bradford assay (Bio-Rad) was used to quantify protein concentration according to the manufacturers guide. Absorbance was measured at 595 nm using recombinant mRFP protein as a standard. Samples were analysed using the TECAN infinite 200PRO multimode reader.

2.3.3 Cell culture of NIH3T3, CGR-8 and HUES7 cells

NIH3T3, CGR-8 and HUES7 cells were grown and maintained as previously described (Dixon et al., 2016). NIH3T3 mouse fibroblast cells are an immortalised cell line. Thus, due to genotypic and/or phenotypic changes these cells may not retain the biological characteristics of their native tissue (Pan et al., 2009). Despite this, NIH3T3 cells have been widely used for screening uptake efficiency and investigating intracellular trafficking (Gao et al., 2016, Choi et al., 2015). We have previously demonstrated that uptake of 8R conjugated to mRFP was high in somatic cells (including NIH3T3 cells) and poor in mouse embryonic stem cells and human embryonic stem cells (Dixon et al., 2016). Therefore, in addition to NIH3T3 cells, uptake was also investigated in CGR-8 mouse embryonic stem cells and HUES7 human embryonic stem cells.

NIH3T3 mouse fibroblast cells were maintained in Dulbecco's modified Eagle's medium (DMEM) with 10% (v/v) fetal calf serum (FCS) supplemented with 2 mM L-glutamine and 100 μg/ml streptomycin. NIH3T3 cells were used between passages 32-55. CGR-8 mouse embryonic stem cells were maintained in DMEM with 20% (v/v) FCS supplemented with 1000 units/mL leukaemia inhibitory factor (LIF), 100 μM β-mercaptoethanol, 2 mM L-glutamine and 100 μg/mL streptomycin. CGR-8 cells were used between passages 21-30. HUES7 human embryonic stem cells were cultured on gelatin coated flasks in DMEM with 20% (v/v) FCS supplemented with 1000 units/mL LIF, 100 μM β-mercaptoethanol, 2 mM L-glutamine and 100 μg/mL streptomycin. HUES7 cells were used between passages 17-27. All cells were incubated at 37^0C under humidified 5% CO_2

conditions, grown in T-75 culture flasks and passaged (with a standard trypsinisation protocol using 0.25% (w/v) trypsin/2 mM EDTA solution) every 2-3 days or when they reached 80% confluency.

2.3.4 Protein delivery to cells

NIH3T3, CGR-8 and HUES7 cells were treated with peptides conjugated to fluorescent reporter protein mRFP to investigate their uptake efficiency (protein sequences are shown on Appendix Table 6.1). Experimental conditions, including the concentration and timing of protein application, were previously evaluated both in terms of minimal cytotoxicity and as an effective dose to allow the quantification of uptake by fluorescence measurements (Dixon et al., 2016). Cells were seeded at 2 x 10^5 cells/well in 12-well plates for 2 h in 1 mL of relevant growth media (GM) at 37^0C in a 5% CO_2 humidified incubator. Each well of cells was aspirated, washed with phosphate buffered saline (PBS) and treated with protein (20 μg/mL, 500 μL) in GM. The cells were incubated with the protein for 20 h at 37^0C in a 5% CO_2 humidified atmosphere.

2.3.5 Maintenance and differentiation of Bry-GFP ES cells, generation of EBs

Bry-GFP cells were maintained on feeders in DMEM with 15% (v/v) FCS supplemented with 1.5 x 10^5 M monothioglycerol (MTG), 10 ng/mL LIF and 2 mM L-glutamine (DMEM-ES).

Bry-GFP murine embryonic stem cells were differentiated as described by Baldwin *et al* (Baldwin et al., 2008). Prior to differentiation the cells were passaged twice, first onto a gelatin coated flask in DMEM-ES and second in Iscove's modified Dulbecco's medium (IMDM) with 15% (v/v) FCS supplemented with 1.5 x 10^4 M MTG, 10 ng/mL LIF and 2 mM L-glutamine (IMDM-ES). Cells were differentiated as embryoid bodies (EBs) for 2.8 days in IMDM with 15% (v/v) FCS supplemented with 4 x 10^4 M MTG, 300 μg/mL transferrin, 25 μg/mL ascorbic acid and 2 mM L-glutamine in Petri-grade dishes. 3 h prior to dissociation, EBs were treated with 50 μg/mL of HS4C3 mRFP or HS4C3 mRFP 8R. EBs were separated into single cells by 10 min incubation and agitation in cell dissociation buffer and fixed in 3.7% (w/v) PFA.

2.3.6 Flow cytometry analysis

The CPPs were coupled to reporter protein mRFP to allow cellular uptake to be evaluated through measuring the fluorescence intensity of treated cells. Following treatment, cells were treated with 25% (w/v) trypsin/2 mM EDTA to remove any surface bound protein/fluorescence and fixed in 3.7% (w/v) paraformaldehyde (PFA) in preparation for flow cytometry. Alternative analysis techniques such as confocal microscopy were considered for analysis of uptake and internalisation. However, drawbacks of confocal microscopy include that only small numbers of cells can be analysed which can lead to problems with statistical analysis (Madani et al., 2011). Flow cytometry facilitates the rapid analysis of large cell numbers, can be used to determine the mean fluorescence intensity and can facilitate the calculation of the percentage of fluorescent cells.

RFP fluorescence expression was analysed on a MoFloTM DP (DAKO) Flow Cytometer using a 561 nm green laser (40,000 cells; gated on live cells by forward/side scatter). Median fluorescence was used for statistical analyses with background from untreated cells subtracted and values taken as ratios to the experimental control (mRFP). Data was analysed on flow cytometry analysis software (WEASEL).

2.3.7 Microscopy

Cells were treated with mRFP reporter proteins as described in Section 2.3.4, washed twice with PBS and imaged live. Bright field and fluorescence images were taken with an inverted Nikon Eclipse microscope TS100 (default settings were used to image the samples and exposure was set based on control samples). RFP fluorescence expression of the cells was captured using a green excitation filter (560 nm). Image J software was used to view the images and add scale bars.

2.3.8 Statistical analysis

Mean and standard deviation (SD) were compiled from three individual experiments (n=3) carried out in duplicate. The number of experiments (n) refers to experiments carried out on cells at different numbers of cell culture passages. Data was analysed by Prism statistical analysis software (GraphPad). ANOVA with Dunnett's test was used for the multiple comparison of each treatment group with unmodified CPP (mRFP 8R).

2.4 Results and discussion

2.4.1 Glycosaminoglycan-binding enhanced transduction (GET)

GF-derived HS-GAG binding sequences were coupled to reporter protein mRFP to allow their uptake to be evaluated through measuring the fluorescence of treated cells by flow cytometry. NIH3T3 murine fibroblast cells, CGR8 murine embryonic stem cells and HUES-7 human embryonic stem cells were treated with the proteins to investigate whether any demonstrated cell type specific activity. It was confirmed that thirteen out of the fifteen tested proteins demonstrated significantly enhanced delivery compared to cells treated with unmodified CPP (mRFP 8R) (Figure 2.3). Furthermore, different HS GAG binding sequences increased uptake preferentially in certain cell types. The diverse delivery profiles of the modified CPPs into the three cell types suggests that the HS-GAG binding domains derived from different GFs may preferentially target and bind different cell surface HS-epitopes. However, it cannot be ruled out that media interactions could also influence uptake. There are over twenty-four heparan sulfate and chondroitin sulfate motifs have been identified in human and bovine serum alone that could interfere with the HS-binding domains (Lu et al., 2010).

It is clear that multifunctional system incorporating cell surface HS GAG targeting domains and CPPs improve uptake into cells. The level of efficiency in different cell types can vary according to the HS-binder. HS binding sequences that show preferential uptake to specific cell types could be utilised for the selection of peptide vectors that are more suitable for their application.

GET moieties P21 and FGF2B demonstrated significant and synergistically enhanced delivery into all three cell types when conjugated to 8R, therefore they were selected as promising candidates for DNA delivery (Figure 2.4).

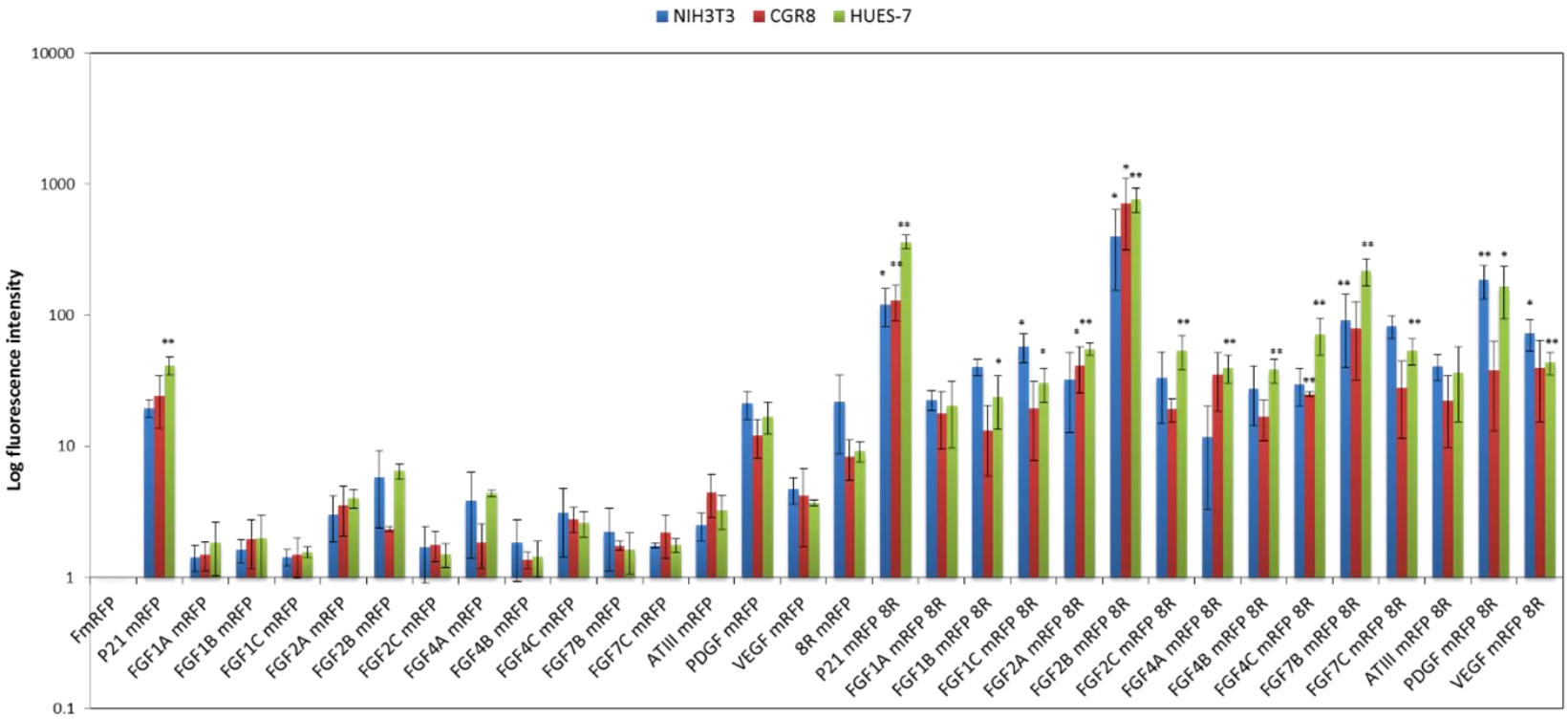


Figure 2.3 Graph showing NIH3T3, CGR8 and HUES-7 cells treated with mRFP conjugated peptides (20 µg/mL, 20 h). Flow cytometry analysis was used to quantify mean fluorescence intensity of cells. Error bars indicate SD, n = 3. One-way ANOVA with Dunnett's test was used for multiple comparison of each treatment group with unmodified CPP (mRFP 8R), *P < 0.05, **P < 0.01.

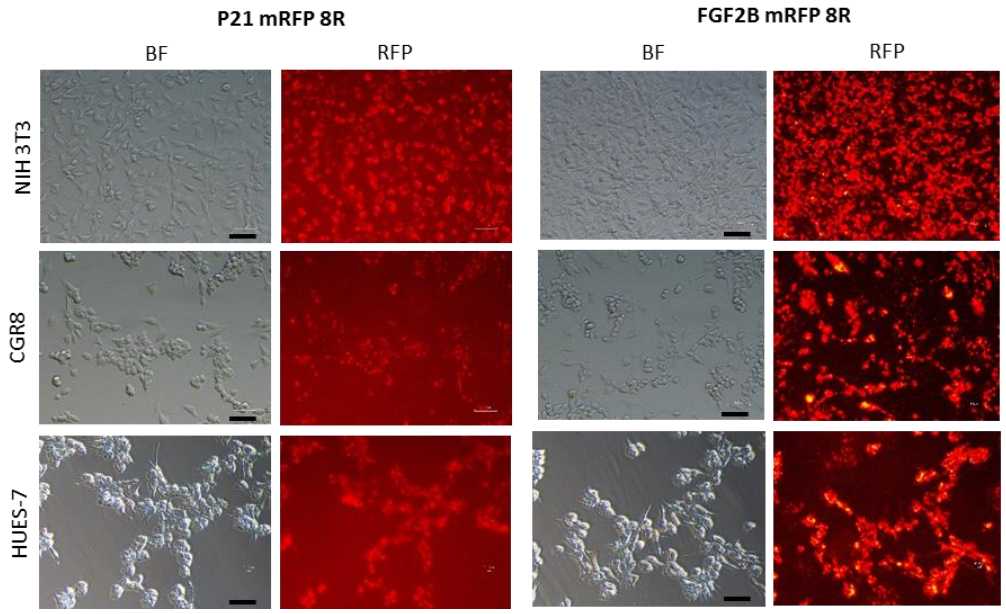


Figure 2.4 Efficient delivery of mRFP to cells via modified CPPs shown to promote GET. Bright field (left) and fluorescence (right) microscopy images of NIH3T3, CGR8 and HUES-7 cells treated with P21 mRFP 8R and FGF2B mRFP 8R peptides (20 µg/mL, 20 h). Following treatment cells were washed twice in PBS to remove background fluorescence and imaged live. Scale bar, 100 µm.

2.4.2 GET-mediated cell type specific targeting of the pre-hemangioblast cell

In this study, the variable region of the HS4C3 antibody was conjugated to 8R to demonstrate GET-facilitated targeting and delivery to a subpopulation of cells during mesodermal differentiation. Baldwin *et al* reported that an antibody (HS4C3) could be used to target a developmentally regulated HS-epitope expressed by the pre-hemangioblast cell (Baldwin et al., 2008). The HS4C3 antibody strongly binds 3-O-sulfated oligosaccharides and weakly binds to N-, 2-O-, and 6-O- sulfated oligosaccharides (ten Dam et al., 2006). During the differentiation process 3-O-sulfotransferases are upregulated which can lead to changes in cell surface epitope presentation. Therefore HS4C3 antibody highly labelled cells are likely to represent a subpopulation that exhibit increased 3-O-sulfation epitopes (Baldwin et al., 2008). A hemangioblast cell is defined as a cell type that is positive for Brachyury (Bry) and Tyrosine Kinase Receptor (FLK-1). The majority FLK-1 positive cells appeared to arise from the Bry positive/HS4C3 high population of cells. Furthermore, Bry positive/HS4C3 high precedes FKL-1, therefore the HS4C3 antibody acts as a novel target for pre-hemangioblast cells with maximal hemangioblast potential during mesodermal differentiation.

Bry-GFP murine embryonic stem cells express GFP when they are Bry positive. These cells were differentiated down a mesodermal lineage for 2.8 days and then treated with truncated HS4C3 peptides that were conjugated to mRFP to allow quantification of highly ($HS4C3^{HIGH}$) and lowly ($HS4C3^{LOW}$) labelled cells by

flow cytometry. A subpopulation of cells (~22%) were Bry positive and showed HS4C3^{HIGH} expression following differentiation vs. Bry negative cells (undifferentiated Bry-GFP cells) that showed HS4C3^{LOW} expression (Figure 2.5) (Baldwin et al., 2008). These results were in agreement with those obtained by Baldwin *et al*, indicating that the conformation of the HS4C3 antibody remained functional when it was shortened to include just the variable region and expressed recombinantly (protein sequences shown in Appendix Table 6.2). The truncated antibody was then conjugated to 8R and cells were treated with the peptide following a 2.8 day differentiation. The HS4C3 mRFP 8R protein did not show any specificity towards Bry positive cells (Figure 2.5). This could be due to the non-selective membrane interaction of 8R masking the specificity of the antibody binding. Future studies are needed to resolve the loss of specificity observed with the HS4C3 mRFP 8R protein.

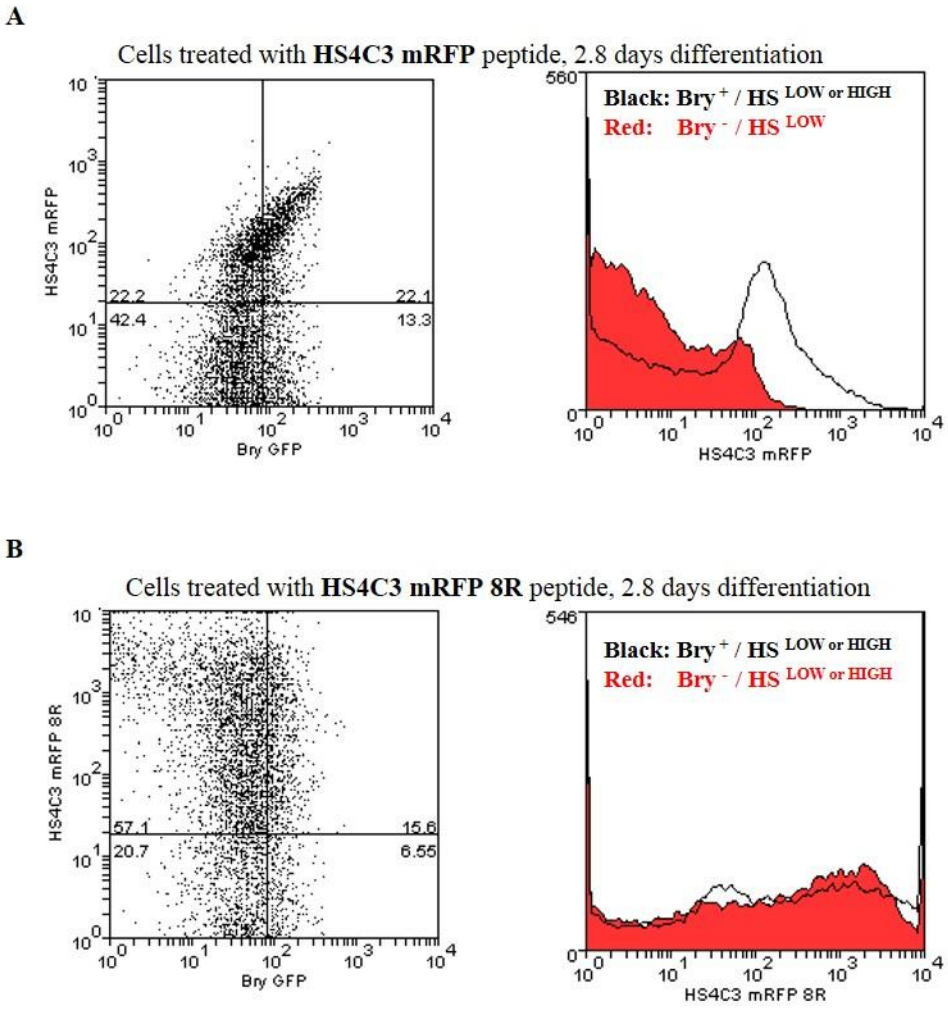


Figure 2.5. Representative flow cytometry profiles of the expression of HS4C3 versus Brachyury (Bry) expression of stem cells following a 2.8 day mesodermal differentiation. Bry-GFP embryonic stem cells were differentiated as EBs for 2.8 days, disaggregated and treated with (A) HS4C3 mRFP or (B) HS4C3 mRFP 8R peptides (50 µg/mL, 3 h). HS4C3 peptides were conjugated to mRFP to allow quantification of highly (HS^{HIGH}) and lowly (HS^{LOW}) labelled cells. Baldwin *et al* defined HS4C3 highly labelled cells as a subpopulation that expressed increased 3-O-sulfation epitopes and HS4C3 lowly labelled as cells in which 3-O-sulfation epitopes were not up-regulated (Baldwin et al., 2008).

2.5 Summary

A panel of CPPs that were modified to include GF derived cell surface HS-GAG binding domains demonstrated 30-100 fold increased delivery to cells, compared to unmodified CPPs. GET-mediated delivery wass due to the dual functionality of the proteins in i) increasing interaction with the cell membrane via the HS-GAG binding domain, and ii) intracellular uptake of proteins into cells via the CPP. The modified CPPs showed preferential delivery profiles of mRFP into the different cell types tested. Furthermore, GET technology overcomes some of the major challenges in efficient uptake into stem cells.

HS4C3, an antibody known to target a HS-epitope during mesodermal differentiation was conjugated to CPP (8R) for cell type specific targeting of the pre-hemangioblast cell. Following conjugation to 8R, antibody specificity was lost. This could be due to the non-specific membrane interaction of the 8R masking the specificity of the antibody. If loss of specificity due to the CPP region could be overcome, these data demonstrates that it may be possible to specifically target and deliver to a desired cell type through fusing HS GAG binding antibodies and CPPs. There are a limited number of specific oligosaccharide sequences that have been identified. To truly exploit HS GAGs for cell type specific targeting, technologies such as phage display must be utilised for screening and identification of target HS-GAG binding sequences (Arap, 2005, Schoonbroodt et al., 2008).

CHAPTER 3 GET peptides for efficient gene transfer

3.1 Introduction

For successful delivery of nucleic acids, CPP-mediated delivery vehicles must be able to form stable complexes with nucleic acids, efficiently deliver them across the cell membrane, protect them from degradation by nucleases, promote their escape from endosomes and facilitate release of the nucleic acid into the cytoplasm or nucleus. In addition, CPP transfection reagents must be able to deliver DNA to the entire cell population, demonstrate high transfection efficiency, transfect a broad cell spectrum, be serum-resistant and cause minimal cytotoxicity. Thus far, the poor delivery efficiency of CPP-based gene carriers have inhibited their clinical application (Karmali and Chaudhuri, 2007).

Due to their ability to deliver cargo into cells much more efficiently than unmodified CPPs, GET technology may provide a powerful tool for the delivery of exogenous genes into cells (Dixon et al., 2016). Amphipathic peptide LK15 was fused to GET moieties P21 or FGF2B and 8R to improve the DNA binding ability of the modified CPP. Santos *et al* reported that fusion of LK15 to TAT significantly improved gene transfer of pDNA into HT29/HT1080 cultured cells by improving the DNA condensation ability of the peptide and increasing delivery of DNA across the cell membrane (Santos et al., 2011). GET transfection peptides (P21 LK15 8R and FGF2B LK15 8R) were designed to include a HS-GAG binding region (P21 or FGF2B), amphipathic region (LK15) and CPP region (8R) for enhanced delivery and transfection (Figure 3.1).

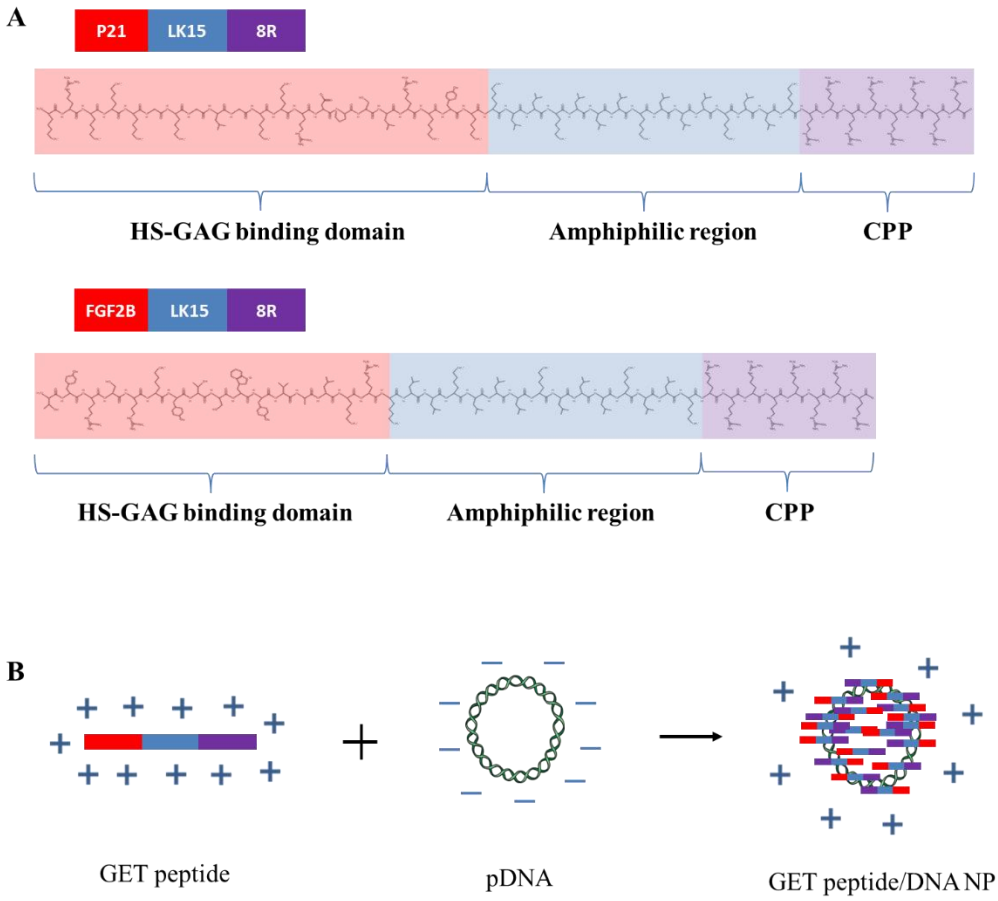


Figure 3.1 Schematic of GET transfection peptides P21 LK15 8R and FGF2B LK15 8R. (A) GET peptide structure. HS GAG binding domain (red), amphiphilic region (blue) and CPP (purple). (B) GET peptide and DNA complex formation. Cationic GET peptides form electrostatic interactions with negatively charged phosphate groups of pDNA to form nanoparticles (NPs).

..

3.2 Aims of the project

1. To optimise the GET-mediated gene transfer of a reporter plasmid for efficient and non-cytotoxic transfection.
2. To compare GET gene carriers to commercially available non-viral transfection reagents.
3. To investigate whether GET peptides can overcome some of the limitations of current non-viral transfection systems such as transfection of multiple plasmids and gene delivery into difficult-to-transfect cell types.

3.3 Materials and methods

3.3.1 Peptide synthesis

Peptides were synthesised by Protein Peptide Research Ltd (PPR) using solid phase tert-Butyloxycarbonyl (t-Boc) chemistry and purified to be >90% (PPR, UK) (Schnolzer et al., 1992). Solid phase synthesis involved repeated cycles of deprotection-wash-coupling. In each cycle the free N-terminal amine of the peptide was coupled to the C-terminal of an N-t-Boc-protected amine. Excess reagent was removed during the washing cycles with the growing peptide chain retained on the solid phase. Peptide sequences are shown in Table 3.1.

Table 3.1 Amino acid sequences of 8R, P21, P21 HA2, P21 8R, LK15, LK15 HA2, P21 LK15, LK15 8R, P21 LK15 8R and FGF2B LK15 8R peptides.

Peptide	Amino acid sequence
8R	RRRRRRRR
P21	KRKKKGKGLGKKRDPCLRKYK
P21 HA2	KRKKKGKGLGKKRDPCLRKYKGDIMGEWGNEIFGAIAGFLG
P21 8R	KRKKKGKGLGKKRDPCLRKYKRRRRRRRR
LK15	KLLKLLLKLLLKLLK
LK15 HA2	KLLKLLLKLLLKLLKGDIMGEWGNEIFGAIAGFLG
P21 LK15	KRKKKGKGLGKKRDPCLRKYKKLLKLLLKLLLKLLK
LK15 8R	KLLKLLLKLLLKLLKRRRRRRRR

P21 LK15 8R	KRKKKGKGLGKKRDPCLRKYKKLLKLLLKLLLK LLKRRRRRRRR
FGF2B LK15 8R	TYRSRKYTSWYVALKRKLLKLLLKLLLKLLKRRR RRRRR

3.3.2 Cell culture

NIH3T3 murine fibroblast cell and CGR-8 mouse embryonic stem cell culture conditions were described in Section 2.3.3. HeLa human cervical cancer cells and MCF-7 human breast adenocarcinoma cells were maintained in DMEM with 10% (v/v) FCS media supplemented with 2 mM L-glutamine and 100 µg/mL streptomycin. HeLa cells and MCF-7 cells were used between passages 45-50 and 33-42, respectively. HUES7fib human fibroblasts derived from HUES7 human embryonic stem cells were maintained in DMEM with 20% (v/v) FCS supplemented with 2 mM L-glutamine and 100 µg/ml streptomycin. HUES7fib cells were used between passages 26-32. Human induced pluripotent stem cells (hiPSCs) (a kind gift from Prof. C. Denning, University of Nottingham, UK; (Dick et al., 2011)) were maintained on Matrigel (Corning, UK) coated flasks with Essential 6 Medium (E6) supplemented with 2 mM L-glutamine and 100 µg/ml streptomycin. HiPSCs were used between passages 12-21. Cells were incubated at 37^0C under humidified 5% CO_2 conditions. All cells were grown in T-75 culture flasks and passaged (with a standard trypsinisation protocol using 0.25% (w/v) trypsin/2 mM EDTA solution) every 2-3 days or when they reached 80% confluency.

3.3.3 Preparation of DNA

Reporter plasmids pSIN GFP and pSIN RFP containing a mammalian promoter elongation factor 1 (EF-1α) were amplified in E. coli (plasmid maps are shown in Appendix Figures 6.1 and 6.2). DNA was extracted and purified using a QIAGEN Plasmid Maxi kit (Qiagen). Bacterial culture was harvested overnight by centrifugation (6000xg, 15 min). The bacterial pellet was resuspended in 10 mL of Buffer P1 (and RNase A solution). 10 mL of Buffer P2 was added, the solution was mixed vigorously by inverting 4-6 times and incubated for 5 min at RT (solution turned blue). 10 mL of Buffer P3 was added, the solution was mixed by inverting 4-6 times, incubated on ice for 20 min (solution turned colourless) and centrifuged (14000xg, 10 min). The QIAGEN tip was equilibrated by running 10 mL Buffer QBT through it. Following centrifugation, the supernatant was applied to the QIAGEN tip and run through the resin by gravity flow. The QIAGEN tip was washed twice with 30 mL Buffer QC. The DNA was eluted into a clean 50 mL vessel using 15 mL Buffer QF. The DNA was precipitated by the addition of 10.5 mL isopropanol and centrigufed (15000xg, 3 min). The supernatant was discarded, the DNA pellet was washed with 5 mL 70% (v/v) ethanol and air-dried for 5-10 min. The DNA was re-dissolved in water (dH_2O) and plasmid purity was confirmed using the NanoDrop 1000 spectrophotometer (ThermoFisher).

3.3.4 DNA complexation assay

The optimal DNA binding ratio of peptide to reporter gene (pSIN GFP) was determined using YO-PRO-1 fluorescence-based assay. 10 µg DNA was diluted

in 60 µL 4-(2-hydroxyethyl)-1-piperazineethanesulfonic acid (HEPES)-buffered saline (10 mM HEPES, 150 mM sodium chloride (NaCl) solution, pH 7.4). 1 mM YO-PRO-1 stock solution was diluted to 0.1 mM in dimethyl sulfoxide (DMSO). 2.7 µL of 0.1 mM YO-PRO-1 solution was made up to 60 µL in HEPES-buffered saline and added dropwise to the diluted DNA. The DNA/YO-PRO-1 solution was mixed, wrapped in foil and incubated for 5 h at RT. Following incubation, the DNA/YO-PRO-1 solution was made up to 1 mL in HEPES-buffered saline and 100 µL aliquots were pipetted into Eppendorf tubes per treatment condition. Peptide amounts corresponding to the desired (+/-) charge ratios (CRs) were added to each Eppendorf. Peptide/DNA/YO-PRO-1 solutions were mixed and incubated at RT for 10 min. Fluorescence measurements were analysed using the TECAN infinite 200PRO multimode reader. Similarly, a no DNA control was made by diluting 2.7 µL of the diluted YO-PRO-1 solution in 120 µL HEPES-buffered saline and following the procedure above.

Table 3.2 GET peptide/DNA CRs. GET peptide was added to 1 µg of DNA at increasing (+/-) CRs.

Peptide/DNA (+/-) CR	Concentration of peptide (µM)	Volume of peptide (µL)
1:5	0.49	0.05
1:3	0.82	0.07
1:2	1.23	0.12
1:1	2.47	0.24
2:1	4.94	0.49
3:1	7.41	0.74

5:1	12.35	1.23
10:1	24.7	2.46

3.3.5 Characterisation of GET peptide/DNA complexes

Hydrodynamic diameter and PDI of P21 LK15 8R/pSIN GFP and FGF2B LK15 8R/pSIN GFP NPs were determined in water by dynamic light scattering (DLS) and assessed in disposable low volume cuvettes. Zeta-potentials were measured in 10 mM NaCl at pH 7.0 by laser Doppler anemometry. Measurements of hydrodynamic size and zeta-potential were performed at RT using Zetasizer Nano ZS90 apparatus (Malvern Instruments), for each sample 3 measurements were taken and each measurement was set to 10 runs.

3.3.6 Cellular uptake assay

NIH3T3 cells were treated with fluorescently-labelled oligonucleotide to investigate cellular uptake. Fluorescein amidite (FAM)-hActin (TTT TTG GTC GCA ATG GAA GAA G) and hActin-comp (CTT CTT CCA TTG CGA CCA AAA A) were designed and purchased from Eurofins (Eurofins, UK). A 10 µM mix of both oligonucleotides in water (dH_2O) was heated to 100°C on a heat block and cooled to RT over an hour to form double stranded FAM-labelled oligonucleotide.

Cells were seeded at 4 x 10^4 cells/well on a 24 well plate and incubated overnight in 500 µL GM. 1 µg FAM-labelled oligo was diluted in 25 µL Opti-MEM. P21 LK15 8R or FGF2B LK15 8R was added to 25 µL Opti-MEM and mixed with

diluted oligo at different CRs. The peptide/oligo solution was mixed and incubated for 20 min at RT. The wells were aspirated and replaced with 200 µL GM. Each well of cells was treated with 50 µL peptide/oligo complex (1 µg DNA/well) and incubated for 2 h at 37^0C under humidified 5% CO_2 conditions.

3.3.7 Endocytosis inhibitors assay

To investigate the mechanism of uptake, NIH3T3 cells were treated with FAM-labelled DNA in the presence of endocytosis inhibitors methyl-β-cyclodextrin (0-10 mM) an inhibitor for calveolae independant endocytosis or amiloride (0-5 mM) an inhibitor of Na+/H+ exchange required for macropinocytosis. Experimental conditions, including effective concentrations and treatment times of the endocytosis inhibitors, were previously validated when assessing the mechanism of internalisation of GET peptides using a Cre assay system (Dixon et al., 2016). It has previously been reported that the treatment of NIH3T3 cells with methyl- β-cyclodextrin (0-5 mM) or amiloride (0-5 mM) did not negatively affect cell viability (Wadia et al., 2004).

Cells were seeded at 4 x 10^4 cells/well on 24 well plates and incubated overnight in 500 µL of GM. For each well of cells to be treated, 1 µg FAM-labelled DNA was diluted in 25 µL Opti-MEM and mixed. The peptide in 25 µL Opti-MEM was added to the diluted DNA. The solution was mixed and incubated for 20 min at RT. The wells were aspirated and replaced with 200 µL GM containing the endocytosis inhibitor. The cells were pre-treated with the endocytosis inhibitor for 15 min prior to addition of GET peptide/FAM-labelled DNA NPs. Following pre-treatment, cells were treated with GET peptide/FAM-labelled

DNA NPs in the presence of the endocytosis inhibitor for 2 h at 37^0C under humidified 5% CO_2 conditions.

3.3.8 *In vitro* transfection

NIH3T3 cells were seeded at 8 x 10^4 cells/well on 12 well plates and incubated overnight in 1 mL of GM. For each well of cells to be transfected, DNA (pSIN GFP) was diluted in 50 µL Opti-MEM and mixed. Peptide in 50 µL Opti-MEM was added to the diluted DNA at the optimal CR. The solution was mixed and incubated for 20 min at RT. The cells were aspirated, washed with PBS and replaced with 400 µL transfection media (Opti-MEM, Opti-MEM + 10% FCS or GM). Each well of cells was treated with 100 µL of peptide/DNA complex solution and incubated. Following treatment, cells were incubated for 24 h at 37^0C under humidified 5% CO_2 conditions.

For serial transfection experiments, NIH3T3 cells were transfected with 1 µg pSIN GFP every day for 3 days. NIH3T3 cells were seeded at 4 x 10^4 cells per well on 24 well plates and incubated overnight in 500 µL of GM. For each well of cells to be transfected, 1 µg DNA was diluted in 25 µL Opti-MEM and mixed. Peptide in 25 µL Opti-MEM was added to the diluted DNA. The solution was mixed and incubated for 20 min at RT. The wells were aspirated and replaced with 200 µL GM. Each well of cells was treated with 50 µL of peptide/DNA complex solution and incubated for 24 h at 37^0C under humidified 5% CO_2 conditions. Cells were treated at 24 h (Day 1), 48 h (Day 2) and 72 h (Day 3) time points. Transfection efficiency, cell viability (PrestoBlue assay, Section

3.3.8) and total cell number were measured every 24 h post transfection for three days.

Next, the performance of GET transfection peptides was tested against leading commercial transfection reagents. GET peptides, P21 LK15 8R and FGF2B LK15 8R were compared to Lipofectamine 2000 (Life Technologies), Lipofectamine 3000 (Life Technologies), JetPEI (Polyplus-transfection), TransIT-LT1 (Mirus Bio) and FuGENE HD (Promega) in terms of transfection efficiency and toxicity (PrestoBlue assay described in Section 3.3.8) To fairly compare the different transfection systems, each reagent was used to transfect 1 µg pSIN GFP according to their manufacturers guide. NIH3T3 cells were seeded at 4 x 10^4 cells/well on 24 well plates and incubated overnight in 500 µL GM. Each well of cells to be transfected was aspirated, washed with PBS and replaced with 200 µL GM. Cells were treated with 50 µL of transfection reagent/DNA complex solution and incubated for 24 h at 37^0C under humidified 5% CO_2 conditions. For Lipofectamine 2000, 1 µg DNA was diluted in 25 µL Opti-MEM. 1.5 µL Lipofectamine 2000 was diluted in 25 µL Opti-MEM and added to the diluted DNA. The solution was mixed and incubated for 20 min at RT. For Lipofectamine 3000, 1 µg DNA and 2 µL P3000 reagent were diluted in 25 µL Opti-MEM. 1.5 µL of Lipofectamine 3000 was diluted in 25 µL Opti-MEM and added to the diluted DNA. The solution was mixed and incubated for 20 min at RT. For JetPEI, 1 µg DNA was diluted in 25 µL 150 mM NaCl solution. 2 µL of JetPEI was diluted in 25 µL 150 mM NaCl solution and added to the diluted DNA. The solution was mixed and incubated for 20 min at RT. For TransIT-LT1, 1 µg DNA was diluted in 25 µL Opti-MEM. 3 µL of TransIT-LT1 was

diluted in 25 µL Opti-MEM and added to the diluted DNA. The solution was mixed and incubated for 20 min at RT.

3.3.9 Cell viability assay

Cell viability was assessed using Trypan Blue (Life Technologies) or PrestoBlue (Invitrogen) cell viability assays. For Trypan Blue, cells were trypsinised (with a standard trypsinisation protocol using 0.25% (w/v) trypsin/2 mM EDTA solution) and resuspended in PBS. 6 µL cell suspension was mixed with 6 µL Trypan Blue and transferred to a haemocytometer. The cells were counted in triplicate, and the ratio of stained to unstained cells were expressed as a percentage of viable cells. Cells were counted at 24 h (Day 1), 48 h (Day 2) and 72 h (Day 3) post transfection. The total cell number at each time point was used to plot growth curves.

For PrestoBlue, 10X solution of PrestoBlue reagent was diluted to a 1X solution in Hanks' balanced salt solution (HBSS). Cells cultured on 24 well plates were aspirated and washed with PBS. 250 µL 1X PrestoBlue reagent solution was added to each well, the plate was covered in foil (PrestoBlue assay is light sensitive) and incubated at 37°C for 15 min. Following incubation, 100 µL of PrestoBlue solution was transferred to a black 96 well plate. Fluorescence intensity was measured in duplicate using a TECAN infinite 200PRO multimode reader at excitation/emission 560 nm/590 nm. Relative fluorescence units (RFU) values of treated cells were divided by the fluorescence values of untreated cells for percentage cell viability.

3.3.10 Endosomal escape reagents

NIH3T3 cells were treated with endosomal escape reagents chloroquine and HA2 peptides to investigate endosomal entrapment of P21 LK15 8R/DNA complexes following internalisation. Cells were seeded at 4 x 10^4 cells per well on 24 well plates and incubated overnight in 500 µL GM. For each well of cells to be transfected, 5 µg DNA was diluted in 25 µL Opti-MEM and mixed. Peptide in 25 µL Opti-MEM was added to the diluted DNA at CR2. The solution was mixed and incubated for 20 min at RT. The wells were aspirated and replaced with 200 µL GM. Cells were pre-treated for 1 h with 100 µM chloroquine or 4.5 uL of 1 mM P21 HA2 or LK15 HA2. Following pre-treatment, each well of cells was treated with 50 µL of peptide/DNA complex solution in the presence of the endosomal escape reagent and incubated at 37^0C under humidified 5% CO_2 conditions for 4 h.

3.3.11 Flow cytometry analysis

The CPPs were transfected with a reporter gene (GFP and/or RFP). Following treatment, cells were treated with 25% (w/v) trypsin/2 mM EDTA and fixed in 3.7% (w/v) paraformaldehyde (PFA) in preparation for flow cytometry. GFP and/or RFP positive cells were analysed on a Beckman Coulter FC500 flow cytometer using a blue 488 nm and/or green 561 nm co-linear laser, respectively (40,000 cells; gated on live cells by forward/side scatter). Transfection efficiency was determined by the percentage of cells expressing GFP. For the uptake studies, FAM-labelled cells were analysed on a Beckman Coulter Astrios EQ Cell Sorter using a 488 nm blue laser (40,000 cells; gated on live cells by

forward/side scatter). Positive cells were gated using negative controls and/or mean fluorescence intensity was used for statistical analysis. Data was analysed on flow cytometry analysis software (WEASEL).

3.3.12 Microscopy

For uptake studies, cells were treated with FAM-labelled DNA as described in Section 3.3.6, stained with Hoechst (Thermofisher) nuclear counterstain 1 mg/mL in water (dH2O) for 10 min and imaged live. For transfection experiments, cells were transfected with GFP reporter gene as described in Section 3.3.8 and imaged live. FAM, Hoechst (Thermofisher) and GFP fluorescence expression were visualised on an inverted Nikon Eclipse microscope TS100 (default settings were used to image the samples and exposure was set based on control samples). Hoechst was excited using a violet (405 nm) laser. FAM and GFP expression was captured using blue (488 nm) laser. Image J software was used to view and add scale bars to the images.

3.3.13 Statistical analysis

Mean and SD were compiled from three individual experiments (n=3). The number of experiments (n) refers to experiments carried out on cells at different numbers of cell culture passages. Data was analysed by Prism statistical analysis software (GraphPad) and compared by one-way analysis of variance (ANOVA) with Bonferroni's multiple comparison test for post-hoc analysis. For the cell viability experiments, each treatment group was compared with control (untreated) by ANOVA with Dunnett’s test.

3.4 Results and discussion

3.4.1 GET peptide/DNA NP formation

Cationic CPPs can form NPs when mixed with DNA due to the electrostatic interactions of the peptide with the negatively charged phosphate groups of the nucleic acid (de Figueiredo et al., 2014). A fluorescence-based competition assay (YO-PRO-1) was used to investigate the DNA condensation ability of the peptides (Marie et al., 1996). YO-PRO-1 is a cyanine dye that binds DNA to form a fluorescent DNA/dye complex. GET peptides, P21 LK15 8R and FGF2B LK15 8R, were added to the fluorescent DNA/dye complex at increasing CRs (Petty et al., 2000). As the peptide out competed the dye by binding the DNA a reduction in fluorescence intensity was observed. A graph of CR was plotted against fluorescence to investigate the optimum CR of peptide to DNA (Figure 3.2). P21 LK15 8R and FGF2B LK15 8R complexed ~97% of the gene at a peptide to DNA ratio of CR2. The LK15 domain improved the DNA condensation ability of the peptides, the 8R peptide lacking the LK15 region was only able to bind ~85% of the DNA compared to LK15 8R, P21 LK15 8R and FGF2B LK15 8R peptides (~97%).

The physiochemical properties of GET peptide/DNA NPs were investigated through hydrodynamic size and zeta potential measurements. Both GET peptides were able to form positively charged, small and stable NPs of < 100 nm (Table 3.3). The polydispersity index (PDI) of P21 LK15 8R/DNA NPs and FGF2B LK15 8R/DNA NPs was 0.2, which indicated relatively uniform size distribution of the complexes and a lack of large aggregates or sedimentation.

Table 3.3 Characterisation of GET peptide/DNA NP hydrodynamic size, polydispersity index and zeta potential.

Peptide	Z-average (d.nm)	Polydispersity index (PDI)	ζ-potential (mV)
P21 LK15 8R	97.3	0.2	24.5
FGF2B LK15 8R	76.3	0.2	20.3

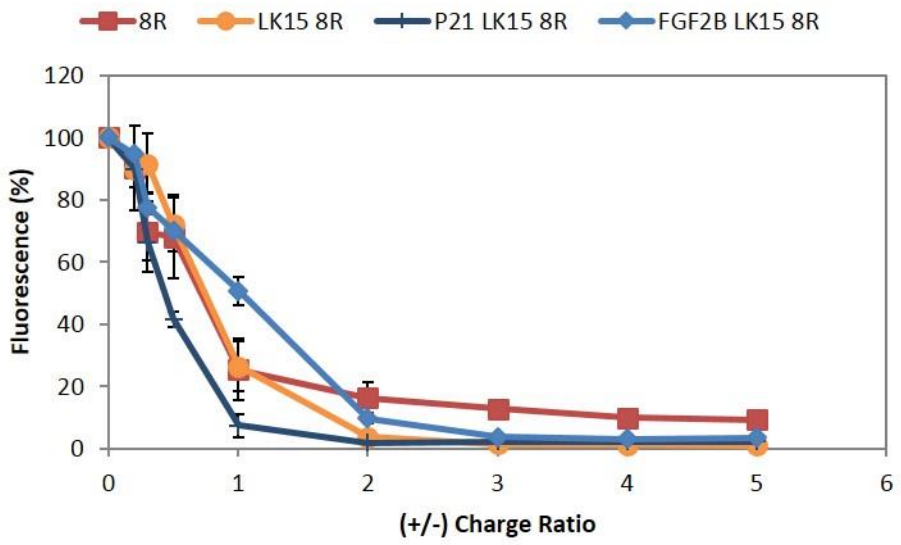


Figure 3.2 GET peptides efficiently bind DNA. Optimization of (+/-) charge ratio of 8R, LK15 8R, P21 LK15 8R and FGF2B LK15 8R to pSIN GFP. The graph shows a decrease in the percentage fluorescence as peptide binds DNA. Error bars indicate SD, n = 3.

3.4.2 DNA delivery

Following successful formation of GET peptide/DNA NPs, the ability of GET peptides to transport DNA into cells was investigated. P21 LK15 8R or FGF2B LK15 8R peptides were complexed with FAM-labelled DNA at CR2, CR3, CR4 and CR5. Cells were treated with the complexes for 4 h, trypsinised to remove any extracellularly bound DNA and fluorescence intensity was measured using flow cytometry (Richard et al., 2003). DNA alone was not able to enter the cells, highlighting the need for an effective gene carrier. Efficient DNA delivery was observed in cells treated with P21 LK15 8R/DNA NPs or FGF2B LK15 8R/DNA NPs at all tested CRs (Figure 3.3). These data showed that GET peptides efficiently delivered DNA to the entire cell population, however efficient uptake does not always correlate with bioavailability. The localisation of DNA appeared to be punctate in the cytoplasm of the cells, which is indicative of endosomal entrapment (Figure 3.3) (Bareford and Swaan, 2007).

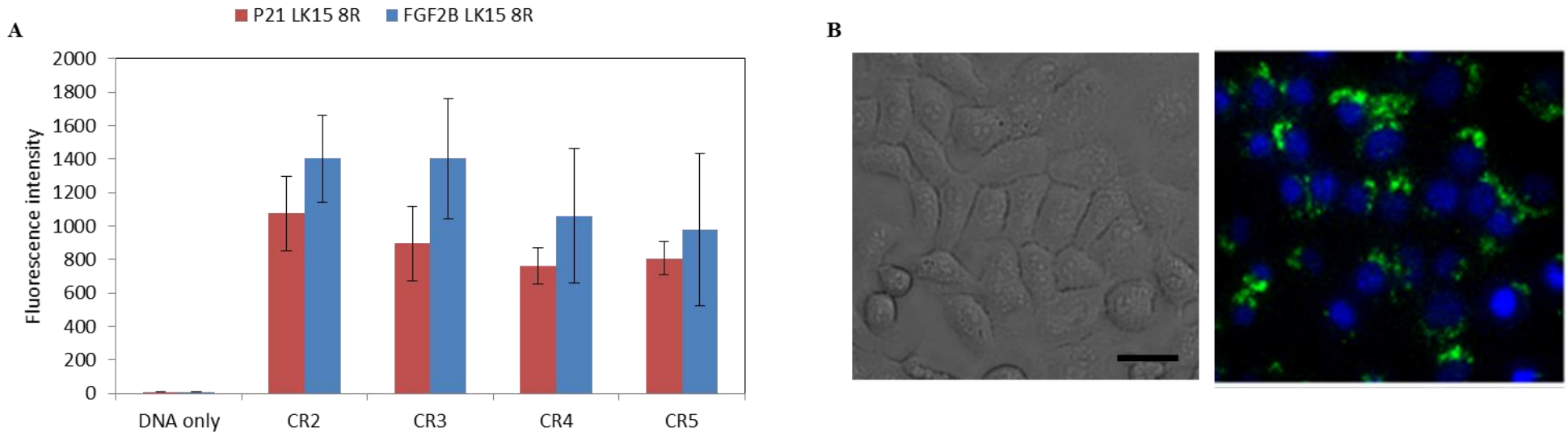


Figure 3.3 GET peptide/DNA complexes are efficiently taken up by cells. (A) Uptake of GET peptide/FAM-labelled DNA complexes in NIH3T3 cells at CR2, CR3, CR4 and CR5. Cells were treated with P21 LK15 8R/FAM-labelled DNA NPs or FGF2B LK15 8R/FAM-labelled DNA NPs for 2 h and fluorescence intensity was determined by flow cytometry. (B) Brightfield (left) and fluorescence (right) microscopy images showing cells following 2 h incubation with P21 LK15 8R/FAM-labelled DNA/ NPs at CR3. FAM-labelled DNA (green). Cell nuclei stained with Hoechst (blue). Scale bar, 15 µm. Error bars indicate SD, n = 3.

3.4.3 NPs are taken up by macropinocytosis

The mechanism of uptake of GET peptide/DNA NPs was investigated in the presence of endocytosis inhibitors. It is important to mention that there is no one conclusive method for assessing internalisation. The drawbacks of this quantification method include that the inhibitors may not be fully specific and that by shutting down one pathway this may stimulate a different mechanism of uptake that is normally inactive (Vercauteren et al., 2010, Madani et al., 2011). We have previously determined that the cellular uptake of GET-proteins occurred via macropinocytosis through employing a Cre assay system in the presence of endocytosis inhibitors (Dixon et al., 2016). This was in agreement with recent findings suggesting that internalisation of arginine-rich CPPs is primarily by macropinocytosis rather than other endocytic pathways (Futaki et al., 2007).

In order to investigate the pathway of internalisation, NIH3T3 cells were treated with P21 LK15 8R/FAM-labelled DNA complexes in the presence of methyl-β-cyclodextrin an inhibitor for calveolae independent endocytosis and amiloride an inhibitor of Na+/H+ exchange required for macropinocytosis. Treatment with methyl-β-cyclodextrin resulted in dose-dependent inhibition of DNA delivery, demonstrating that GET peptide/DNA uptake requires calveolae independent endocytosis (Figure 3.4). Macropinocytosis is a clathrin- and caveolae independent pathway of endocytosis (Doherty and McMahon, 2009). To confirm that macropinocytosis was the endocytotic pathway of uptake, cells were treated with amiloride (Koivusalo et al., 2010). At increasing doses of amiloride

treatment a reduction of DNA uptake was observed, confirming that GET peptide/DNA NPs were taken up by macropinocytosis (Figure 3.4).

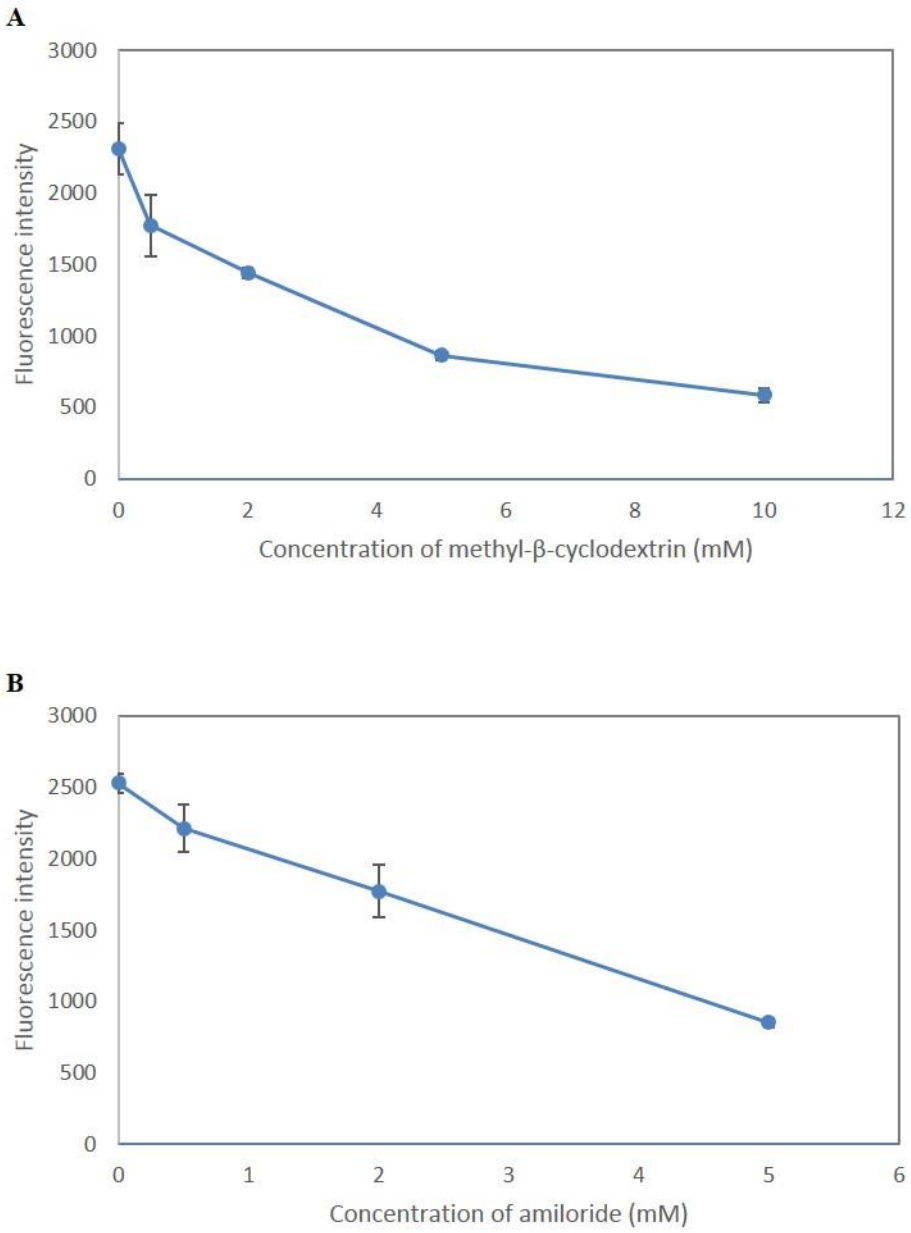


Figure 3.4 Uptake of GET peptide/DNA NPs is inhibited in the presence of endocytosis inhibitors. NIH3T3 cells were treated with P21 LK15 8R/FAM-labelled DNA complexes in the presence of (A) methyl-β-cyclodextrin (0-10 mM) an inhibitor for calveolae independant endocytosis and (B) amiloride (0-5 mM) an inhibitor of Na+/H+ exchange required for macropinocytosis to investigate the mechanism of internalisation. Error bars indicate SD, n = 3.

3.4.4 Serum-resistant transfection

The transfection efficiency of P21 LK15 8R and its components were compared in NIH3T3 cells via transfection of reporter gene pSIN GFP. Cells were fixed 24 h post treatment to allow time for the transient expression of GFP to be captured and percentage of transfected cells to be quantified by flow cytometry (Figure 3.5). The P21 LK15 8R peptide, that combined all three functional segments, exhibited two-fold higher transfection efficiency than the unmodified CPP (LK15 8R) (Figure 3.6). Peptide vectors without the LK15 component were the least efficient.

Next, P21 LK15 8R-mediated transfection of the GFP reporter gene was optimised in terms of transfection media, amount of DNA and transfection time (Figure 3.7). Interestingly, the optimal transfection conditions for P21 LK15 8R were observed when cells were transfected for 24 h in serum conditions (Figure 3.7). This could be due to an up regulation of the intracellular trafficking of complexes/NPs in the presence of serum (Wu et al., 2011). The majority of cationic gene carries, including commercial transfection systems such as Lipofectamine 2000, have demonstrated steep decreases in transfection efficiency in serum containing media (Mao et al., 2010). This is believed to be because serum molecules competitively bind the gene carrier, therefore outcompeting binding of the DNA and/or causing aggregation of gene carrier/DNA NPs. There are several disadvantages to carrying out transfections in serum free conditions including increased cytotoxicity and that gene carriers are limited to *in vitro* applications (*in vivo* transfections are carried out in the presence of serum/biological fluid) (Gollapudi and Oblinger, 1999).

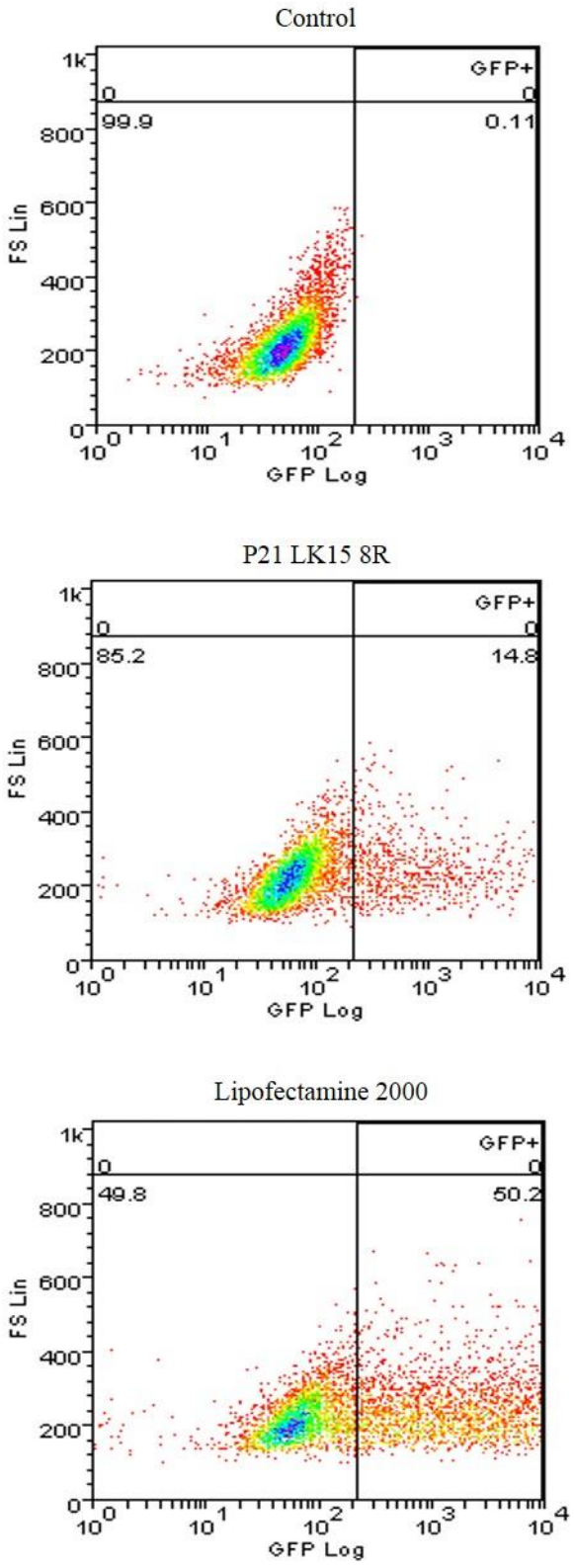


Figure 3.5 Representative flow cytometry dot plots showing GFP expression of NIH3T3 cells following transfection with 1 µg pSIN GFP for 6 h. Following transfection, cells were fixed at a 24 h time point. Flow cytometry analysis was used to quantify the percentage of GFP positive cells.

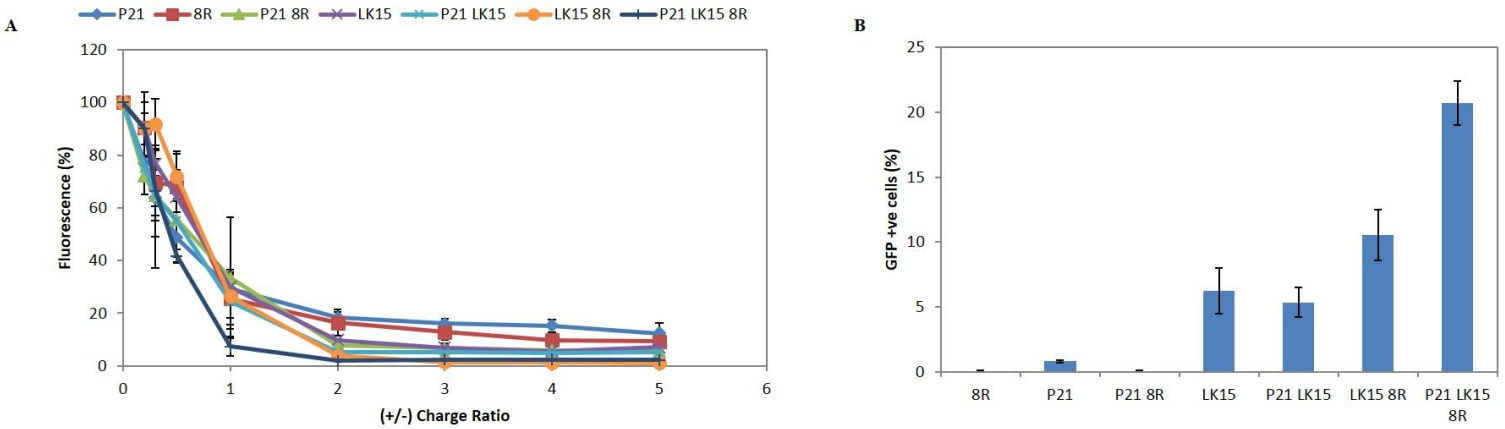


Figure 3.6 Transfection of 1 µg pSIN GFP via P21 LK15 8R and its component peptides in NIH3T3 cells for 24 h. (A) YO-PRO-1 assay was used to demonstrate the DNA condensation ability of peptides at different CRs. (B) Transfection efficiency of 8R, P21, LK15, P21 LK15, LK15 8R and P21 LK15 8R peptides.. Flow cytometry analysis was used to quantify the percentage of GFP positive cells. Error bars indicate SD, n = 3.

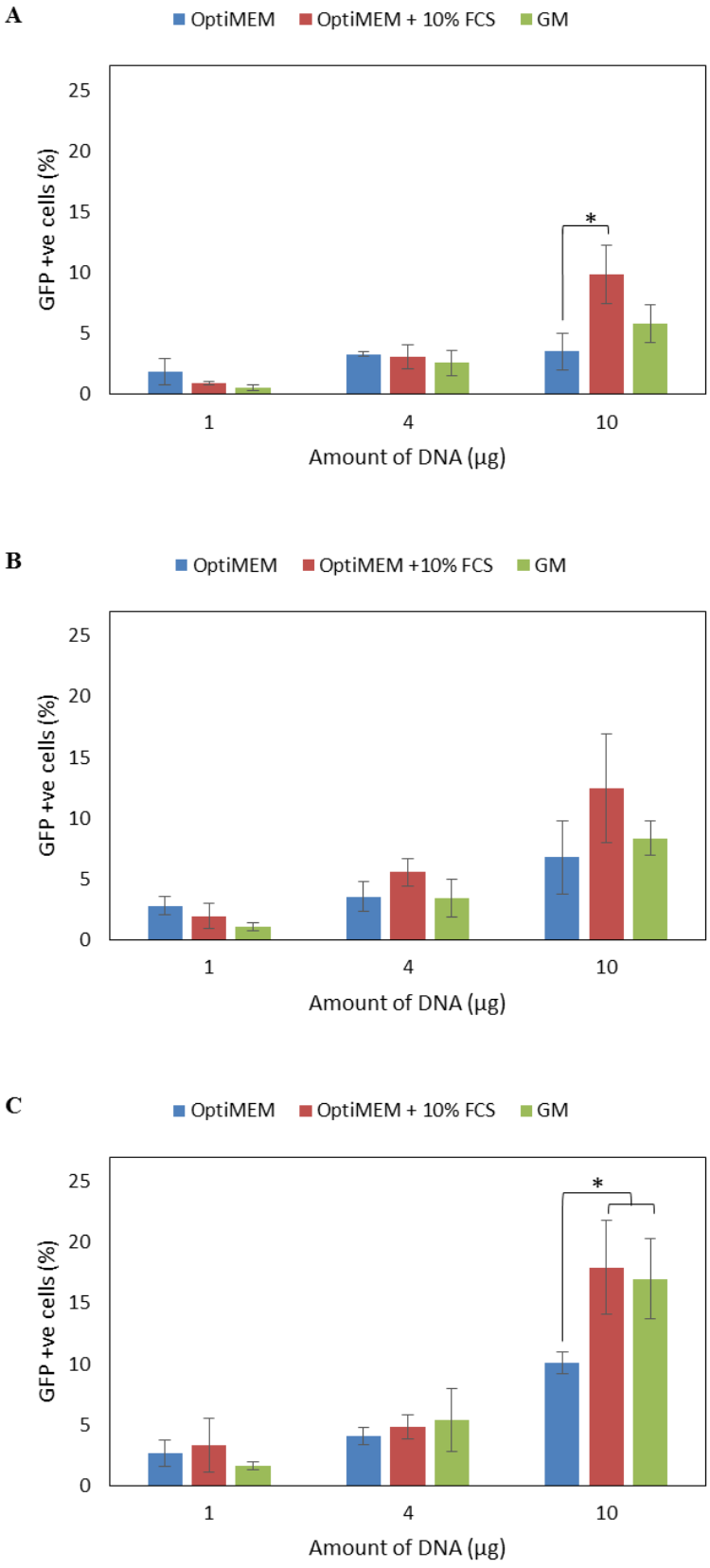


Figure 3.7 Optimisation of the transfection of pSIN GFP in NIH3T3 cells by P21 LK15 8R peptide at CR2. Transfections were carried out in OptiMEM, OptiMEM + 10% FCS and GM. Cells were transfected for (A) 3 h, (B) 6 h and (C) 24 h. Following transfection, cells were fixed at a 24 h time point. Error bars indicate SD, n = 3. One-way ANOVA with Bonferroni's post-tests; *P < 0.05, **P < 0.01.

3.4.5 Endosomal escape

Due to the endocytic mechanism of uptake, peptide/genetic cargo can remain trapped in endosomes following intracellular uptake. CPP-based transfection reagents can be coupled to endosomal escape reagents to facilitate release of DNA from endosomes prior to their degradation in late endosomes/lysosomes (Foerg and Merkle, 2008). The most widely used endosomal escape strategy is co-treatment with chloroquine, a detergent-based chemical that disrupt endosomes by preventing their acidification (Ciftci and Levy, 2001). More recent studies have found that some peptides have endosome disruptive properties that have led to their exploitation as endosomal escape reagents. One such example is the influenza virus derived endosomal escape peptide hemagglutinin protein (HA2) (Wadia et al., 2004). HA2 peptide is a pH-sensitive fusogenic peptide that was reported to increase TAT-Cre recombination, with no reported cytotoxicity.

The effect of incorporating an endosomal escape strategy with P21 LK15 8R was investigated. NIH3T3 cells were co-treated with GET peptide/DNA complexes and chloroquine or HA2. Wadia *et al* found that HA2 alone had little to no effect unless it was fused to delivery peptide TAT (Wadia et al., 2004). Therefore, in this study HA2 was conjugated to P21 or LK15 to facilitate its uptake and co-localisation in the endosome. The co-treatment of cells with the endosomal escape reagents improved transfection efficiency by ~2-20%, however transfection was only significantly improved when cells were treated with 100 μM chloroquine (Figure 3.8). Despite demonstrating only limited enhancement of transfection, these results show that there is potential for the

GET system to be further optimised by the incorporation of an endosomal escape strategy.

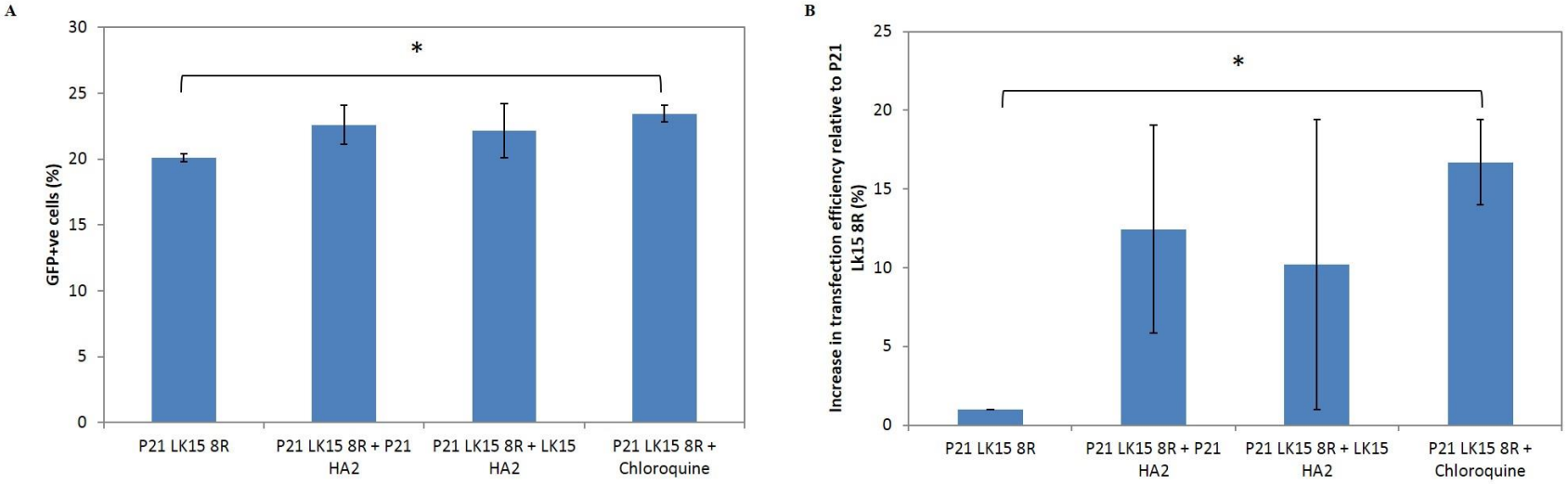


Figure 3.8 Endosomal escape reagents improve transfection of P21 LK15 8R. NIH3T3 cells were co-treated with P21 LK15 8R/FAM-labelled DNA NPs and 18 µM P21 HA2, 18 µM LK15 HA2 or 100 µM chloroquine for 24 h. Graphs of (A) transfection efficiency and (B) fold increase in transfection. Error bars indicate SD, n = 3. One-way ANOVA with Bonferroni's post-tests; *P < 0.05, **P < 0.01.

3.4.6 Optimal CR for transfection – adding excess peptide improves transfection efficiency

The optimal CR of GET peptide to DNA for DNA binding was determined using the YO-PRO-1 assay (Section 3.4.1). The membrane active residues of the peptide can be inhibited through their interaction with DNA therefore the effect of varying CR on transfection efficiency was investigated. To determine the optimal CR for transfection, cells were treated with GET peptide/DNA complexes at CR1, CR2, CR3, CR4 and CR5. Transfection efficiency was enhanced at higher CRs where more cationic GET peptide component was present in the NPs (Figure 3.9). Excess cationic gene carriers can be associated with increased cytotoxicity (Lv et al., 2006). However, by using a slight excess of GET peptide, superior transfection performance could be achieved. The improved transfection efficiency at higher CR facilitated transfection of even very low DNA amounts (100 ng), reducing the reagent/DNA dose required for efficient transfection and potentially minimising any toxicity risks (Appendix Figure 6.3).

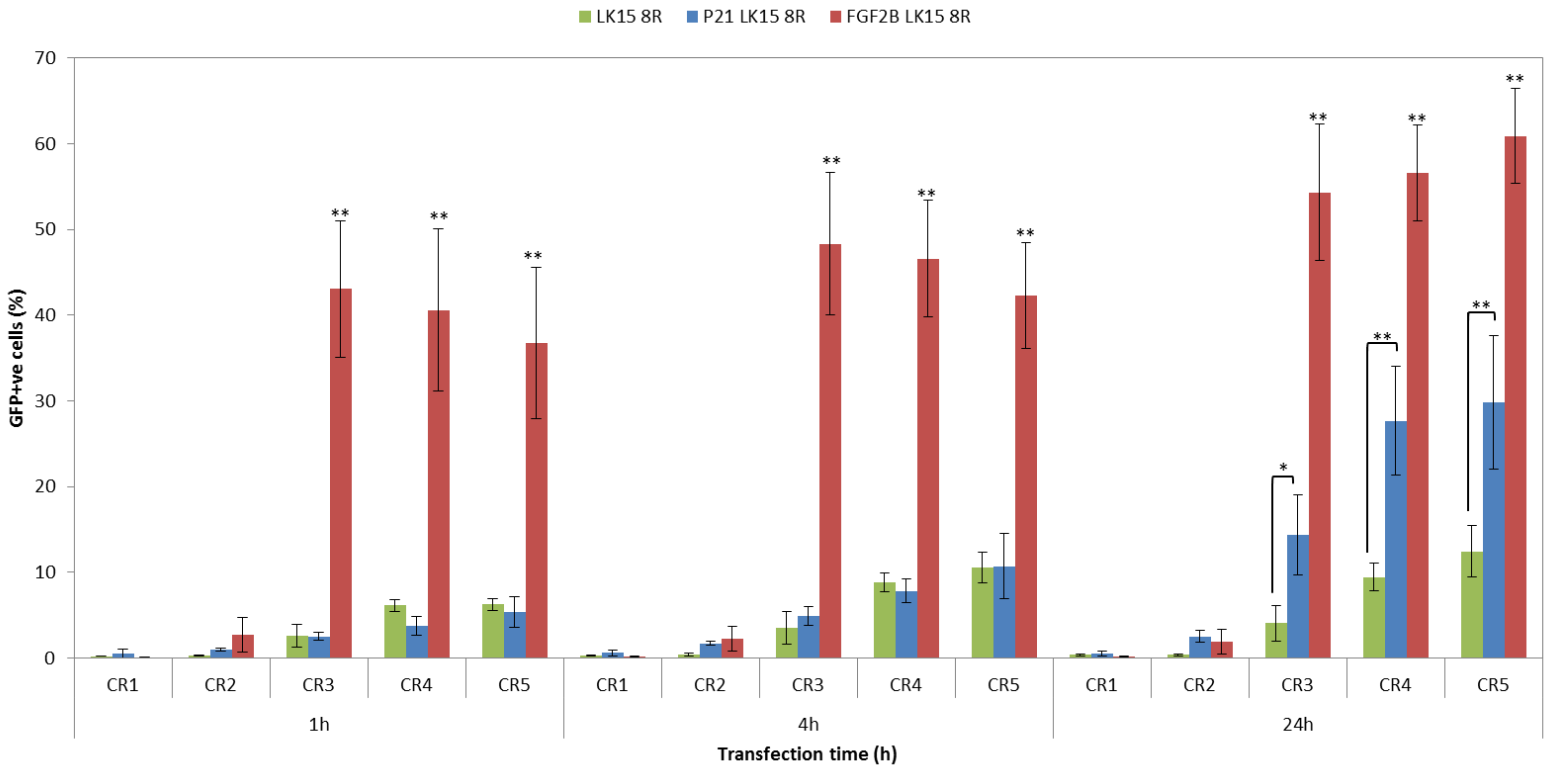


Figure 3.9 Optimisation of CR for efficient GET-mediated transfection. Transfection of 1 µg pSIN GFP in NIH3T3 cells by LK15 8R, P21 LK15 8R and FGF2B LK15 8R peptides at CR1, CR2, CR3, CR4 and CR5. Cells were transfected for 1 h, 4 h and 24 h. Following transfection, cells were fixed at 24 h time point. Error bars indicate SD, n = 3. One-way ANOVA with Bonferroni's post-tests; *P < 0.05, **P < 0.01.

3.4.7 GET vs. commercial transfection reagents

In this study, GET transfection peptides, P21 LK15 8R and FGF2B LK15 8R, were compared to a variety of leading commercial transfection reagents Lipofectamine 2000, Lipofectamine 3000, JetPEI, TransIT-LT1 and FuGENE HD. The transfection of GET peptides and commercial transfection reagents were compared in terms of efficiency and cytotoxicity (Figure 3.10). The majority of the tested transfection reagents demonstrated comparable transfection efficiency, with TransIT LT1 demonstrating the lowest efficiency. PrestoBlue assay was used to measure toxicity of gene carriers. NIH3T3 cells treated with P21 LK15 8R, Lipofectamine 2000 and JetPEI exhibited reduced viability compared to control. FGF2B LK15 8R outperformed the majority 'gold standard' transfection reagents by demonstrating both high transfection efficiency and minimal cytotoxicity (Figure 3.10).

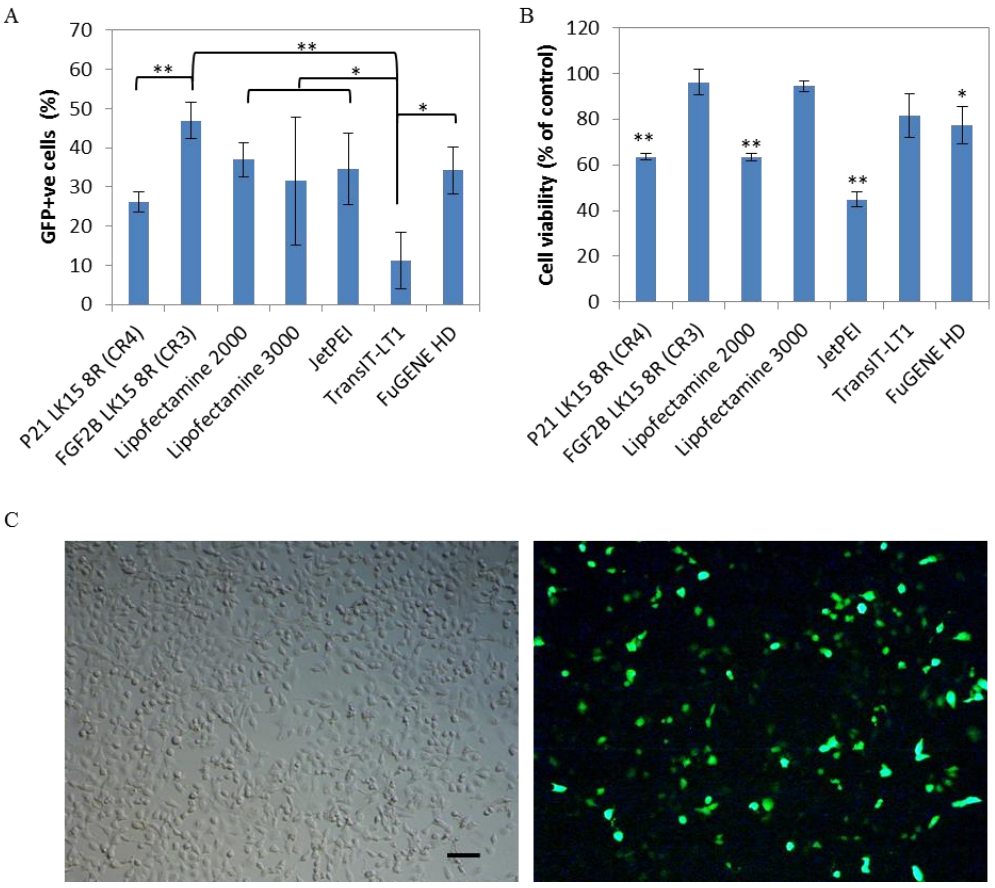


Figure 3.10 Transfection of GET peptides vs. commercial transfection reagents. NIH3T3 cells were transfected with 1 µg pSIN GFP. GET peptides P21 LK15 8R and FGF2B LK15 8R were compared to leading transfection reagents Lipofectamine 2000, Lipofectamine 3000, JetPEI, TransIT-LT1 and FuGENE HD in terms of (A) transfection efficiency and (B) cell viability (PrestoBlue assay). (C) Bright field (left) and fluorescence (right) microscopy images of transfected cells expressing GFP (green) following 24 h transfection with FGF2B LK15 8R (CR3). Scale bar, 150 µm. Error bars indicate SD, n = 3**.** One-way ANOVA with Bonferroni's post-test (for transfection efficiency) or One-way ANOVA with Dunnett's test for the comparison of each treatment group with the control (for cell viability), *P < 0.05, **P < 0.01.

3.4.8 Efficient gene transfer of difficult-to-transfect cell types

FGF2B LK15 8R peptide showed high efficiency and low cytotoxicity in the transfection of NIH3T3 cells, therefore the GET peptide was tested in the transfection of a variety of different cell types including HeLa, MCF-7 and HUES7fib cells (Figure 3.11). HeLa human cervical cancer cells and MCF-7 human breast adenocarcinoma cells are some of the most common cell lines used for the *in vitro* study of cancer ((Lee et al., 2015)). HUES7fib are a human fibroblasts cell line derived from human embryonic stem cells (hESCs). FGF2B LK15 8R efficiently transfected all tested cells, demonstrating GET technology as a robust gene transfer system with a broad cell spectrum (Figure 3.11).

Next, hiPSCs were transfected with the GET peptide (Figure 3.12). HiPSCs are of biological significance in the study of disease pathology, manipulation of cellular process and/or for cell therapies as they have the ability to differentiate into any cell type and retain the genetic information of the donor (Okita and Yamanaka, 2011). The transfection efficiency of GET peptide at optimal CR was comparable to Lipofectamine 3000 (Figure 3.12). However, the viability of hiPSCs treated with the GET peptide was significantly better than with Lipofectamine 3000 (Figure 3.12). Furthermore, high transfection efficiency was maintained when hiPSCs were treated in 24 well plates, 6 well plates and T25 flasks, demonstrating scalable transfection (Figure 3.12). This data highlights that with minimum optimisation GET technology can be used to efficiently transfect challenging cell types such as pluripotent cells.

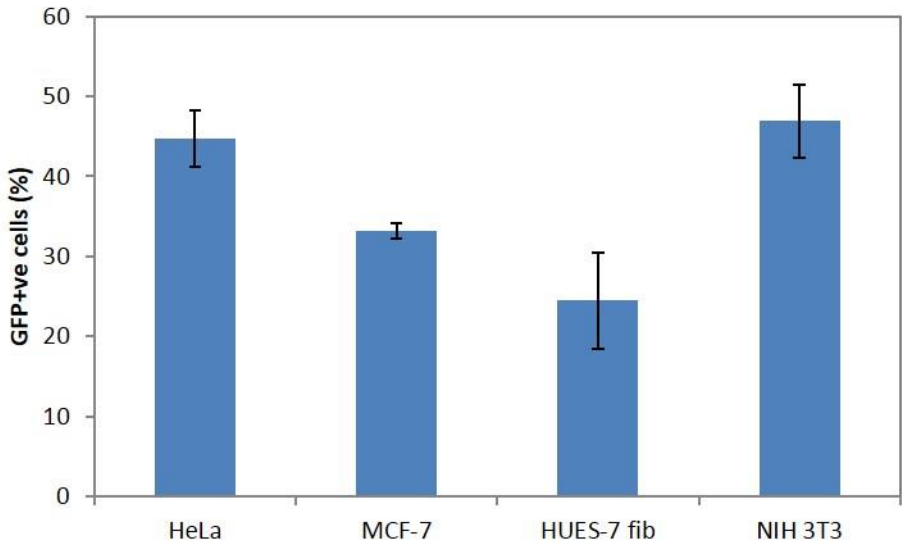


Figure 3.11 GET peptide transfection of HeLa, MCF-7, HUES-7 fib and NIH3T3 cells. Cells were transfected with 1 μg pSIN GFP using FGF2B LK15 8R (CR3). Error bars indicate SD, n = 3.

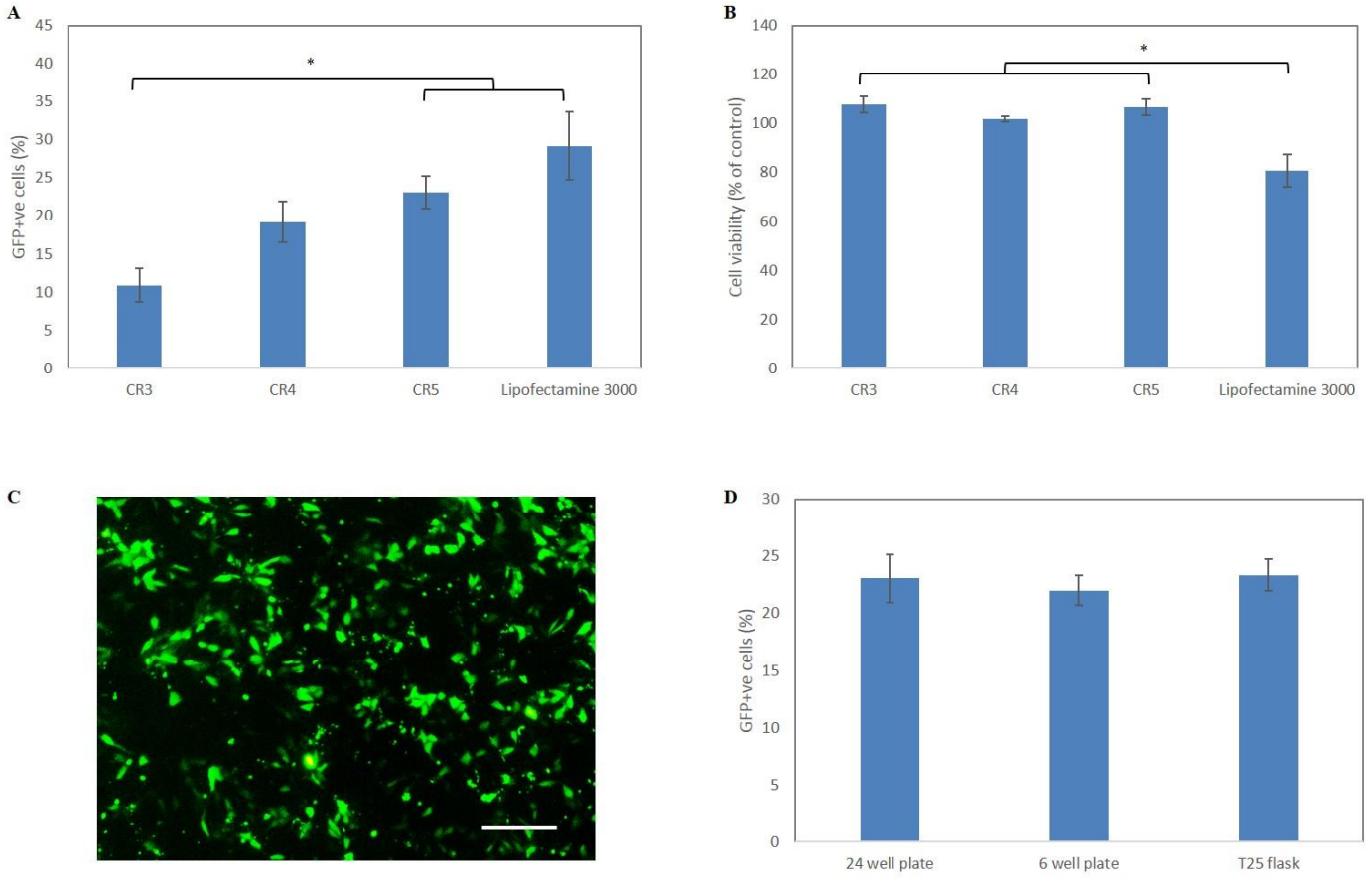


Figure 3.12 Efficient and scalable transfection of hiPSCs via GET. (A) Transfection efficiency and (B) cell viability (PrestoBlue assay) of hiPSCs treated with FGF2B LK15 8R or Lipofectamine 3000. (C) Fluorescence image of FGF2B LK15 8R transfected hiPSCs expressing GFP (green) and (D) scale-up of transfection. Error bars indicate SD, n = 3. One-way ANOVA with Bonferroni's post-tests; *P < 0.05, **P < 0.01.

3.4.9 Sustained delivery and expression of DNA

Multiple transfections can be important for sustained protein expression, improving transfection efficiency or for transfections of multiple plasmid DNAs (Cohen et al., 2000). The serial transfection of pSIN GFP reporter gene by FGF2B LK15 8R was assessed every day for three days. The transfection efficiency of the GET peptide was compared to commercial transfection reagent Lipofectamine 3000 in terms of cell viability, growth curves of treated cells, transfection efficiency and numbers of transfected cells (Figure 3.13). Treatment with GET peptide did not cause cytotoxicity or effect the growth of the cells. However, cells treated with Lipofectamine 3000 exhibited inhibited growth/proliferation. Thus, the application of Lipofectamine 3000 is detrimental in cell therapies where timely expansion of cells and efficient gene transfer are necessary for therapeutic efficacy. Transfection efficiency was comparable between both of the tested transfection reagents (Figure 3.13). However, due to the lower cell viability and inhibited proliferation of cells treated with Lipofectamine 3000, the numbers of transfected cells calculated for GET peptide transfection were considerably greater. To summarise, cells treated with Lipofectamine 3000 showed inhibited cell growth and exhibited lower cell viability than treatment with FGF2B LK15 8R. Following a three day serial transfection, a two-fold increase of GFP positive cells was detected using GET gene-transfer compared to Lipofectamine 3000.

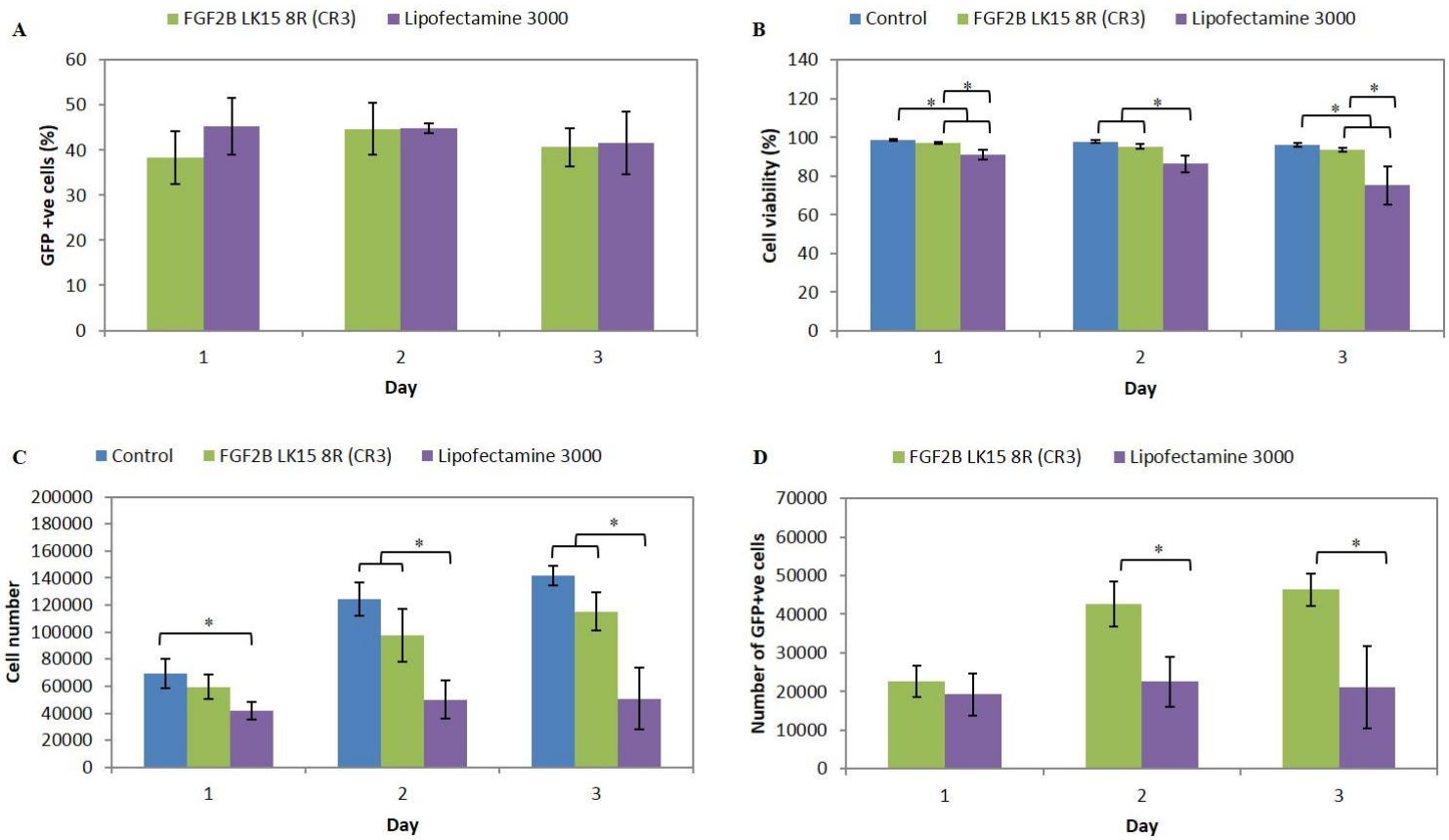


Figure 3.13 NIH3T3 cells were treated with FGF2B LK15 8R peptide or commercial transfection reagent Lipofectamine 3000 at Day 1 (24 h), Day 2 (48 h) and Day 3 (72 h) over a 3 day serial transfection of pSIN GFP. Transfections were compared in terms of (A) transfection efficiency, (B) cell viability (PrestoBlue assay), (C) cell proliferation/growth and (D) numbers of transfected cells. Error bars indicate SD, n = 3. One-way ANOVA with Bonferroni's post-tests; *P < 0.05, **P < 0.01.

3.4.10 Multiple plasmid delivery

Delivery of a cocktail of genes can be necessary for genetic manipulation, such as in the reprogramming of cells where four Yamanaka factors (Oct3/4, Sox2, Klf4, c-Myc) are over-expressed to induce pluripotency (Takahashi and Yamanaka, 2006). The ability of GET peptides to transfect multiple plasmids was explored. FGF2B LK15 8R was complexed with a GFP reporter gene and/or RFP reporter gene. Flow cytometry results demonstrated a proportion of cells treated with FGF2B LK15 8R/pSIN GFP NPs or FGF2B LK15 8R/pSIN RFP NPs expressed GFP or RFP, respectively (Figure 3.14). Cells treated with FGF2B LK15 8R complexed with a mixture of pSIN GFP and pSIN RFP expressed both GFP and RFP, confirming multiple plasmid transfection.

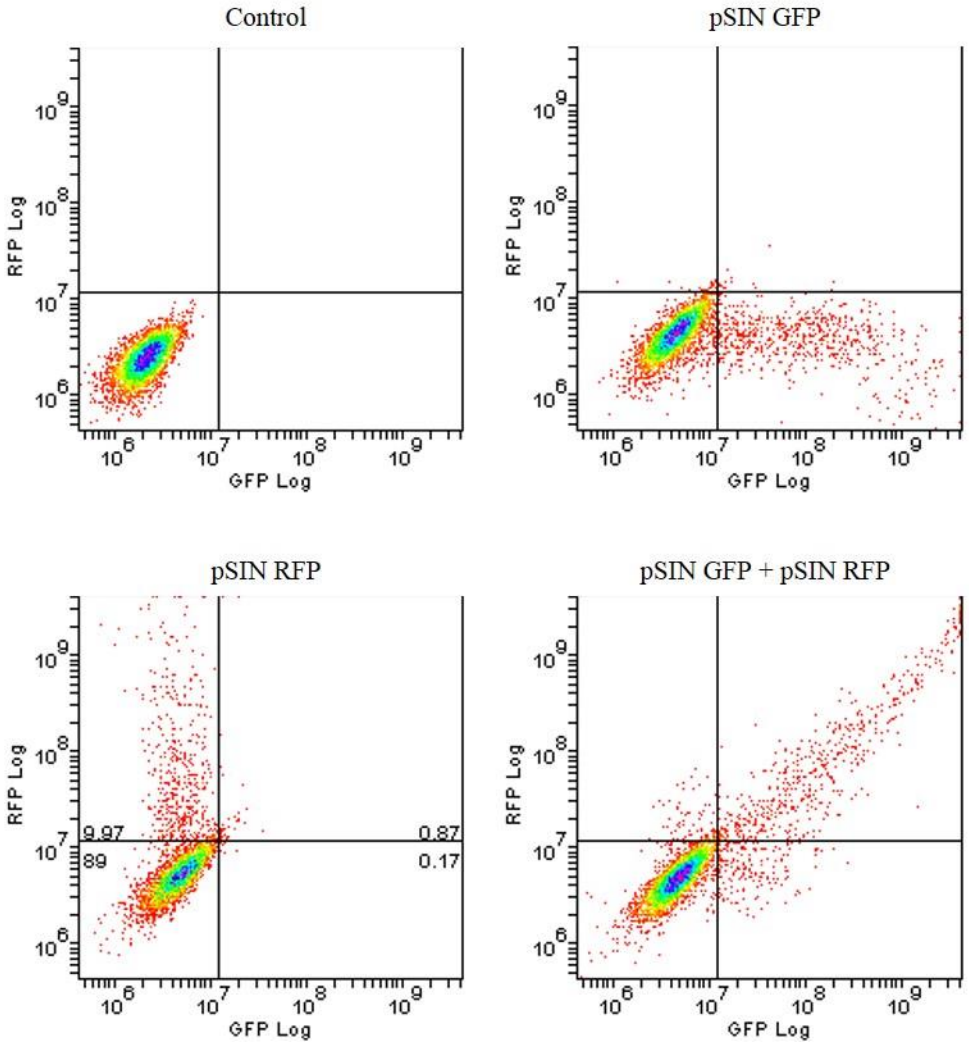


Figure 3.14 FGF2B LK15 8R-mediated transfection of multiple genes. Representative flow cytometry dot plots showing RFP and GFP expression of NIH3T3 cells transfected with 1 µg pSIN GFP, 1 µg pSIN RFP or a mixture 0.5 µg pSIN GFP + 0.5 µg pSIN RFP plasmids. Control was untreated cells.

3.5 Summary

GET transfection peptides were designed for enhanced cellular uptake and efficient transfection of a reporter gene in NIH3T3 cells. GET peptides utilise three functional segments:

- **HS-GAG targeting sequence:** for enhanced cellular delivery
- **LK15 amphipathic peptide:** for DNA binding and membrane activity
- **CPP:** for efficient translocation

These results collectively demonstrate that GET peptides fulfil many of the criteria required of an "optimal" transfection reagent including efficient serum-resistant transfection and minimal cytotoxicity. Furthermore, serial transfections with GET peptide did not affect proliferation/expansion of cells. The GET system overcomes one of the great challenges in CPP-mediated delivery of DNA by greatly improving membrane association and cellular uptake. However, endosomal entrapment still remains a challenge and future work should focus on the intelligent modification/incorporation of targeted endosomal escape strategies for minimal cytotoxicity and maximum transfection efficiency (Eguchi et al., 2009, Santos et al., 2011).

CHAPTER 4 PEGylated GET peptides for inhaled lung gene therapy

4.1 Introduction

Cystic fibrosis (CF) is an inherited incurable disease that affects greater than 7000 patients in the UK (Mehta, 2010). The disease is caused by an underlying genetic mutation in the cystic fibrosis transmembrane conductance regulator (CFTR) gene. Over 1990 different mutations of the CFTR gene have been reported (Griesenbach et al., 2015). The most common mutation, F508del, affects 70% of CF patients causing the production of a defective CFTR protein that is no longer able to regulate cAMP-dependent chloride secretion, bicarbonate secretion and epithelial sodium channels (ENaCs). Eventually this leads to incorrect transport of ions, mucus stasis/plugging and chronic lung infections (Rowe et al., 2005). There are a number of clinically available drugs for CFTR correction that act to block sodium channels or stimulate chloride channels (such as Ivacaftor (Vertex Pharmaceuticals)). These drugs often demonstrate low efficacy and are frequently combined with other drugs which increases the likelihood of adverse side effects (Verkman et al., 2006).

Developing successful lung gene therapy is complex as the agent must reach the airways, penetrate lung mucus and not be removed by mucociliary clearance (Jones and Helm, 2009). This navigation is even more difficult in CF patients due to increased amounts of thicker mucus that must be penetrated to reach target cells (Sanders et al., 2000) (Figure 4.1). CF mucus is a sticky mesh made up of

mucin fibres which contains a high density of negatively charged biomolecules, bacteria and endogenous DNA. As a consequence many particles are sterically immobilised or become entrapped by adhesive interactions with sputum components. The majority of viral technologies cannot penetrate mucosal secretions and/or have safety concerns inhibiting their clinical adoption (Schuster et al., 2014). In 2015, the outcome of the first-in-man non-viral gene therapy for CF was published by the UK Cystic Fibrosis Gene Therapy Consortium (UK CFGTC) (Alton et al., 2015). This was a one year phase 2b trial designed to assess clinical efficacy following monthly repeated delivery of a cationic liposome-based gene therapy in patients with CF. Results showed that inhaling the liposomal vector was safe over a 1 year period, could prevent disease progression (stabilise lung function) and had a moderate beneficial effect on lung function. Despite demonstrating only limited and variable efficacy, this is the first demonstration of non-viral gene carriers as a feasible approach for gene therapy treatment of CF.

Efficacious gene delivery systems must be able to navigate the mucus mesh as well as transfect cells efficiently. Non-viral cationic gene carriers are able to effectively complex DNA and efficiently transfect cells *in vitro* (Midoux et al., 2009). However, *in vivo* they are rapidly entrapped and cleared from mucus due to steric hindrance and/or mucoadhesion. The surface of cationic gene carriers can be coated with PEG to form “mucus penetrating” particles (Lai et al., 2009). PEG acts as an inert shield that inhibits interaction of the NP with mucus components and increases colloidal stability. Colloidal stability is a physical state in which particles remain dispersed in a solution at equilibrium. When

kinetically unstable particles coagulate and form aggregates (Suk et al., 2016). In addition, PEG coatings have been reported to reduce cytotoxicity and prolong the half-life of therapeutic agents *in vivo* (Veronese and Pasut, 2005). Importantly, PEGylation of polymer-based vectors has been shown to significantly improve distribution and gene transfer in mouse lung models (Mastorakos et al., 2015).

GET peptides have demonstrated efficient and non-cytotoxic transfection *in vitro*. Functionalisation of GET NPs with PEG could produce multifunctional gene carriers for effective *in vivo* lung gene delivery that go beyond the current approaches used for the treatment of diseases such as CF.

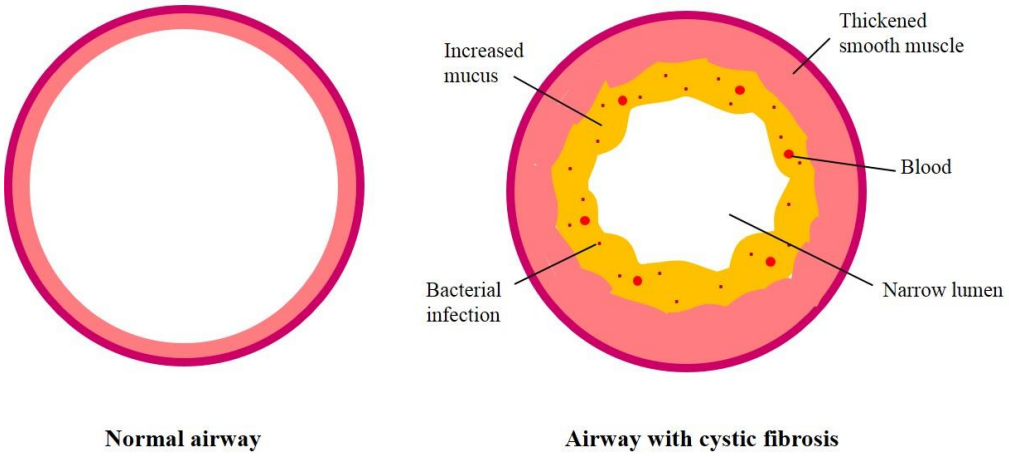


Figure 4.1 Schematic of healthy and cystic fibrosis airway sections.

4.2 Aims of the project

1. To engineer PEGylated GET complexes with tuneable properties for enhanced colloidal stability and rapid CF mucus penetration.
2. To demonstrate efficient and widespread transgene expression via PEGylated GET peptide NPs in healthy mouse lung models *in vivo*.

4.3 Materials and methods

4.3.1 Peptide synthesis

PEGylated peptides were synthesised by Protein Peptide Research Ltd (PPR, UK). FGF2B LK15 8R peptide was synthesised using solid phase t-Boc chemistry as described in Section 3.3.1. For the synthesis of PEGylated peptides, 5 KDa PEG chain was conjugated to FGF2B LK15 8R through a maleimide-thiol coupling reaction (PPR, UK). PEG maleimide was reacted with the thiol group of the terminal cysteine residue of the peptide. The PEG to peptide bond was formed through formation of a stable thioether linkage.

4.3.2 Preparation of DNA

The luciferase-expressing plasmid driven by a cytomegalovirus (CMV) promoter and fluorescently labelled versions of the plasmid DNA with Cyanine3 (Cy3) or Cyanine5 (Cy5) fluorophore were a kind gift from Dr Jung Soo Suk, Johns Hopkins University (Suk et al., 2009, Mastorakos et al., 2015).

4.3.3 Formation of PEGylated GET/DNA NPs

NPs were formulated by the dropwise addition of DNA (0.1 μg/μL) to a volume of swirling 1 mM peptide solution at CR3. The peptide solution was a mixture of nonPEGylated and PEGylated peptide at different PEGylation rates of 0, 10, 20, 40, 60, 80 and 100%. PEGylation rate was defined as the ratio of PEGylated to nonPEGylated peptide (for example 20% PEG would represent a mixture of 20% PEGylated peptide and 80% nonPEGylated peptide). Following the addition of DNA to peptide the NPs were incubated for 30 min at RT.

Polyethylenimine (PEI) NPs were made freshly by Mr Namho Kim, Johns Hopkins University as previously described (Johns Hopkins University, USA) (Mastorakos et al., 2015). NPs were washed three times with ultrapure distilled water and re-concentrated to 0.5 μg/μL using Amicon Ultra Centrifugal Filters (100,000 molecular weight cut-off; Millipore).

4.3.4 Characterisation of PEGylated NPs

Hydrodynamic diameter of NPs was determined in water by dynamic light scattering (DLS) and assessed in disposable low volume cuvettes. Zeta potential was measured in 10 mM NaCl at pH 7.0 by laser Doppler anemometry. NPs were measured by DLS following 1 h incubation in ultrapure water or 10% (v/v) bronchoalveolar lavage fluid (BALF) in PBS. Measurements of hydrodynamic size and zeta-potential were performed at RT using Zetasizer Nano ZS90 apparatus (Malvern Instruments). For each sample 3 measurements were taken, and each measurement was set to 10 runs.

0%, 40% and 60% PEGylated FGF2B LK15 8R/DNA NPs were imaged using transmission electron microscopy (TEM) to determine their morphology. The complexes were prepared as described in Section 4.3.3 and diluted to 0.1 μg/μL in ultrapure water. A drop of the sample was cast onto a copper TEM grid and air-dried at RT for several hours before examination. The TEM (H7600; Hitachi High Technologies America, Johns Hopkins University USA) was operated at 80 kV and 3-5 images were taken per grid.

4.3.5 *In vitro* transfection

NIH3T3 cells were maintained as described in Section 3.3.2. NIH3T3 cells were seeded 4 x 10^4 cells/well on 24 well-plates and incubated overnight. For each well of cells to be transfected, 1 µg DNA was diluted in 25 µL Opti-MEM and mixed. The peptide in 25 µL Opti-MEM was added to the diluted DNA. The solution was mixed and incubated for 20 min at RT. The wells were aspirated and replaced with 200 µL GM. Each well of cells was treated with 50 µL of peptide/DNA complex solution and incubated for 24 h. Following treatment wells were aspirated, washed with PBS and replaced with 200 µL GM and 50 µL fresh peptide/DNA complex solution.

4.3.6 Multiple particle tracking

The diffusion of Cy3 and Cy5-labelled DNA NPs were tracked in freshly expectorated CF mucus of patients from Johns Hopkins Cystic Fibrosis Centre as previously described (Schuster et al., 2014). CF sputum samples were collected after receiving written informed consent and approval from the Johns Hopkins Institutional Review Board (study NA_00046768). There were no specific exclusion criteria for patients based on their clinical status. However, patient samples could be excluded based on quality (i.e. noticeable amounts of saliva contamination).

A blend of nonPEGylated FGF2B LK15 8R and PEGylated FGF2B LK15 8R peptides were complexed with Cy3 or Cy5-labelled DNA (DNA concentration 0.5 µg/µL). 0.75 µL of fluorescently labelled complexes were added to 30 µL of

a CF sputum sample and mixed. Sputum aliquots were used on the day of collection and kept sealed to prevent dehydration of the sample. Following 1 h incubation, 20 s movies of NP displacement were captured using an inverted epifluorescence microscope (Axio Observer; Zeiss). NP trajectories were analysed using multiple particle tracking (MTP) software based on a previously developed algorithm (Schuster et al., 2015). The algorithm was written on MATLAB software and used to calculate the time-averaged mean squared displacement (MSD) of particles through the sputum. An intensity threshold was used to identify x and y position of complexes and the moving distance between frames was used to calculate the particle trajectories. Particles were distinguished by brightness, size, and eccentricity parameters. The time-averaged MSD of each trajectory was calculated. For each sputum sample, 3–5 videos were collected.

4.3.7 Animal studies

Animal studies were carried out by Miss Jane Chisholm (Johns Hopkins University, USA) on 6-8 week female BALB/c mice as previously described (Mastorakos et al., 2015) in accordance with Johns Hopkins University Animal Care and Use Committee guidelines.

Mice were anesthetised with an i.p. injection of 2,2,2-tribromoethanol (SigmaAldrich) working solution. 50 µL GET peptide/DNA NPs (DNA concentration 0.2 µg/µL) were administered by intratracheal microspray (Penn-Century). For distribution studies, mice were treated with Cy3-labelled DNA NPs. 30 min post administration lungs were harvested and flash frozen in

Optimal Cutting Temperature (OCT) compound (Fisher Healthcare). To determine bio-distribution, lung slices were cryosectioned (CM1950 cryostat, Leica Biosystems) and stained with DAPI. Images were taken on Carl Zeiss LSM-710 confocal microscope and quantified using ImageJ software (> 30 sections were analysed per mouse).

For transgene expression studies, mice were treated with luciferase expressing reporter plasmid driven by CMV promotor. 48 h post administration lungs were harvested and homogenised. The luciferase activity was measured using a luciferase assay kit (Thermo Scentific Pierce). Briefly, samples were freeze thawed 3 times in the presence of 1X reporter lysis buffer and centrifuged (10000xg, 10 min). 20 μL of supernatant was mixed with the luciferase substrate and relative light units (RLU) was immediately measured on 20/20n luminometer. BCA protein assay kit was used to normalise luciferase activity (Thermo Scentific Pierce).

For the safety study, mice were treated with 0 % or 40 % PEGylated NPs. 24 h post administration lungs were washed with 2.5 mL PBS x 3 to collect BALF for cell counts or lung tissue sections were stained with hematoxylin and eosin and cryosectioned (CM1950 cryostat, Leica Biosystems) for hematoxylin and eosin staining. Tissue slices were imaged on Carl Zeiss LSM-710 confocal microscope (Mastorakos et al., 2015) (n = 1 mouse/group).

4.3.8 Statistical analysis

For MPT experiments, median and SD were compiled from human CF patient mucus samples. Due to the heterogeneity of sputum samples, particles were tracked in n = 5/6 patient samples. For biodistribution and transgene expression experiments, mean and SD were compiled from n = 3 mice/group. Data were presented as mean ± SD and analysed by Prism statistical analysis software (GraphPad). Statistical significance was measured between two groups using a two-tailed Student's t test for comparison or between multiple groups by ANOVA with Bonferroni's multiple comparison test for post-hoc analysis.

4.4 Results and discussion

4.4.1 PEGylated GET peptide NP formation

GET peptide NPs were functionalised with PEG to shield their cationic surface, preventing unwanted interactions with components of biological fluid and ECM *in vivo*. PEG 5 KDa was coupled to GET peptide (FGF2B LK15 8R) via a maleimide-thiol coupling reaction (Shen et al., 2012). A blend of nonPEGylated FGF2B LK15 8R and PEG 5 KDa FGF2B LK15 8R peptides were mixed with DNA at CR3 to form PEGylated GET peptide/DNA NPs (Figure 4.2). The term PEGylation rate was used to describe the ratio of nonPEGylated to PEGylated peptide in the complex (for example 40 % PEGylation would indicate a ratio of 40 % PEG 5 KDa FGF2B LK15 8R to 60 % FGF2B LK15 8R). This strategy was utilised by Veiman *et al,* who demonstrated that varying the PEGylation rates of a CPP gene carrier led to the formation of particles with a tuneable/controllable density of PEG coating (Veiman et al., 2015). The hydrodynamic diameter and zeta potential of GET peptide/DNA complexes at 0%, 10%, 20%, 40%, 60%, 80% and 100% PEGylation rates were measured in water using DLS (Figure 4.3). The size of GET peptide complexes at all tested PEGylation rates were < 100 nm, indicating that the presence of PEG did not inhibit the ability of GET peptides to condense DNA into compact NPs. The surface charge of nonPEGylated complexes was ~ 20 mV. The zeta potential dropped at increasing PEGylation rates (particles exhibited a near neutral surface charge at high PEGylation rates). This signifies that adjusting proportions of PEGylated GET peptide facilitates control of cell surface PEG shielding.

TEM images of 0%, 40% and 60% PEGylated FGF2B LK15 8R/DNA complexes were taken to confirm their size and shape (Figure 4.4). NP dimensions were in agreement with hydrodynamic size measurements. The shape of complexes was spherical, indicating the formation of compact NPs.

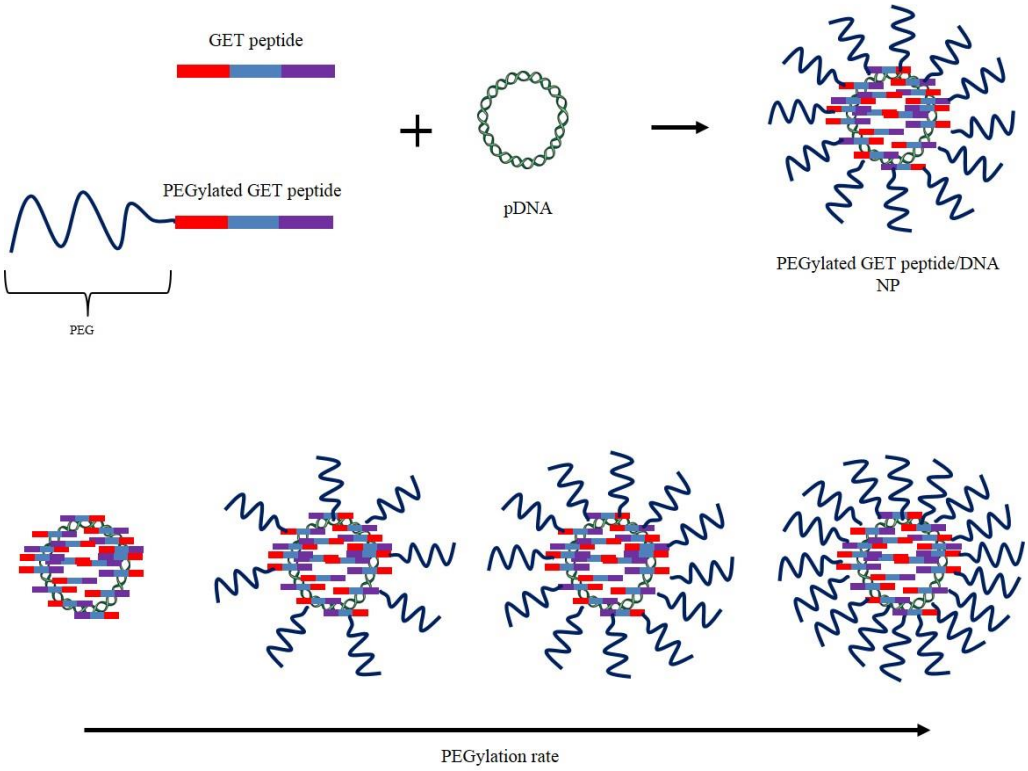


Figure 4.2 Schematic of PEGylated GET peptide/DNA complex formation. NonPEGylated and PEGylated peptides were blended at different ratios to control the density of PEG coating on the outer shell of NPs.

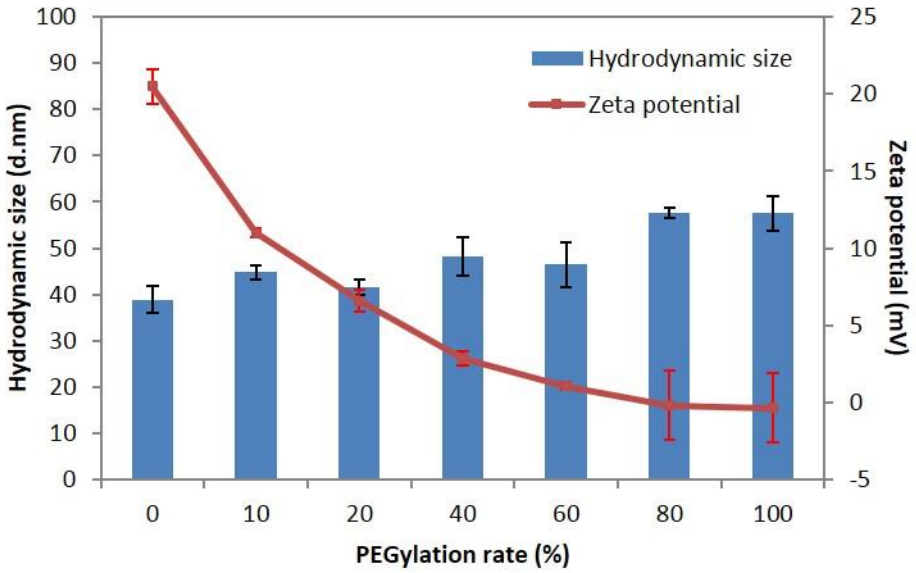


Figure 4.3 Graph of hydrodynamic size and zeta potential of GET peptide/DNA NPs at 0%, 10%, 20%, 40%, 60%, 80% and 100% PEGylation rates. The hydrodynamic size was measured in ultrapure water and zeta-potentials were measured in 10 mM NaCl at pH 7.0. Error bars indicate SD, n = 3.

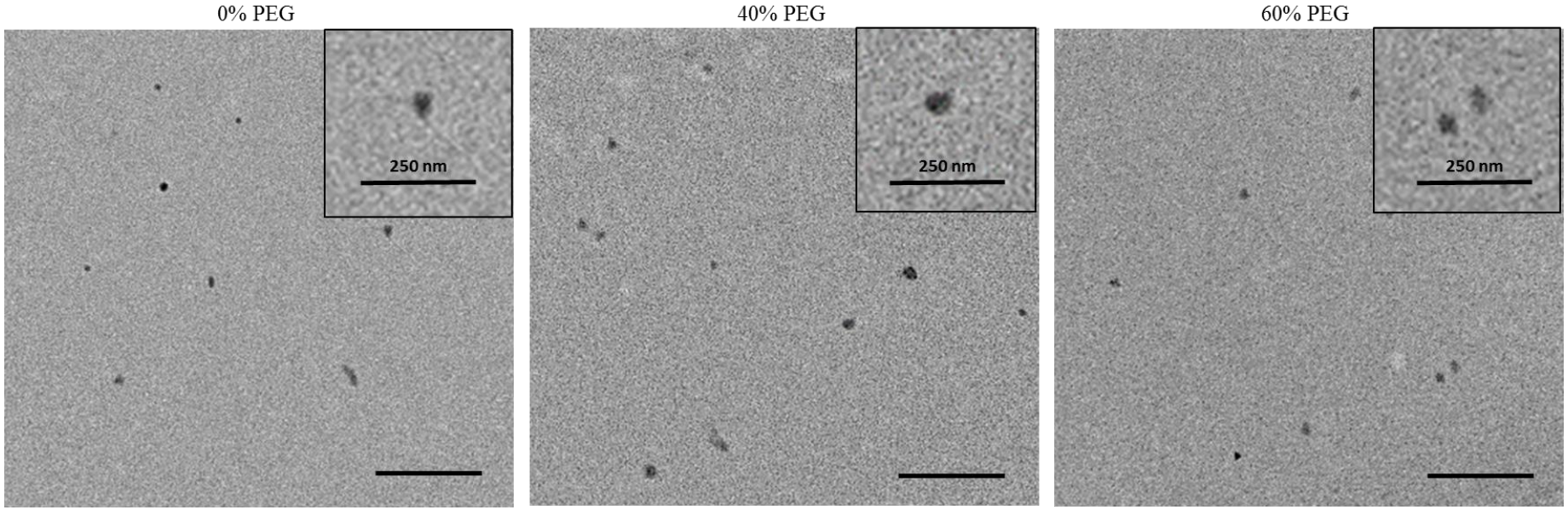


Figure 4.4 Representative transmission electron micrographs of FGF2B LK15 8R/DNA NPs at 0%, 40% and 60% PEGylation rates. Scale bar, 500 nm on original images and 250 nm on inserts.

4.4.2 Stability of NPs in biological fluid

Aggregates or large particles cannot overcome biological barriers for *in vivo* lung gene therapy due to steric hindrance inhibiting their movement through airway mucus before they reach the airway epithelium (Khandare and Minko, 2006). This is especially true for CF patients where a thick mucus mesh and rapid mucociliary clearance inhibit gene therapy (Suk et al., 2009). Therefore, ideally NPs *in vivo* should maintain colloidal stability to give them the best chance of navigating the mucus and reaching airway epithelium prior to being removed by clearance (Zhang et al., 2009). The hydrodynamic size of NPs incubated for 1 h in water or bronchoalveolar lavage fluid (BALF) was investigated. Following incubation in water, the size of FGF2B LK15 8R NPs remained < 100 nm at all tested PEGylation rates (NPs retained colloidal stability) (Figure 4.5). However when incubated in BALF, complexes of low PEGylation rates exhibited up to 20 fold increase in hydrodynamic size compared to their dimensions in water. Colloidal stability in BALF was achieved at high PEGylation rates, NPs of ≥ 40% PEGylation demonstrated hydrodynamic size < 100 nm.

PEG sheilds can greatly improve colloidal stability however this is often achieved at the expense of masking the activity of the gene carrier thereby inhibiting its transfection capacity (Kleemann et al., 2005). The effect of PEGylation on transfection efficiency *in vitro* was explored (Figure 4.6). Transfection was severely inhibited at higher PEGylation rates (transfection efficiency dropped from ~45% at 0% PEGylation to ~3% at 100 % PEGylation). Due to the adaptability of the PEG coating, PEGylation rates at which both colloidal stability and *in vitro* transfection efficiency were retained could be

identified for maximal *in vivo* potential. 40% PEGylated GET NPs were selected as a good candidate for *in vivo* studies as they retained colloidal stability in BALF and demonstrated *in vitro* transfection efficiency of ~10%.

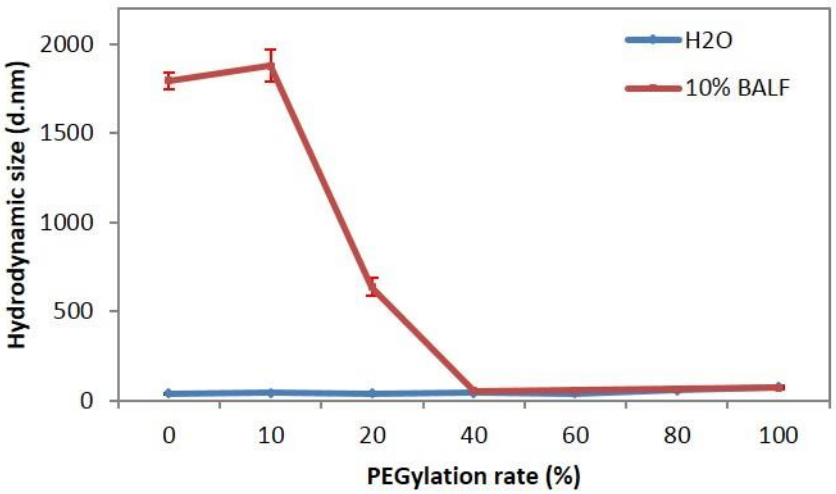


Figure 4.5 Stability of PEGylated GET peptide/DNA complexes at 10%, 20%, 40%, 60%, 80% and 100% PEGylation rates following 1 h incubation in water or 10% (v/v) BALF in PBS. Error bars indicate SD, n = 3.

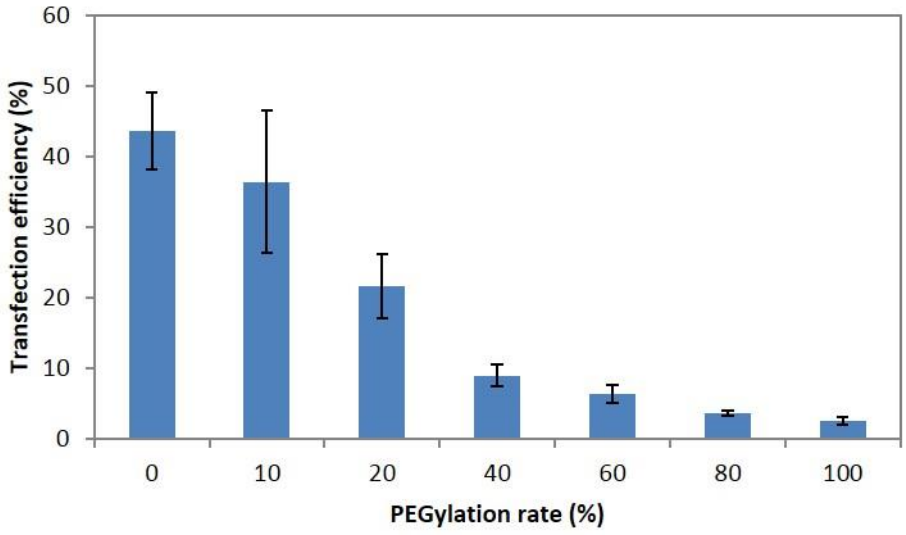


Figure 4.6 *In vitro* transfection efficiency of PEGylated GET NPs. NIH3T3 cells were transfected with 1 μg reporter gene expressing GFP for 24 h. Flow cytometry analysis was used to quantify the percentage of GFP positive cells. Error bars indicate SD, n = 3**.**

4.4.3 *Ex vivo* NP tracking in CF patient sputum samples

Despite the lung being an easily accessible target, the inability of viral and non-viral gene carriers to penetrate CF mucus has inhibited *in vivo* efficacy (Montier et al., 2004, Robinson et al., 2000). It is estimated that CF mucus has an average pore size of 140 ± 50 nm, therefore NPs that aggregate (> 200 nm) are likely to be immediately entrapped within the mucus mesh and cleared by enzymes and macrophages (Suk et al., 2009). It was hypothesised that PEGylated GET peptides that showed enhanced colloidal stability in BALF/biological fluid would demonstrate superior diffusion through CF sputum. The diffusion of 0%, 40% and 60% PEGylated GET particles through CF patient sputum samples was investigated *ex vivo*. Multiple particle tracking technology was used to track the diffusion of Cy3 and/or Cy5-labelled DNA NPs (Schuster et al., 2015). It has been reported that inhaled particles are cleared rapidly from mucus of CF patients within the first hour (Fahy and Dickey, 2010). Thus, particles able to diffuse through sputum MSD $\geq$ 1 μm^2 at 1 second were defined as "mucus penetrating" as these particles are most likely to navigate the CF sputum barrier fast enough to reach the underlying epithelium prior to being cleared from the lung. CF sputum strongly inhibited the transport of 0% PEGylated NPs, only ~ 5% were classified as diffusive. PEGylation significantly increased the proportion of diffusive particles by 5 fold (Figure 4.7).

Schuster *et al* have demonstrated that sputum hindered diffusion of clinically and pre-clinically tested adeno–associated virus' (AAVs) (Schuster et al., 2014). It was estimated that only between 5-10% AAV particles were "mucus penetrating" (this was thought to be a contributing factor to their limited clinical

success). A larger proportion of 40% and 60% PEGylated GET particles were able to diffuse through CF sputum (32% and 27%, respectively). These findings suggest that GET peptides could potentially overcome some of the major challenges for successful *in vivo* CF gene therapy.

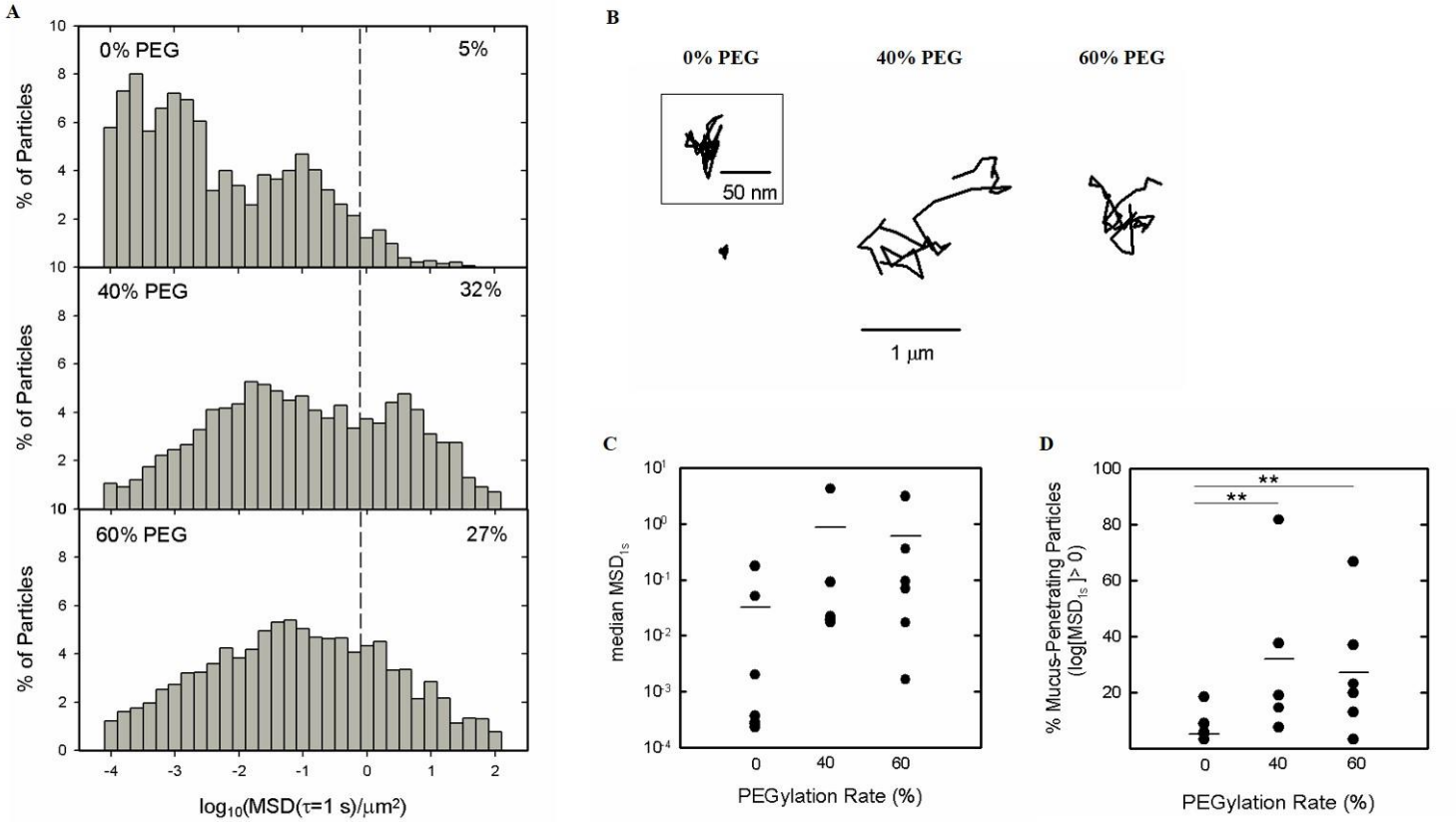


Figure 4.7 Multiple particle tracking of PEGylated GET NPs in *ex vivo* CF sputum samples. (A) Distribution of particle log MSD at a timescale of 1 s. (B) Representative trajectories of particles. Dot plots of (C) ensemble-median MSD and (D) percentage mucus penetrating particles (MSD ≥ 1 μm^2). Error bars indicate SD, n = 5-6 patient samples. One-way ANOVA with Bonferroni's post-tests; *P < 0.05, ** P < 0.01.

4.4.4 Biodistribution of NPs in lung model

It is thought that successful treatment of CF can be achieved by restoring as little as 10% CFTR expression per cell (Sheridan, 2011). Therefore, wide spread transgene expression of even low level expression is crucial for successful therapy. The bio-distribution of PEGylated GET NPs was investigated in mouse lung models *in vivo*. PEGylated and nonPEGylated GET NPs containing Cy5-labelled DNA were administered by intratracheal microspray directly to the mouse lung. 30 min post administration, lungs were harvested to analyse the bio-distribution of the particles. 0% PEGylated NPs appeared to be sparsely distributed in the tissue compared to the widespread and uniform distribution observed in the lungs treated with 40% PEGylated NPs (Figure 4.8). Image-based quantification of fluorescence confirmed that PEGylated NPs exhibited significantly better coverage in large airways and distribution in the lung parenchyma. The superior bio-distribution of the PEGylated NPs was likely to be a result of their enhanced colloidal stability.

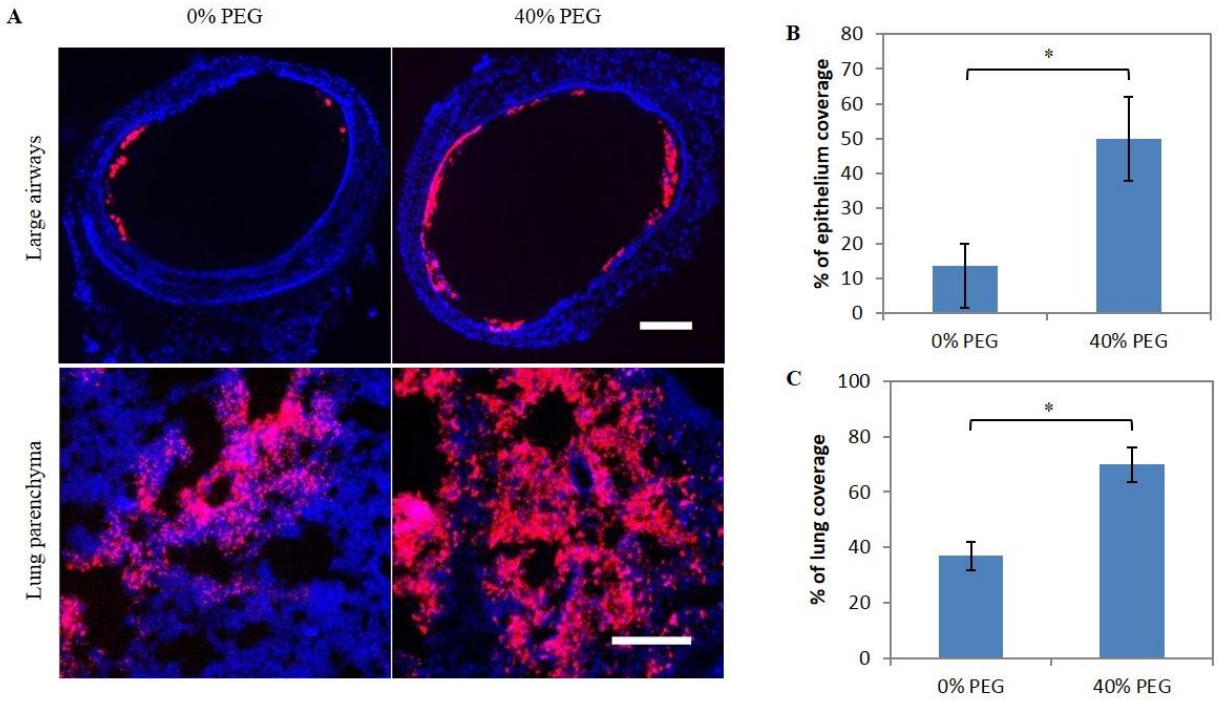


Figure 4.8 *In vivo* distribution of PEGylated GET peptide complexes in healthy mouse lung models. Cy5-labelled DNA was complexed with FGF2B LK15 8R at CR3. (A) Representative images of NP distribution in large airways and lung parenchyma following intratracheal administration of the respective NPs (red). Cell nuclei were stained with DAPI (blue). (B and C) Image-based quantification of (B) coverage of NPs in large airways and (C) distribution of NPs in the lung parenchyma. Tissues were harvested 30 min following intratracheal administration of NPs. Error bars indicate SD, n = 3 mice/group. Two-tailed Student's t-test, *P < 0.05, **P < 0.01.

4.4.5 *In vivo* transfection

40% PEGylated GET peptide/DNA complexes displayed superior stability, mucus penetration and bio-distribution compared to nonPEGylated complexes. Next, we sought to determine whether PEGylation improved gene transfer *in vivo*. FGF2B LK15 8R/DNA complexes of 0% and 40% PEGylation rates were administered to 6 to 8 week female Balb/C mice. Each mouse was treated with 10 μg of luciferase expressing plasmid via intratracheal microspray. Transfection efficiency of GET peptides was compared to PEI, a leading non-viral polymer-based gene carrier for *in vivo* transfection (Mastorakos et al., 2015). The lung luciferase activity of mice treated with 0% PEG complexes was not significantly different to control despite 0% PEGylation rate demonstrating the highest *in vitro* transfection efficiency (Figure 4.9). Mice treated with 40% PEGylated GET complexes demonstrated significantly superior gene transfer to nonPEGylated GET NPs and PEI NPs.

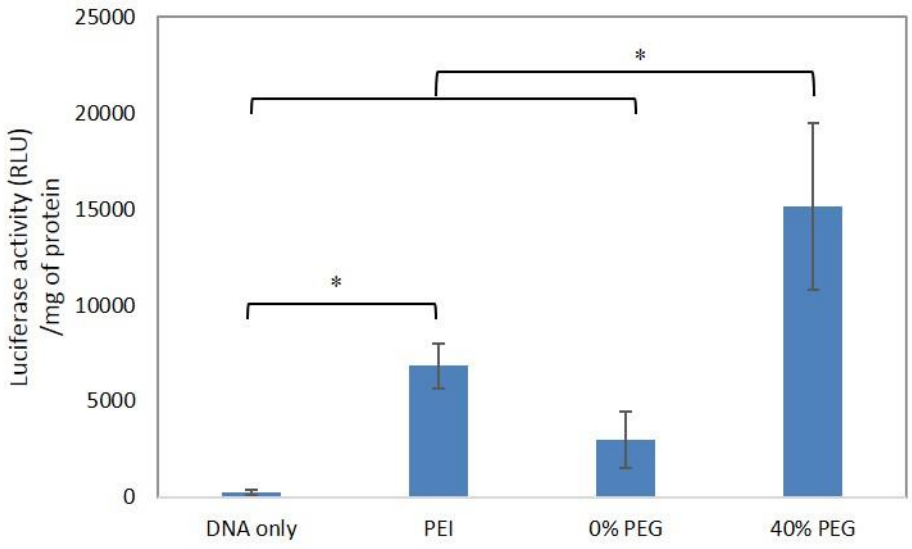


Figure 4.9 *In vivo* mouse lung transgene expression of luciferase activity following PEGylated GET/DNA NP administration. Error bars indicate SD, n = 3 mice/group. One-way ANOVA with Bonferroni's post-tests; *P < 0.05, **P < 0.01.

4.4.6 *In vivo* safety

PEGylation has been shown to improve the safety of cationic particles by shielding their positive charge and inhibiting non-specific interactions (Xiao et al., 2011, Zhang et al., 2008). The acute toxicity of PEGylated GET peptide/DNA complexes was assessed by analysis of cell counts from BALF and lung histology 24 h post administration. Cell counts give an indication of immune cell infiltration, a higher number of cells in the collected BALF indicates an increased host immune response. The cell count of mice treated with nonPEGylated complexes was significantly higher than 40% PEGylated complexes (Figure 4.10). Furthermore, histology images of lungs treated with 0% PEGylated NPs appeared to show a higher number of cell nuclei and congestion (n = 1 mouse/group) (Figure 4.10). Semi-quantification of lung inflammation in histology samples is currently dependent on visual scoring by an expert. Further studies are needed to expand sample group of treated mice to facilitate scoring of the tissue samples.

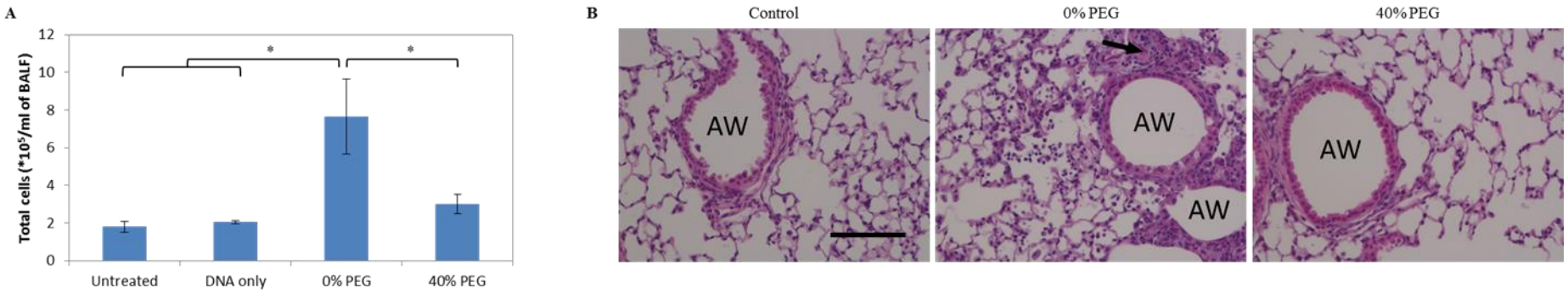


Figure 4.10 Safety profile of lungs treated with PEGylated GET NPs 24 h post administration. (A) Cell counts from BALF of treated lungs (n = 3 mice/group) and (B) representative images of lung sections stained with hematoxylin and eosin (n = 1 mouse/group). AW, airway, arrow indicates cellular infiltrate. Scale bar, 100 µm. Error bars indicate SD. One-way ANOVA with Bonferroni's post-tests; *P < 0.05, **P < 0.01.

4.5 Summary

To summarise, PEGylated GET peptide NPs were engineered for *in vivo* DNA delivery. PEGylation greatly improved colloidal stability however this was achieved at the expense of masking the activity of the gene carrier thereby limiting its transfection capacity *in vitro*. 40% PEGylated particles were capable of maintaining colloidal stability in biological fluids and navigating human CF sputum samples. These particles demonstrated superior bio-distribution, transgene expression and safety profiles compared to nonPEGylated particles in mouse lung models *in vivo*. This data collectively highlights the potential clinical utility of PEGylated GET particles for efficacious gene therapy of CF.

CHAPTER 5 Conclusions and future work

This project reports the efficient GET-mediated *in vitro* and *in vivo* transfection of DNA. GET peptides overcome some of the challenges of non-viral DNA delivery by exhibiting superior gene transfer and minimal cytotoxicity. Furthermore, PEGylated GET NPs have demonstrated the ability to penetrate the mucus barrier for efficient and widespread DNA delivery in mouse lung models.

This work presents an approach that combines a CPP and a HS GAG targeting sequence for enhanced delivery to cells. A variety of GF derived HS targeting sequences were conjugated to 8R and screened for their transduction efficiency. Four modified CPPs demonstrated 30-100 fold GAG-binding enhanced transduction (GET) of a reporter protein, compared to the unmodified CPP (8R alone). It is also worthy to mention that GET peptides demonstrated enhanced delivery to difficult-to-transduce cell types such as pluripotent cell lines.

Cell surface HS-GAG expression can vary greatly between different cell types and disease states, therefore it was hypothesised that selective HS motifs could be targeted for preferential delivery to selected cells. The GF derived HS-GAG binding domain was replaced with a HS-specific antibody (HS4C3) for cell type specific targeting and delivery to prehemangioblast cells during mesodermal differentiation. Baldwin *et al* demonstrated that HS4C3 antibody targeted a HS epitope that was expressed transiently by cells with maximal hemangioblast potential during mesodermal differentiation (Baldwin et al., 2008). Following

conjugation to mRFP, a truncated version of HS4C3 retained its ability to bind pre-hemangioblast cells. However, when fused with 8R the cell type specificity of the antibody was masked through non-specific cell interaction of the CPP with the membrane. If loss of specificity due to CPP region could be overcome, this data demonstrates that it may be possible to specifically target and deliver to a desired cell type in a heterogeneous population of cells through utilising truncated HS GAG binding antibodies fused to CPPs.

There are a limited number of specific oligosaccharide sequences that have been identified. To truly exploit GET for cell type specific targeting, technologies such as phage display must be utilized for screening and identification of target HS-GAG binding peptides (Arap, 2005, Schoonbroodt et al., 2008). Phage display techniques have already demonstrated effectiveness for identifying sequences that bind specific HS epitopes, as evidenced by Kuppevelt *et al* who created a human antibody phage display library of anti-HS epitope antibodies (van Kuppevelt et al., 1998).

Due to their ability to deliver cargo into cells much more efficiently than unmodified CPPs, GET peptides were designed for efficient DNA delivery. Conjugation of amphipathic peptide LK15 to GET moieties P21 or FGF2B and 8R improved the DNA binding ability and transfection efficiency of the peptides. Transfection of reporter gene (pSIN GFP) was optimised in NIH3T3 cells and compared with commercial transfection reagent Lipofectamine 2000, Lipofectamine 3000, JetPEI, FuGENE HD and TransIT-LT1. GET peptide, FGF2B LK15 8R, outperformed most of the ‘gold standard’ transfection

reagents by demonstrating both high transfection efficiency and minimal cytotoxicity. GET peptides were able to non-covalently bind DNA for efficient and non-cytotoxic transfection of a variety of cell types, including difficult-to-transfect cell types such as hiPSCs. Furthermore, FGF2B LK15 8R demonstrated sustained delivery and expression of the reporter gene following repeat transfections. Following a 3 day serial transfection, 2-fold more GFP positive cells were detected using GET gene-transfer compared to Lipofectamine 3000.

The data collectively demonstrates that GET peptides fulfil many of the criteria required for an optimal transfection reagent including:

- **Efficient serum-resistant transection:** comparable and in some cases exceeding transfection efficiency of leading commercial transfection reagents
- **Low cellular toxicity**
- **Broad cell spectrum:** transfection of a variety of cell lines including difficult-to-transfect cell types (such as pluripotent cells)
- **Transfection of single or multiple plasmids**
- **Low cost**

GET peptides were not only able to transfect cells efficiently *in vitro* but they also demonstrated efficient *in vivo* gene transfer when PEGylated. PEG GET NPs were engineered for DNA delivery in mouse lung models. At PEGylation rates ≥ 40 %, PEG shielding greatly improved colloidal stability and prevented unwanted interactions of the cationic CPPs with bio-components in BALF. Furthermore, 40 % and 60 % PEGylated GET NPs were able to efficiently

penetrate CF patient sputum samples. Results have demonstrated that PEG GET NPs can navigate biological barriers for wide spread and highly efficient gene transfer without toxicity in mouse lung models.

This work has highlighted the huge potential of GET-technology as a gene therapy for CF and other lung diseases. Future work will be focused on adapting the GET-system for efficient correction of the CF mutation using Cas9/CRISPR (Figure 5.1). The use of an effective gene delivery system with leading gene-editing technologies (such as Cas9/CRISPR) has the potential to produce a successful treatment for CF that goes beyond the current approaches used in conventional gene therapy.

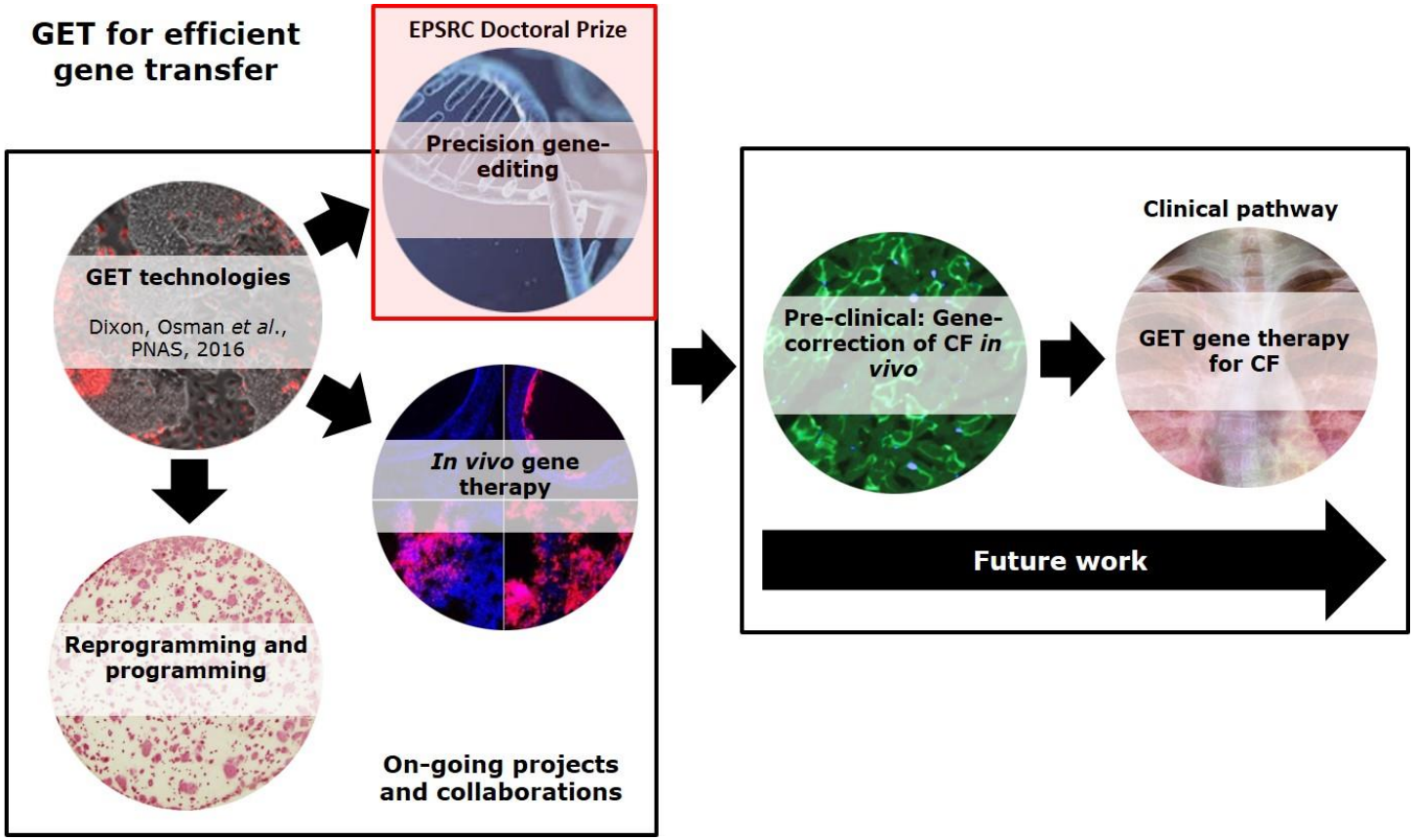


Figure 5.1 Future work plan: translation of GET technology for precision CF gene therapy.

CHAPTER 6 Appendix

Table 6.1 Amino acid sequences of the recombinant proteins.

Protein	Amino acid sequence
mRFP	MASSEDVIKEFMRFKVRMEGSVNGHEFEIEGEGEGR PYEGTQTAKLKVTKGGPLPFAWDILSPQFQYGSKAY VKHPADIPDYLKLSFPEGFKWERVMNFEDGGVVTV TQDSSLQDGEFIYKVKLRGTNFPSDGPVMQKKTMG WEASTERMYPEDGALKGEIKMRLKLKDGGHYDAE VKTTYMAKKPVQLPGAYKTDIKLDITSHNEDYTIVE QYERAEGRHSTGATSEFGRPGSTM
P21 mRFP	KRKKKGKGLGKKRDPCLRKYKMASSEDVIKEFMRF KVRMEGSVNGHEFEIEGEGEGRPYEGTQTAKLKVT KGGPLPFAWDILSPQFQYGSKAYVKHPADIPDYLKL SFPEGFKWERVMNFEDGGVVTVTQDSSLQDGEFIYK VKLRGTNFPSDGPVMQKKTMGWEASTERMYPEDG ALKGEIKMRLKLKDGGHYDAEVKTTYMAKKPVQL PGAYKTDIKLDITSHNEDYTIVEQYERAEGRHSTGAT SEFGRPGSTM
FGF1A mRFP	KKPKLLYCSNGGHFLRILPDGTVDGTRDRSDQHIQL QLSAESVGEVYIKSTMASSEDVIKEFMRFKVRMEGS VNGHEFEIEGEGEGRPYEGTQTAKLKVTKGGPLPFA WDILSPQFQYGSKAYVKHPADIPDYLKLSFPEGFKW ERVMNFEDGGVVTVTQDSSLQDGEFIYKVKLRGTN

	FPSDGPVMQKKTMGWEASTERMYPEDGALKGEIK MRLKLKDGGHYDAEVKTTYMAKKPVQLPGAYKTD IKLDITSHNEDYTIVEQYERAEGRHSTGATSEFGRPG STM
FGF1B mRFP	TYISKKHAEKNWFVGLKKMASSEDVIKEFMRFKVR MEGSVNGHEFEIEGEGEGRPYEGTQTAKLKVTKGGP LPFAWDILSPQFQYGSKAYVKHPADIPDYLKLSFPEG FKWERVMNFEDGGVVTVTQDSSLQDGEFIYKVKLR GTNFPSDGPVMQKKTMGWEASTERMYPEDGALKG EIKMRLKLKDGGHYDAEVKTTYMAKKPVQLPGAY KTDIKLDITSHNEDYTIVEQYERAEGRHSTGATSEFG RPGSTM
FGF1C mRFP	KNGSCKRGPRTHYGQKMASSEDVIKEFMRFKVRME GSVNGHEFEIEGEGEGRPYEGTQTAKLKVTKGGPLP FAWDILSPQFQYGSKAYVKHPADIPDYLKLSFPEGF KWERVMNFEDGGVVTVTQDSSLQDGEFIYKVKLRG TNFPSDGPVMQKKTMGWEASTERMYPEDGALKGEI KMRLKLKDGGHYDAEVKTTYMAKKPVQLPGAYKT DIKLDITSHNEDYTIVEQYERAEGRHSTGATSEFGRP GSTM
FGF2A mRFP	KDPKRLYCKNGGFFLRIHPDGRVDGVREKSDPHIKL QLQAEERGVVSIKGVMASSEDVIKEFMRFKVRMEG SVNGHEFEIEGEGEGRPYEGTQTAKLKVTKGGPLPF AWDILSPQFQYGSKAYVKHPADIPDYLKLSFPEGFK WERVMNFEDGGVVTVTQDSSLQDGEFIYKVKLRGT

	NFPSDGPVMQKKTMGWEASTERMYPEDGALKGEIK MRLKLKDGGHYDAEVKTTYMAKKPVQLPGAYKTD IKLDITSHNEDYTIVEQYERAEGRHSTGATSEFGRPG STM
FGF2B mRFP	TYRSRKYTSWYVALKRMASSEDVIKEFMRFKVRME GSVNGHEFEIEGEGEGRPYEGTQTAKLKVTKGGPLP FAWDILSPQFQYGSKAYVKHPADIPDYLKLSFPEGF KWERVMNFEDGGVVTVTQDSSLQDGEFIYKVKLRG TNFPSDGPVMQKKTMGWEASTERMYPEDGALKGEI KMRLKLKDGGHYDAEVKTTYMAKKPVQLPGAYKT DIKLDITSHNEDYTIVEQYERAEGRHSTGATSEFGRP GSTM
FGF2C mRFP	RTGQYKLGSKTGPGQKMASSEDVIKEFMRFKVRME GSVNGHEFEIEGEGEGRPYEGTQTAKLKVTKGGPLP FAWDILSPQFQYGSKAYVKHPADIPDYLKLSFPEGF KWERVMNFEDGGVVTVTQDSSLQDGEFIYKVKLRG TNFPSDGPVMQKKTMGWEASTERMYPEDGALKGEI KMRLKLKDGGHYDAEVKTTYMAKKPVQLPGAYKT DIKLDITSHNEDYTIVEQYERAEGRHSTGATSEFGRP GSTM
FGF4A mRFP	KRLRRLYCNVGIGFHLQALPDGRIGGAHADTRDSLL ELSPVERGVVSIFGVMASSEDVIKEFMRFKVRMEGS VNGHEFEIEGEGEGRPYEGTQTAKLKVTKGGPLPFA WDILSPQFQYGSKAYVKHPADIPDYLKLSFPEGFKW ERVMNFEDGGVVTVTQDSSLQDGEFIYKVKLRGTN

	FPSDGPVMQKKTMGWEASTERMYPEDGALKGEIK MRLKLKDGGHYDAEVKTTYMAKKPVQLPGAYKTD IKLDITSHNEDYTIVEQYERAEGRHSTGATSEFGRPG STM
FGF4B mRFP	AYESYKYPGMFIALSKMASSEDVIKEFMRFKVRME GSVNGHEFEIEGEGEGRPYEGTQTAKLKVTKGGPLP FAWDILSPQFQYGSKAYVKHPADIPDYLKLSFPEGF KWERVMNFEDGGVVTVTQDSSLQDGEFIYKVKLRG TNFPSDGPVMQKKTMGWEASTERMYPEDGALKGEI KMRLKLKDGGHYDAEVKTTYMAKKPVQLPGAYKT DIKLDITSHNEDYTIVEQYERAEGRHSTGATSEFGRP GSTM
FGF4C mRFP	KNGKTKKGNRVSPTMKMASSEDVIKEFMRFKVRME GSVNGHEFEIEGEGEGRPYEGTQTAKLKVTKGGPLP FAWDILSPQFQYGSKAYVKHPADIPDYLKLSFPEGF KWERVMNFEDGGVVTVTQDSSLQDGEFIYKVKLRG TNFPSDGPVMQKKTMGWEASTERMYPEDGALKGEI KMRLKLKDGGHYDAEVKTTYMAKKPVQLPGAYKT DIKLDITSHNEDYTIVEQYERAEGRHSTGATSEFGRP GSTM
FGF7B mRFP	TYASAKWTHNGGEMFVALNQMASSEDVIKEFMRF KVRMEGSVNGHEFEIEGEGEGRPYEGTQTAKLKVT KGGPLPFAWDILSPQFQYGSKAYVKHPADIPDYLKL SFPEGFKWERVMNFEDGGVVTVTQDSSLQDGEFIYK VKLRGTNFPSDGPVMQKKTMGWEASTERMYPEDG

	ALKGEIKMRLKLKDGGHYDAEVKTTYMAKKPVQL PGAYKTDIKLDITSHNEDYTIVEQYERAEGRHSTGAT SEFGRPGSTM
FGF7C mRFP	QKGIPVRGKKTKKEQKMASSEDVIKEFMRFKVRME GSVNGHEFEIEGEGEGRPYEGTQTAKLKVTKGGPLP FAWDILSPQFQYGSKAYVKHPADIPDYLKLSFPEGF KWERVMNFEDGGVVTVTQDSSLQDGEFIYKVKLRG TNFPSDGPVMQKKTMGWEASTERMYPEDGALKGEI KMRLKLKDGGHYDAEVKTTYMAKKPVQLPGAYKT DIKLDITSHNEDYTIVEQYERAEGRHSTGATSEFGRP GSTM
ATIII mRFP	AKLNCRLYRKANKSSKLVSANRMASSEDVIKEFMR FKVRMEGSVNGHEFEIEGEGEGRPYEGTQTAKLKVT KGGPLPFAWDILSPQFQYGSKAYVKHPADIPDYLKL SFPEGFKWERVMNFEDGGVVTVTQDSSLQDGEFIYK VKLRGTNFPSDGPVMQKKTMGWEASTERMYPEDG ALKGEIKMRLKLKDGGHYDAEVKTTYMAKKPVQL PGAYKTDIKLDITSHNEDYTIVEQYERAEGRHSTGAT SEFGRPGSTM
PDGF mRFP	GRPRESGKKRKRKRLKPTMASSEDVIKEFMRFKVR MEGSVNGHEFEIEGEGEGRPYEGTQTAKLKVTKGGP LPFAWDILSPQFQYGSKAYVKHPADIPDYLKLSFPEG FKWERVMNFEDGGVVTVTQDSSLQDGEFIYKVKLR GTNFPSDGPVMQKKTMGWEASTERMYPEDGALKG EIKMRLKLKDGGHYDAEVKTTYMAKKPVQLPGAY

	KTDIKLDITSHNEDYTIVEQYERAEGRHSTGATSEFG RPGSTM
VEGF mRFP	ARQENPCGPCSERRKHLFVQDPQTCKCSCKNTDSRC KARQLELNERTCRCDKPRRMASSEDVIKEFMRFKVR MEGSVNGHEFEIEGEGEGRPYEGTQTAKLKVTKGGP LPFAWDILSPQFQYGSKAYVKHPADIPDYLKLSFPEG FKWERVMNFEDGGVVTVTQDSSLQDGEFIYKVKLR GTNFPSDGPVMQKKTMGWEASTERMYPEDGALKG EIKMRLKLKDGGHYDAEVKTTYMAKKPVQLPGAY KTDIKLDITSHNEDYTIVEQYERAEGRHSTGATSEFG RPGSTM
8R mRFP	RRRRRRRRMASSEDVIKEFMRFKVRMEGSVNGHEF EIEGEGEGRPYEGTQTAKLKVTKGGPLPFAWDILSP QFQYGSKAYVKHPADIPDYLKLSFPEGFKWERVMN FEDGGVVTVTQDSSLQDGEFIYKVKLRGTNFPSDGP VMQKKTMGWEASTERMYPEDGALKGEIKMRLKLK DGGHYDAEVKTTYMAKKPVQLPGAYKTDIKLDITS HNEDYTIVEQYERAEGRHSTGATSEFGRPGSTM
P21 mRFP 8R	KRKKKGKGLGKKRDPCLRKYKMASSEDVIKEFMRF KVRMEGSVNGHEFEIEGEGEGRPYEGTQTAKLKVT KGGPLPFAWDILSPQFQYGSKAYVKHPADIPDYLKL SFPEGFKWERVMNFEDGGVVTVTQDSSLQDGEFIYK VKLRGTNFPSDGPVMQKKTMGWEASTERMYPEDG ALKGEIKMRLKLKDGGHYDAEVKTTYMAKKPVQL

	PGAYKTDIKLDITSHNEDYTIVEQYERAEGRHSTGAT SEFGRPGSTMRRRRRRRR
FGF1A mRFP 8R	KKPKLLYCSNGGHFLRILPDGTVDGTRDRSDQHIQL QLSAESVGEVYIKSTMASSEDVIKEFMRFKVRMEGS VNGHEFEIEGEGEGRPYEGTQTAKLKVTKGGPLPFA WDILSPQFQYGSKAYVKHPADIPDYLKLSFPEGFKW ERVMNFEDGGVVTVTQDSSLQDGEFIYKVKLRGTN FPSDGPVMQKKTMGWEASTERMYPEDGALKGEIK MRLKLKDGGHYDAEVKTTYMAKKPVQLPGAYKTD IKLDITSHNEDYTIVEQYERAEGRHSTGATSEFGRPG STMRRRRRRRR
FGF1B mRFP 8R	TYISKKHAEKNWFVGLKKMASSEDVIKEFMRFKVR MEGSVNGHEFEIEGEGEGRPYEGTQTAKLKVTKGGP LPFAWDILSPQFQYGSKAYVKHPADIPDYLKLSFPEG FKWERVMNFEDGGVVTVTQDSSLQDGEFIYKVKLR GTNFPSDGPVMQKKTMGWEASTERMYPEDGALKG EIKMRLKLKDGGHYDAEVKTTYMAKKPVQLPGAY KTDIKLDITSHNEDYTIVEQYERAEGRHSTGATSEFG RPGSTMRRRRRRRR
FGF1C mRFP 8R	KNGSCKRGPRTHYGQKMASSEDVIKEFMRFKVRME GSVNGHEFEIEGEGEGRPYEGTQTAKLKVTKGGPLP FAWDILSPQFQYGSKAYVKHPADIPDYLKLSFPEGF KWERVMNFEDGGVVTVTQDSSLQDGEFIYKVKLRG TNFPSDGPVMQKKTMGWEASTERMYPEDGALKGEI KMRLKLKDGGHYDAEVKTTYMAKKPVQLPGAYKT

	DIKLDITSHNEDYTIVEQYERAEGRHSTGATSEFGRP GSTMRRRRRRRR
FGF2A mRFP 8R	KDPKRLYCKNGGFFLRIHPDGRVDGVREKSDPHIKL QLQAEERGVVSIKGVMASSEDVIKEFMRFKVRMEG SVNGHEFEIEGEGEGRPYEGTQTAKLKVTKGGPLPF AWDILSPQFQYGSKAYVKHPADIPDYLKLSFPEGFK WERVMNFEDGGVVTVTQDSSLQDGEFIYKVKLRGT NFPSDGPVMQKKTMGWEASTERMYPEDGALKGEIK MRLKLKDGGHYDAEVKTTYMAKKPVQLPGAYKTD IKLDITSHNEDYTIVEQYERAEGRHSTGATSEFGRPG STMRRRRRRRR
FGF2B mRFP 8R	TYRSRKYTSWYVALKRMASSEDVIKEFMRFKVRME GSVNGHEFEIEGEGEGRPYEGTQTAKLKVTKGGPLP FAWDILSPQFQYGSKAYVKHPADIPDYLKLSFPEGF KWERVMNFEDGGVVTVTQDSSLQDGEFIYKVKLRG TNFPSDGPVMQKKTMGWEASTERMYPEDGALKGEI KMRLKLKDGGHYDAEVKTTYMAKKPVQLPGAYKT DIKLDITSHNEDYTIVEQYERAEGRHSTGATSEFGRP GSTMRRRRRRRR
FGF2C mRFP 8R	RTGQYKLGSKTGPGQKMASSEDVIKEFMRFKVRME GSVNGHEFEIEGEGEGRPYEGTQTAKLKVTKGGPLP FAWDILSPQFQYGSKAYVKHPADIPDYLKLSFPEGF KWERVMNFEDGGVVTVTQDSSLQDGEFIYKVKLRG TNFPSDGPVMQKKTMGWEASTERMYPEDGALKGEI KMRLKLKDGGHYDAEVKTTYMAKKPVQLPGAYKT

	DIKLDITSHNEDYTIVEQYERAEGRHSTGATSEFGRP GSTMRRRRRRRR
FGF4A mRFP 8R	KRLRRLYCNVGIGFHLQALPDGRIGGAHADTRDSLL ELSPVERGVVSIFGVMASSEDVIKEFMRFKVRMEGS VNGHEFEIEGEGEGRPYEGTQTAKLKVTKGGPLPFA WDILSPQFQYGSKAYVKHPADIPDYLKLSFPEGFKW ERVMNFEDGGVVTVTQDSSLQDGEFIYKVKLRGTN FPSDGPVMQKKTMGWEASTERMYPEDGALKGEIK MRLKLKDGGHYDAEVKTTYMAKKPVQLPGAYKTD IKLDITSHNEDYTIVEQYERAEGRHSTGATSEFGRPG STMRRRRRRRR
FGF4B mRFP 8R	AYESYKYPGMFIALSKMASSEDVIKEFMRFKVRME GSVNGHEFEIEGEGEGRPYEGTQTAKLKVTKGGPLP FAWDILSPQFQYGSKAYVKHPADIPDYLKLSFPEGF KWERVMNFEDGGVVTVTQDSSLQDGEFIYKVKLRG TNFPSDGPVMQKKTMGWEASTERMYPEDGALKGEI KMRLKLKDGGHYDAEVKTTYMAKKPVQLPGAYKT DIKLDITSHNEDYTIVEQYERAEGRHSTGATSEFGRP GSTMRRRRRRRR
FGF4C mRFP 8R	KNGKTKKGNRVSPTMKMASSEDVIKEFMRFKVRME GSVNGHEFEIEGEGEGRPYEGTQTAKLKVTKGGPLP FAWDILSPQFQYGSKAYVKHPADIPDYLKLSFPEGF KWERVMNFEDGGVVTVTQDSSLQDGEFIYKVKLRG TNFPSDGPVMQKKTMGWEASTERMYPEDGALKGEI KMRLKLKDGGHYDAEVKTTYMAKKPVQLPGAYKT

	DIKLDITSHNEDYTIVEQYERAEGRHSTGATSEFGRP GSTMRRRRRRRR
FGF7B mRFP 8R	TYASAKWTHNGGEMFVALNQMASSEDVIKEFMRF KVRMEGSVNGHEFEIEGEGEGRPYEGTQTAKLKVT KGGPLPFAWDILSPQFQYGSKAYVKHPADIPDYLKL SFPEGFKWERVMNFEDGGVVTVTQDSSLQDGEFIYK VKLRGTNFPSDGPVMQKKTMGWEASTERMYPEDG ALKGEIKMRLKLKDGGHYDAEVKTTYMAKKPVQL PGAYKTDIKLDITSHNEDYTIVEQYERAEGRHSTGAT SEFGRPGSTMRRRRRRRR
FGF7C mRFP 8R	QKGIPVRGKKTKKEQKMASSEDVIKEFMRFKVRME GSVNGHEFEIEGEGEGRPYEGTQTAKLKVTKGGPLP FAWDILSPQFQYGSKAYVKHPADIPDYLKLSFPEGF KWERVMNFEDGGVVTVTQDSSLQDGEFIYKVKLRG TNFPSDGPVMQKKTMGWEASTERMYPEDGALKGEI KMRLKLKDGGHYDAEVKTTYMAKKPVQLPGAYKT DIKLDITSHNEDYTIVEQYERAEGRHSTGATSEFGRP GSTMRRRRRRRR
ATIII mRFP 8R	AKLNCRLYRKANKSSKLVSANRMASSEDVIKEFMR FKVRMEGSVNGHEFEIEGEGEGRPYEGTQTAKLKVT KGGPLPFAWDILSPQFQYGSKAYVKHPADIPDYLKL SFPEGFKWERVMNFEDGGVVTVTQDSSLQDGEFIYK VKLRGTNFPSDGPVMQKKTMGWEASTERMYPEDG ALKGEIKMRLKLKDGGHYDAEVKTTYMAKKPVQL

	PGAYKTDIKLDITSHNEDYTIVEQYERAEGRHSTGAT SEFGRPGSTMRRRRRRRR
PDGF mRFP 8R	GRPRESGKKRKRKRLKPTMASSEDVIKEFMRFKVR MEGSVNGHEFEIEGEGEGRPYEGTQTAKLKVTKGGP LPFAWDILSPQFQYGSKAYVKHPADIPDYLKLSFPEG FKWERVMNFEDGGVVTVTQDSSLQDGEFIYKVKLR GTNFPSDGPVMQKKTMGWEASTERMYPEDGALKG EIKMRLKLKDGGHYDAEVKTTYMAKKPVQLPGAY KTDIKLDITSHNEDYTIVEQYERAEGRHSTGATSEFG RPGSTMRRRRRRRR
VEGF mRFP 8R	ARQENPCGPCSERRKHLFVQDPQTCKCSCKNTDSRC KARQLELNERTCRCDKPRRMASSEDVIKEFMRFKVR MEGSVNGHEFEIEGEGEGRPYEGTQTAKLKVTKGGP LPFAWDILSPQFQYGSKAYVKHPADIPDYLKLSFPEG FKWERVMNFEDGGVVTVTQDSSLQDGEFIYKVKLR GTNFPSDGPVMQKKTMGWEASTERMYPEDGALKG EIKMRLKLKDGGHYDAEVKTTYMAKKPVQLPGAY KTDIKLDITSHNEDYTIVEQYERAEGRHSTGATSEFG RPGSTMRRRRRRRR

Table 6.2 Amino acid sequences of the HS4C3 antibody-derived recombinant proteins.

Protein	Amino acid sequence
HS4C3 mRFP	MEVQLVESGGGLVQPRGSLRLSCAASGFTVSSN EMSWIRQAPGKGLWVSSISGGSTYYADSRKGRF TISRDNSKNTLYLQMNNLRAEGTAAYYCGRRL KDPSTPPTPSPSTPPTPSPSMASSEDVIKEFMRFK VRMEGSVNGHEFEIEGEGEGRPYEGTQTAKLKV TKGGPLPFAWDILSPQFQYGSKAYVKHPADIPD YLKLSFPEGFKWERVMNFEDGGVVTVTQDSSL QDGEFIYKVKLRGTNFPSDGPVMQKKTMGWEA STERMYPEDGALKGEIKMRLKLKDGGHYDAEV KTTYMAKKPVQLPGAYKTDIKLDITSHNEDYTI VEQYERAEGRHSTGATSEFGRPGSTM
HS4C3 mRFP 8R	MEVQLVESGGGLVQPRGSLRLSCAASGFTVSSN EMSWIRQAPGKGLWVSSISGGSTYYADSRKGRF TISRDNSKNTLYLQMNNLRAEGTAAYYCGRRL KDPSTPPTPSPSTPPTPSPSMASSEDVIKEFMRFK VRMEGSVNGHEFEIEGEGEGRPYEGTQTAKLKV TKGGPLPFAWDILSPQFQYGSKAYVKHPADIPD YLKLSFPEGFKWERVMNFEDGGVVTVTQDSSL QDGEFIYKVKLRGTNFPSDGPVMQKKTMGWEA STERMYPEDGALKGEIKMRLKLKDGGHYDAEV KTTYMAKKPVQLPGAYKTDIKLDITSHNEDYTI VEQYERAEGRHSTGATSEFGRPGSTMRRRRRRR R

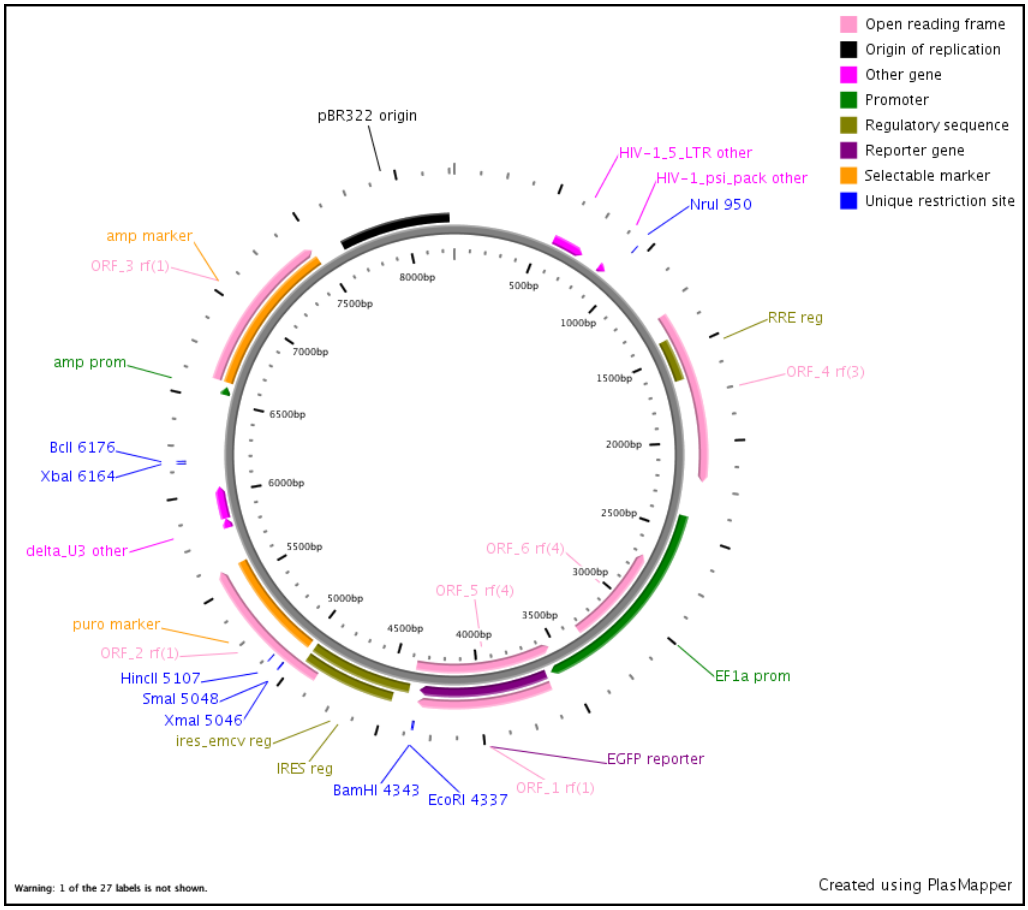


Figure 6.1 Plasmid map of pSIN GFP IRES PURO (Addgene).

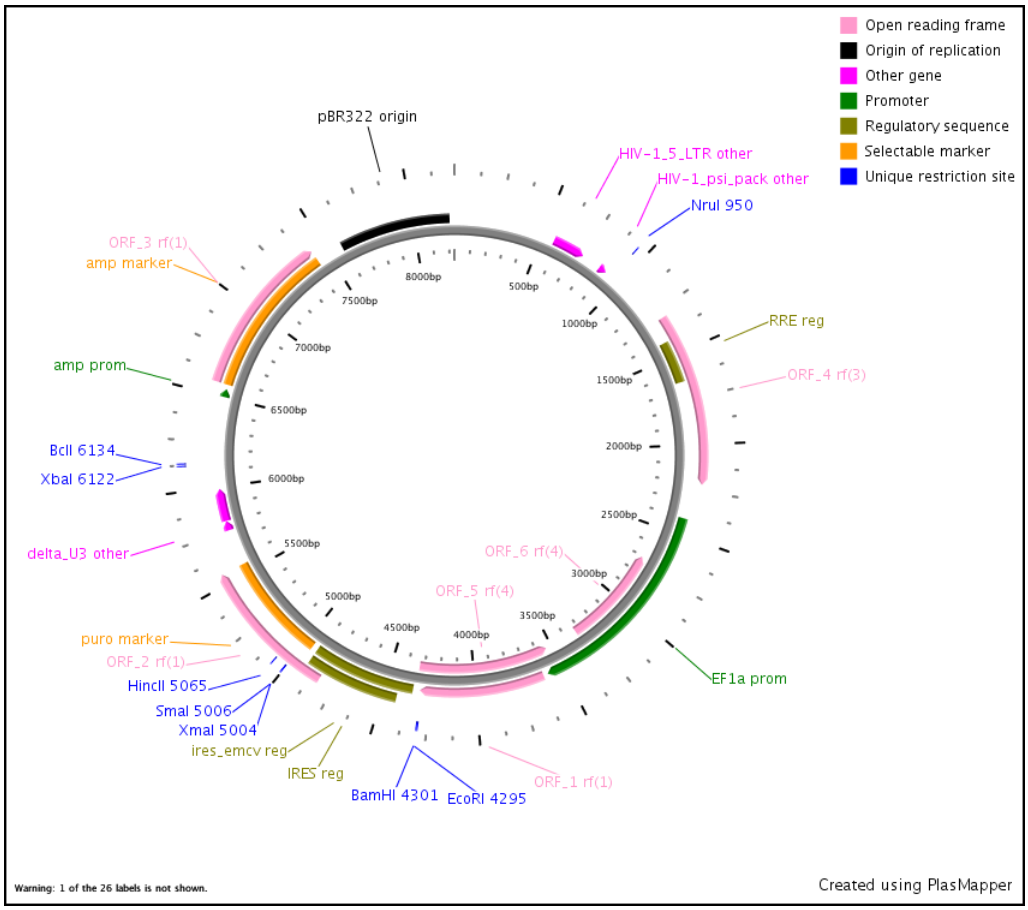


Figure 6.2 Plasmid map of pSIN mRFP NSR IRES PURO (Addgene).

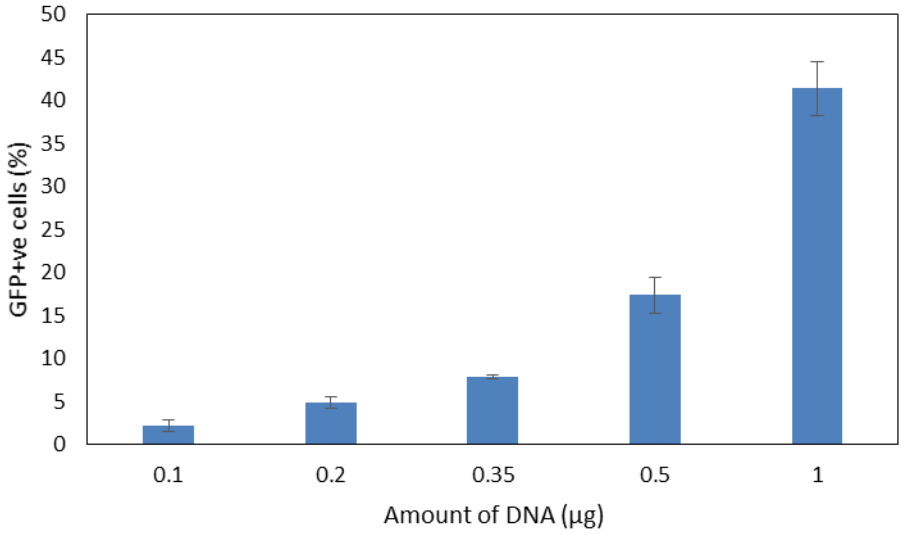


Figure 6.3 NIH3T3 cells were transfected with 0.1, 0.2, 0.35, 0.5 and 1 µg of pSIN GFP by FGF2B LK15 8R (CR3) for 24 h. Flow cytometry analysis was used to quantify the percentage of GFP positive cells. Error bars indicate SD, n = 3.

CHAPTER 7 References

ABRAMSSON, A., KURUP, S., BUSSE, M., YAMADA, S., LINDBLOM, P., SCHALLMEINER, E., STENZEL, D., SAUVAGET, D., LEDIN, J., RINGVALL, M., LANDEGREN, U., KJELLEN, L., BONDJERS, G., LI, J. P., LINDAHL, U., SPILLMANN, D., BETSHOLTZ, C. & GERHARDT, H. 2007. Defective N-sulfation of heparan sulfate proteoglycans limits PDGF-BB binding and pericyte recruitment in vascular development. *Genes & Development,* 21**,** 316-331.

ALLEN, T. M. & CULLIS, P. R. 2013. Liposomal drug delivery systems: From concept to clinical applications. *Advanced Drug Delivery Reviews,* 65**,** 36-48.

ALTON, E., ARMSTRONG, D. K., ASHBY, D., BAYFIELD, K. J., BILTON, D., BLOOMFIELD, E. V., BOYD, A. C., BRAND, J., BUCHAN, R., CALCEDO, R., CARVELLI, P., CHAN, M., CHENG, S. H., COLLIE, D. D. S., CUNNINGHAM, S., DAVIDSON, H. E., DAVIES, G., DAVIES, J. C., DAVIES, L. A., DEWAR, M. H., DOHERTY, A., DONOVAN, J., DWYER, N. S., ELGMATI, H. I., FEATHERSTONE, R. F., GAVINO, J., GEA-SORLI, S., GEDDES, D. M., GIBSON, J. S. R., GILL, D. R., GREENING, A. P., GRIESENBACH, U., HANSELL, D. M., HARMAN, K., HIGGINS, T. E., HODGES, S. L., HYDE, S. C., HYNDMAN, L., INNES, J. A., JACOB, J., JONES, N., KEOGH, B. F., LIMBERIS, M. P., LLOYD-EVANS, P., MACLEAN, A. W., MANVELL, M. C., MCCORMICK, D., MCGOVERN, M., MCLACHLAN, G., MENG, C. X., MONTERO, M. A., MILLIGAN, H., MOYCE, L. J., MURRAY, G. D., NICHOLSON, A. G., OSADOLOR, T., PARRA-LEITON, J., PORTEOUS, D. J., PRINGLE, I. A., PUNCH, E. K., PYTEL, K. M., QUITTNER, A. L., RIVELLINI, G., SAUNDERS, C. J., SCHEULE, R. K., SHEARD, S., SIMMONDS, N. J., SMITH, K., SMITH, S. N., SOUSSI, N., SOUSSI, S., SPEARING, E. J., STEVENSON, B. J., SUMNER-JONES, S. G., TURKKILA, M., URETA, R. P., WALLER, M. D., WASOWICZ, M. Y., WILSON, J. M., WOLSTENHOLME-HOGG, P. & CO, U. K. C. F. G. T. 2015. Repeated nebulisation of non-viral CFTR gene therapy in patients with cystic fibrosis: a randomised, double-blind, placebo-controlled, phase 2b trial. *Lancet Respiratory Medicine,* 3**,** 684-691.

ANDALOUSSI, S. E. L., LEHTO, T., MAGER, I., ROSENTHAL-AIZMAN, K., OPREA, II, SIMONSON, O. E., SORK, H., EZZAT, K., COPOLOVICI, D. M., KURRIKOFF, K., VIOLA, J. R., ZAGHLOUL, E. M., SILLARD, R., JOHANSSON, H. J., HASSANE, F. S., GUTERSTAM, P., SUHORUTSENKO, J., MORENO, P. M. D., OSKOLKOV, N., HALLDIN, J., TEDEBARK, U., METSPALU, A., LEBLEU, B., LEHTIO, J., SMITH, C. I. E. & LANGEL, U. 2011. Design of a peptide-based vector, PepFect6, for efficient delivery of

siRNA in cell culture and systemically in vivo. *Nucleic Acids Research,* 39**,** 3972-3987.

ARAP, M. A. 2005. Phage display technology - Applications and innovations. *Genetics and Molecular Biology,* 28**,** 1-9.

ASHIKARI, S., HABUCHI, H. & KIMATA, K. 1995. CHARACTERIZATION OF HEPARAN-SULFATE OLIGOSACCHARIDES THAT BIND TO HEPATOCYTE GROWTH-FACTOR. *Journal of Biological Chemistry,* 270**,** 29586-29593.

BALDWIN, R. J., TEN DAM, G. B., VAN KUPPEVELT, T. H., LACAUD, G., GALLAGHER, J. T., KOUSKOFF, V. & MERRY, C. L. R. 2008. A Developmentally Regulated Heparan Sulfate Epitope Defines a Subpopulation with Increased Blood Potential During Mesodermal Differentiation. *Stem Cells,* 26**,** 3108-3118.

BAREFORD, L. A. & SWAAN, P. W. 2007. Endocytic mechanisms for targeted drug delivery. *Advanced Drug Delivery Reviews,* 59**,** 748-758.

BECATTINI, G., MATTOS, L. S. & CALDWELL, D. G. 2014. A Fully Automated System for Adherent Cells Microinjection. *Ieee Journal of Biomedical and Health Informatics,* 18**,** 83-93.

BELAYET, H. M., KANAYAMA, N., KHATUN, S., SUMIMOTO, K., KOBAYASHI, T. & TERAO, T. 1999. Binding of interleukin-8 to heparan sulphate enhances cervical maturation in rabbits. *Molecular Human Reproduction,* 5**,** 261-269.

BREUNIG, M., LUNGWITZ, U., LIEBL, R. & GOEPFERICH, A. 2007. Breaking up the correlation between efficacy and toxicity for nonviral gene delivery. *Proceedings of the National Academy of Sciences of the United States of America,* 104**,** 14454-14459.

BRICKMAN, Y. G., FORD, M. D., GALLAGHER, J. T., NURCOMBE, V., BARTLETT, P. F. & TURNBULL, J. E. 1998. Structural modification of fibroblast growth factor-binding heparan sulfate at a determinative stage of neural development. *Journal of Biological Chemistry,* 273**,** 4350-4359.

CARPENTIER, M., DENYS, A., ALLAIN, F. & VERGOTEN, G. 2014. Molecular docking of heparin oligosaccharides with Hep-II heparin-binding domain of fibronectin reveals an interplay between the different positions of sulfate groups. *Glycoconjugate Journal,* 31**,** 161-169.

CARTER, N. M., ALI, S. & KIRBY, J. A. 2003. Endothelial inflammation: the role of differential expression of N-deacetylase/N-sulphotransferase enzymes in alteration of the immunological properties of heparan sulphate. *Journal of Cell Science,* 116**,** 3591-3600.

CHIAPPINI, C., DE ROSA, E., MARTINEZ, J. O., LIU, X., STEELE, J., STEVENS, M. M. & TASCIOTTI, E. 2015. Biodegradable silicon nanoneedles delivering nucleic acids intracellularly induce localized in vivo neovascularization. *Nature Materials,* 14**,** 532-539.

CHOI, S. I., MAENG, Y. S., KIM, T. I., LEE, Y., KIM, Y. S. & KIM, E. K. 2015. Lysosomal Trafficking of TGFBIp via Caveolae-Mediated Endocytosis. *Plos One,* 10.

CIFTCI, K. & LEVY, R. J. 2001. Enhanced plasmid DNA transfection with lysosomotropic agents in cultured fibroblasts. *International Journal of Pharmaceutics,* 218**,** 81-92.

COHEN, H., LEVY, R. J., GAO, J., FISHBEIN, I., KOUSAEV, V., SOSNOWSKI, S., SLOMKOWSKI, S. & GOLOMB, G. 2000. Sustained delivery and expression of DNA encapsulated in polymeric nanoparticles. *Gene Therapy,* 7**,** 1896-1905.

COOMBE, D. R. 2008. Biological implications of glycosaminoglycan interactions with haemopoietic cytokines. *Immunology and Cell Biology,* 86**,** 598-607.

COPOLOVICI, D. M., LANGEL, K., ERISTE, E. & LANGEL, U. 2014. Cell-Penetrating Peptides: Design, Synthesis, and Applications. *Acs Nano,* 8**,** 1972-1994.

CROMBEZ, L., MORRIS, M. C., DESHAYES, S., HEITZ, F. & DIVITA, G. 2008. Peptide-Based Nanoparticle for Ex Vivo and In Vivo Dug Delivery. *Current Pharmaceutical Design,* 14**,** 3656-3665.

DE FIGUEIREDO, I. R., FREIRE, J. M., FLORES, L., VEIGA, A. S. & CASTANHO, M. 2014. Cell-penetrating peptides: A tool for effective delivery in gene-targeted therapies. *Iubmb Life,* 66**,** 182-194.

DEAN, D. A., STRONG, D. D. & ZIMMER, W. E. 2005. Nuclear entry of nonviral vectors. *Gene Therapy,* 12**,** 881-890.

DELEHEDDE, M., DEUDON, E., BOILLY, B. & HONDERMARCK, H. 1997. Proteoglycans in breast cancer. *Pathologie Biologie,* 45**,** 305-311.

DEMETRIOU, M., BINKERT, C., SUKHU, B., TENENBAUM, H. C. & DENNIS, J. W. 1996. Fetuin/alpha 2-HS glycoprotein is a transforming growth factor-beta type II receptor mimic and cytokine antagonist. *Journal of Biological Chemistry,* 271**,** 12755-12761.

DESHAYES, S., KONATE, K., ALDRIAN, G., HEITZ, F. & DIVITA, G. 2011. Interactions of Amphipathic CPPs with Model Membranes. *In:* LANGEL, U. (ed.) *Cell-Penetrating Peptides: Methods and Protocols.* Totowa: Humana Press Inc.

DI PISA, M., CHASSAING, G. & SWIECICKI, J. M. 2015. Translocation Mechanism(s) of Cell-Penetrating Peptides: Biophysical Studies Using Artificial Membrane Bilayers. *Biochemistry,* 54**,** 194-207.

DICK, E., MATSA, E., YOUNG, L. E., DARLING, D. & DENNING, C. 2011. Faster generation of hiPSCs by coupling high-titer lentivirus and column-based positive selection. *Nature Protocols,* 6**,** 701-714.

DIXON, J. E., OSMAN, G., MORRIS, G. E., MARKIDES, H., ROTHERHAM, M., BAYOUSSEF, Z., EL HAJ, A. J., DENNING, C. & SHAKESHEFF, K. M. 2016. Highly efficient delivery of functional cargoes by the synergistic effect of GAG binding motifs and cell-penetrating peptides. *Proceedings of the National Academy of Sciences of the United States of America,* 113**,** E291-E299.

DOHERTY, G. J. & MCMAHON, H. T. 2009. Mechanisms of Endocytosis. *Annual Review of Biochemistry.*

DUCHARDT, F., FOTIN-MLECZEK, M., SCHWARZ, H., FISCHER, R. & BROCK, R. 2007. A comprehensive model for the cellular uptake of cationic cell-penetrating peptides. *Traffic,* 8**,** 848-866.

DURAN, M. C., WILLENBROCK, S., BARCHANSKI, A., MULLER, J. M. V., MAIOLINI, A., SOLLER, J. T., BARCIKOWSKI, S., NOLTE, I., FEIGE, K. & ESCOBAR, H. M. 2011. Comparison of nanoparticle-mediated transfection methods for DNA expression plasmids: efficiency and cytotoxicity. *Journal of Nanobiotechnology,* 9.

EGUCHI, A., MEADE, B. R., CHANG, Y. C., FREDRICKSON, C. T., WILLERT, K., PURI, N. & DOWDY, S. F. 2009. Efficient siRNA delivery into primary cells by a peptide transduction domain-dsRNA binding domain fusion protein. *Nature Biotechnology,* 27**,** 567-U110.

ELMQUIST, A., HANSEN, M. & LANGEL, U. 2006. Structure-activity relationship study of the cell-penetrating peptide pVEC. *Biochimica Et Biophysica Acta-Biomembranes,* 1758**,** 721-729.

ELTAHER, H. M., YANG, J., SHAKESHEFF, K. M. & DIXON, J. E. 2016. Highly efficient intracellular transduction in three-dimensional gradients for programming cell fate. *Acta Biomaterialia,* 41**,** 181-192.

FAHY, J. V. & DICKEY, B. F. 2010. MEDICAL PROGRESS Airway Mucus Function and Dysfunction. *New England Journal of Medicine,* 363**,** 2233-2247.

FEITSMA, K., HAUSSER, H., ROBENEK, H., KRESSE, H. & VISCHER, P. 2000. Interaction of thrombospondin-1 and heparan sulfate from endothelial cells - Structural requirements of heparan sulfate. *Journal of Biological Chemistry,* 275**,** 9396-9402.

FISCHER, R., WAIZENEGGER, T., KOHLER, K. & BROCK, R. 2002. A quantitative validation of fluorophore-labelled cell-permeable peptide conjugates: fluorophore and cargo dependence of import. *Biochimica Et Biophysica Acta-Biomembranes,* 1564**,** 365-374.

FOERG, C. & MERKLE, H. P. 2008. On the biomedical promise of cell penetrating peptides: Limits versus prospects. *Journal of Pharmaceutical Sciences,* 97**,** 144-162.

FONSECA, S. B., PEREIRA, M. P. & KELLEY, S. O. 2009. Recent advances in the use of cell-penetrating peptides for medical and biological applications. *Advanced Drug Delivery Reviews,* 61**,** 953-964.

FRENCH, M. M., SMITH, S. E., AKANBI, K., SANFORD, T., HECHT, J., FARACH-CARSON, M. C. & CARSON, D. D. 1999. Expression of the heparan sulfate proteoglycan, perlecan, during mouse embryogenesis and perlecan chondrogenic activity in vitro. *Journal of Cell Biology,* 145**,** 1103-1115.

FUSTER, M. M. & ESKO, J. D. 2005. The sweet and sour of cancer: Glycans as novel therapeutic targets. *Nature Reviews Cancer,* 5**,** 526-542.

FUTAKI, S., NAKASE, I., TACLOKORO, A., TAKEUCHI, T. & JONES, A. T. 2007. Arginine-rich peptides and their internalization mechanisms. *Biochemical Society Transactions,* 35**,** 784-787.

FUTAKI, S., SUZUKI, T., OHASHI, W., YAGAMI, T., TANAKA, S., UEDA, K. & SUGIURA, Y. 2001. Arginine-rich peptides - An abundant source of membrane-permeable peptides having potential as carriers for intracellular protein delivery. *Journal of Biological Chemistry,* 276**,** 5836-5840.

GAJ, T., GERSBACH, C. A. & BARBAS, C. F. 2013. ZFN, TALEN, and CRISPR/Cas-based methods for genome engineering. *Trends in Biotechnology,* 31**,** 397-405.

GAO, X. X., STANGER, K., KALUARACHCHI, H., MAURER, T., CIEPLA, P., CHALOUNI, C., FRANKE, Y. & HANNOUSH, R. N. 2016. Cellular uptake of a cystine-knot peptide and modulation of its intracellular trafficking. *Scientific Reports,* 6.

GERLZA, T., HECHER, B., JEREMIC, D., FUCHS, T., GSCHWANDTNER, M., FALSONE, A., GESSLBAUER, B. & KUNGL, A. J. 2014. A Combinatorial Approach to Biophysically Characterise Chemokine-Glycan Binding Affinities for Drug Development. *Molecules,* 19**,** 10618-10634.

GIRALDO, A. M. V., APPELQVIST, H., EDERTH, T. & OLLINGER, K. 2014. Lysosomotropic agents: impact on lysosomal membrane permeabilization and cell death. *Biochemical Society Transactions,* 42**,** 1460-1464.

GOLLAPUDI, L. & OBLINGER, M. M. 1999. Stable transfection of PC12 cells with estrogen receptor (ER alpha): Protective effects of estrogen on cell survival after serum deprivation. *Journal of Neuroscience Research,* 56**,** 99-108.

GREEN, M. & LOEWENSTEIN, P. M. 1988. AUTONOMOUS FUNCTIONAL DOMAINS OF CHEMICALLY SYNTHESIZED HUMAN IMMUNODEFICIENCY VIRUS TAT TRANS-ACTIVATOR PROTEIN. *Cell,* 55**,** 1179-1188.

GRIESENBACH, U., PYTEL, K. M. & ALTON, E. 2015. Cystic Fibrosis Gene Therapy in the UK and Elsewhere. *Human Gene Therapy,* 26**,** 266-275.

HUANG, Y. W., LEE, H. J., TOLLIVER, L. M. & ARONSTAM, R. S. 2015. Delivery of Nucleic Acids and Nanomaterials by Cell-Penetrating Peptides: Opportunities and Challenges. *Biomed Research International*.

JIAO, C. Y., DELAROCHE, D., BURLINA, F., ALVES, I. D., CHASSAING, G. & SAGAN, S. 2009. Translocation and Endocytosis for Cell-penetrating Peptide Internalization. *Journal of Biological Chemistry,* 284**,** 33957-33965.

JONES, A. M. & HELM, J. M. 2009. Emerging Treatments in Cystic Fibrosis. *Drugs,* 69**,** 1903-1910.

KAPLAN, I. M., WADIA, J. S. & DOWDY, S. F. 2005. Cationic TAT peptide transduction domain enters cells by macropinocytosis. *Journal of Controlled Release,* 102**,** 247-253.

KARMALI, P. P. & CHAUDHURI, A. 2007. Cationic Liposomes as non-viral carriers of gene medicines: Resolved issues, open questions, and future promises. *Medicinal Research Reviews,* 27**,** 696-722.

KHANDARE, J. & MINKO, T. 2006. Polymer-drug conjugates: Progress in polymeric prodrugs. *Progress in Polymer Science,* 31**,** 359-397.

KIM, T. K. & EBERWINE, J. H. 2010. Mammalian cell transfection: the present and the future. *Analytical and Bioanalytical Chemistry,* 397**,** 3173-3178.

KLEEMANN, E., NEU, M., JEKEL, N., FINK, L., SCHMEHL, T., GESSLER, T., SEEGER, W. & KISSEL, T. 2005. Nano-carriers for DNA delivery to the lung based upon a TAT-derived peptide covalently coupled to PEG-PEI. *Journal of Controlled Release,* 109**,** 299-316.

KOGURE, K., AKITA, H., YAMADA, Y. & HARASHIMA, H. 2008. Multifunctional envelope-type nano device (MEND) as a non-viral gene delivery system. *Advanced Drug Delivery Reviews,* 60**,** 559-571.

KOIVUSALO, M., WELCH, C., HAYASHI, H., SCOTT, C. C., KIM, M., ALEXANDER, T., TOURET, N., HAHN, K. M. & GRINSTEIN, S. 2010. Amiloride inhibits macropinocytosis by lowering submembranous pH and preventing Rac1 and Cdc42 signaling. *Journal of Cell Biology,* 188**,** 547-563.

KOTTERMAN, M. A. & SCHAFFER, D. V. 2014. Engineering adeno-associated viruses for clinical gene therapy. *Nature Reviews Genetics,* 15**,** 445-451.

KWOK, K. Y., PARK, Y., YANG, Y. S., MCKENZIE, D. L., LIU, Y. H. & RICE, K. G. 2003. In vivo gene transfer using sulfhydryl cross-linked PEG-peptide/glycopeptide DNA co-condensates. *Journal of Pharmaceutical Sciences,* 92**,** 1174-1185.

LAI, S. K., WANG, Y. Y. & HANES, J. 2009. Mucus-penetrating nanoparticles for drug and gene delivery to mucosal tissues. *Advanced Drug Delivery Reviews,* 61**,** 158-171.

LAM, A. P. & DEAN, D. A. 2010. Progress and prospects: nuclear import of nonviral vectors. *Gene Therapy,* 17**,** 439-447.

LAMBRICHT, L., LOPES, A., KOS, S., SERSA, G., PREAT, V. & VANDERMEULEN, G. 2016. Clinical potential of electroporation for gene therapy and DNA vaccine delivery. *Expert Opinion on Drug Delivery,* 13**,** 295-310.

LAWRENCE, M. S., PHILLIPS, K. J. & LIU, D. R. 2007. Supercharging proteins can impart unusual resilience. *Journal of the American Chemical Society,* 129**,** 10110-+.

LEE, A. V., OESTERREICH, S. & DAVIDSON, N. E. 2015. MCF-7 Cells-Changing the Course of Breast Cancer Research and Care for 45 Years. *Jnci-Journal of the National Cancer Institute,* 107.

LEHTO, T., ABES, R., OSKOLKOV, N., SUHORUTSENKO, J., COPOLOVICI, D. M., MAGER, I., VIOLA, J. R., SIMONSON, O. E., EZZAT, K., GUTERSTAM, P., ERISTE, E., SMITH, C. I. E., LEBLEU, B., EL ANDALOUSSI, S. & LANGEL, U. 2010. Delivery of nucleic acids with a stearylated (RxR)(4) peptide using a non-covalent co-incubation strategy. *Journal of Controlled Release,* 141**,** 42-51.

LEHTO, T., KURRIKOFF, K. & LANGEL, U. 2012. Cell-penetrating peptides for the delivery of nucleic acids. *Expert Opinion on Drug Delivery,* 9**,** 823-836.

LEHTO, T., SIMONSON, O. E., MAGER, I., EZZAT, K., SORK, H., COPOLOVICI, D. M., VIOLA, J. R., ZAGHLOUL, E. M., LUNDIN, P., MORENO, P. M. D., MAE, M., OSKOLKOV, N., SUHORUTSENKO, J., SMITH, C. I. E. & ANDALOUSSI, S. E. L. 2011. A Peptide-based Vector for Efficient Gene Transfer In Vitro and In Vivo. *Molecular Therapy,* 19**,** 1457-1467.

LI, W. J., NICOL, F. & SZOKA, F. C. 2004. GALA: a designed synthetic pH-responsive amphipathic peptide with applications in drug and gene delivery. *Advanced Drug Delivery Reviews,* 56**,** 967-985.

LI, Y., SUN, C. Y., YATES, E. A., JIANG, C., WILKINSON, M. C. & FERNIG, D. G. 2016. Heparin binding preference and structures in the fibroblast growth factor family parallel their evolutionary diversification. *Open Biology,* 6.

LINHARDT, J. D. E. A. R. J. 2009. Proteins that Bind Sulfated Glycosaminoglycans. *Essentials of Glycobiology. 2nd edition,* 35.

LIPSCOMBE, R. J., NAKHOUL, A. M., SANDERSON, C. J. & COOMBE, D. R. 1998. Interleukin-5 binds to heparin heparan sulfate. A model for an interaction with extracellular matrix. *Journal of Leukocyte Biology,* 63**,** 342-350.

LO, S. L. & WANG, S. 2008. An endosomolytic Tat peptide produced by incorporation of histidine and cysteine residues as a nonviral vector for DNA transfection. *Biomaterials,* 29**,** 2408-2414.

LORTAT-JACOB, H. 2006. Interferon and heparan sulphate. *Biochemical Society Transactions,* 34**,** 461-464.

LU, H., MCDOWELL, L. M., STUDELSKA, D. R. & ZHANG, L. 2010. Glycosaminoglycans in Human and Bovine Serum: Detection of Twenty-Four Heparan Sulfate and Chondroitin Sulfate Motifs Including a Novel Sialic Acid-modified Chondroitin Sulfate Linkage Hexasaccharide. *Glycobiology insights,* 2010**,** 13-28.

LUAN, L., MENG, Q. B., XU, L., MENG, Z., YAN, H. S. & LIU, K. L. 2015. Peptide amphiphiles with multifunctional fragments promoting cellular uptake and endosomal escape as efficient gene vectors. *Journal of Materials Chemistry B,* 3**,** 1068-1078.

LV, H. T., ZHANG, S. B., WANG, B., CUI, S. H. & YAN, J. 2006. Toxicity of cationic lipids and cationic polymers in gene delivery. *Journal of Controlled Release,* 114**,** 100-109.

MA, D. X., SHI, N. Q. & QI, X. R. 2011. Distinct transduction modes of arginine-rich cell-penetrating peptides for cargo delivery into tumor cells. *International Journal of Pharmaceutics,* 419**,** 200-208.

MADANI, F., LINDBERG, S., LANGEL, #220, LO, FUTAKI, S., GR, #228 & SLUND, A. 2011. Mechanisms of Cellular Uptake of Cell-Penetrating Peptides. *Journal of Biophysics,* 2011.

MAHTOUK, K., CREMER, F. W., REME, T., JOURDAN, M., BAUDARD, M., MOREAUX, J., REQUIRAND, G., FIOL, G., DE VOS, J., MOOS, M., QUITTET, P., GOLDSCHMIDT, H., ROSSI, J. F., HOSE, D. & KLEIN, B. 2006. Heparan sulphate proteoglycans are essential for the myeloma cell growth activity of EGF-family ligands in multiple myeloma. *Oncogene,* 25**,** 7180-7191.

MAIOLO, J. R., FERRER, M. & OTTINGER, E. A. 2005. Effects of cargo molecules on the cellular uptake of arginine-rich cell-penetrating epeptides. *Biochimica Et Biophysica Acta-Biomembranes,* 1712**,** 161-172.

MAO, S. R., SUN, W. & KISSEL, T. 2010. Chitosan-based formulations for delivery of DNA and siRNA. *Advanced Drug Delivery Reviews,* 62**,** 12-27.

MARIE, D., VAULOT, D. & PARTENSKY, F. 1996. Application of the novel nucleic acid dyes YOYO-1, YO-PRO-1, and PicoGreen for flow cytometric analysis of marine prokaryotes. *Applied and Environmental Microbiology,* 62**,** 1649-1655.

MARUYAMA, S., CANTU, E., GALILI, U., D'AGATI, V., GODMAN, G., STERN, D. M. & ANDRES, G. 2000. alpha-Galactosyl epitopes on glycoproteins of porcine renal extracellular matrix. *Kidney International,* 57**,** 655-663.

MASTORAKOS, P., DA SILVA, A. L., CHISHOLM, J., SONG, E., CHOI, W. K., BOYLE, M. P., MORALES, M. M., HANES, J. & SUK, J. S. 2015. Highly compacted biodegradable DNA nanoparticles capable of overcoming the mucus barrier for inhaled lung gene therapy. *Proceedings of the National Academy of Sciences of the United States of America,* 112**,** 8720-8725.

MATSUBARA, Y., CHIBA, T., KASHIMADA, K., MORIO, T., TAKADA, S., MIZUTANI, S. & ASAHARA, H. 2014. Transcription activator-like effector nuclease-mediated transduction of exogenous gene into IL2RG locus. *Scientific Reports,* 4.

MCNAUGHTON, B. R., CRONICAN, J. J., THOMPSON, D. B. & LIU, D. R. 2009. Mammalian cell penetration, siRNA transfection, and DNA transfection by supercharged proteins. *Proceedings of the National Academy of Sciences of the United States of America,* 106**,** 6111-6116.

MEHTA, A. 2010. The how (and why) of disease registers. *Early Human Development,* 86**,** 723-728.

MIDOUX, P., PICHON, C., YAOUANC, J. J. & JAFFRES, P. A. 2009. Chemical vectors for gene delivery: a current review on polymers, peptides and lipids containing histidine or imidazole as nucleic acids carriers. *British Journal of Pharmacology,* 157**,** 166-178.

MONTIER, T., DELEPINE, P., PICHON, C., FEREC, C., PORTEOUS, D. J. & MIDOUX, P. 2004. Non-viral vectors in cystic fibrosis gene therapy: progress and challenges. *Trends in Biotechnology,* 22**,** 586-592.

MORIGUCHI, R., KOGURE, K., AKITA, H., FUTAKI, S., MIYAGISHI, M., TAIRA, K. & HARASHIMA, H. 2005. A multifunctional envelope-type nano device for novel gene delivery of siRNA plasmids. *International Journal of Pharmaceutics,* 301**,** 277-285.

NAIMY, H., LEYMARIE, N., BOWMAN, M. J. & ZAIA, J. 2008. Characterization of heparin oligosaccharides binding specifically to antithrombin III using mass spectrometry. *Biochemistry,* 47**,** 3155-3161.

NAKAMURA, Y., KOGURE, K., YAMADA, Y., FUTAKI, S. & HARASHIMA, H. 2006. Significant and prolonged antisense effect of a multifunctional envelope-type nano device encapsulating antisense oligodeoxynucleotide. *Journal of Pharmacy and Pharmacology,* 58**,** 431-437.

OHTSUKI, T., MIKI, S., KOBAYASHI, S., HARAGUCHI, T., NAKATA, E., HIRAKAWA, K., SUMITA, K., WATANABE, K. & OKAZAKI, S. 2015. The molecular mechanism of photochemical internalization of cell penetrating peptide-cargophoto-sensitizer conjugates. *Scientific Reports,* 5.

OKITA, K. & YAMANAKA, S. 2011. Induced pluripotent stem cells: opportunities and challenges. *Philosophical Transactions of the Royal Society B-Biological Sciences,* 366**,** 2198-2207.

ORAVECZ, T., PALL, M., WANG, J. H., RODERIQUEZ, G., DITTO, M. & NORCROSS, M. A. 1997. Regulation of anti-HIV-1 activity of RANTES by heparan sulfate proteoglycans. *Journal of Immunology,* 159**,** 4587-4592.

ORTMANN, C., PICKHINKE, U., EXNER, S., OHLIG, S., LAWRENCE, R., JBOOR, H., DREIER, R. & GROBE, K. 2015. Sonic hedgehog processing and release are regulated by glypican heparan sulfate proteoglycans. *Journal of Cell Science,* 128**,** 2374-2385.

PALM-APERGI, C., LONN, P. & DOWDY, S. F. 2012. Do Cell-Penetrating Peptides Actually "Penetrate" Cellular Membranes? *Molecular Therapy,* 20**,** 695-697.

PAN, C. P., KUMAR, C., BOHL, S., KLINGMUELLER, U. & MANN, M. 2009. Comparative Proteomic Phenotyping of Cell Lines and Primary

Cells to Assess Preservation of Cell Type-specific Functions. *Molecular & Cellular Proteomics,* 8**,** 443-450.

PAN, R., XU, W., DING, Y., LU, S. & CHEN, P. 2016. Uptake Mechanism and Direct Translocation of a New CPP for siRNA Delivery. *Molecular Pharmaceutics,* 13**,** 1366-1374.

PARK, T. G., JEONG, J. H. & KIM, S. W. 2006. Current status of polymeric gene delivery systems. *Advanced Drug Delivery Reviews,* 58**,** 467-486.

PARN, K., VIRU, L., LEHTO, T., OSKOLKOV, N., LANGEL, U. & MERITS, A. 2013. Transfection of Infectious RNA and DNA/RNA Layered Vectors of Semliki Forest Virus by the Cell-Penetrating Peptide Based Reagent PepFect6. *Plos One,* 8.

PETTY, J. T., BORDELON, J. A. & ROBERTSON, M. E. 2000. Thermodynamic characterization of the association of cyanine dyes with DNA. *Journal of Physical Chemistry B,* 104**,** 7221-7227.

POOGA, M., SOOMETS, U., HALLBRINK, M., VALKNA, A., SAAR, K., REZAEI, K., KAHL, U., HAO, J. X., XU, X. J., WIESENFELD-HALLIN, Z., HOKFELT, T., BARTFAI, T. & LANGEL, U. 1998. Cell penetrating PNA constructs regulate galanin receptor levels and modify pain transmission in vivo. *Nature Biotechnology,* 16**,** 857-861.

PRESTA, M., LEALI, D., STABILE, H., RONCA, R., CAMOZZI, M., COCO, L., MORONI, E., LIEKENS, S. & RUSNATI, M. 2003. Heparin derivatives as angiogenesis inhibitors. *Current Pharmaceutical Design,* 9**,** 553-566.

PUJALS, S., SABIDO, E., TARRAGO, T. & GIRALT, E. 2007. all-D proline-rich cell-penetrating peptides: a preliminary in vivo internalization study. *Biochemical Society Transactions,* 35**,** 794-796.

RAUCHER, D. & RYU, J. S. 2015. Cell-penetrating peptides: strategies for anticancer treatment. *Trends in Molecular Medicine,* 21**,** 560-570.

RICHARD, J. P., MELIKOV, K., VIVES, E., RAMOS, C., VERBEURE, B., GAIT, M. J., CHERNOMORDIK, L. V. & LEBLEU, B. 2003. Cell-penetrating peptides - A reevaluation of the mechanism of cellular uptake. *Journal of Biological Chemistry,* 278**,** 585-590.

RICHARDSON, T. P., TRINKAUS-RANDALL, V. & NUGENT, M. A. 2001. Regulation of heparan sulfate proteoglycan nuclear localization by fibronectin. *Journal of Cell Science,* 114**,** 1613-1623.

RIDER, C. C. & MULLOY, B. 2010. Bone morphogenetic protein and growth differentiation factor cytokine families and their protein antagonists. *Biochemical Journal,* 429**,** 1-12.

ROBINSON, M., EBERL, S., TOMLINSON, C., DAVISKAS, E., REGNIS, J. A., BAILEY, D. L., TORZILLO, P. J., MENACHE, M. & BYE, P. T. 2000. Regional mucociliary clearance in patients with cystic fibrosis. *Journal of Aerosol Medicine-Deposition Clearance and Effects in the Lung,* 13**,** 73-86.

ROWE, S. M., MILLER, S. & SORSCHER, E. J. 2005. Mechanisms of disease: Cystic fibrosis. *New England Journal of Medicine,* 352**,** 1992-2001.

SALEH, A. F., AOJULA, H., ARTHANARI, Y., OFFERMAN, S., ALKOTAJI, M. & PLUEN, A. 2010. Improved Tat-mediated plasmid DNA transfer by fusion to LK15 peptide. *Journal of Controlled Release,* 143**,** 233-242.

SANDERS, N. N., DE SMEDT, S. C., VAN ROMPAEY, E., SIMOENS, P., DE BAETS, F. & DEMEESTER, J. 2000. Cystic fibrosis sputum - A barrier

to the transport of nanospheres. *American Journal of Respiratory and Critical Care Medicine,* 162**,** 1905-1911.

SANTOS, J. L., PANDITA, D., RODRIGUES, J., PEGO, A. P., GRANJA, P. L. & TOMAS, H. 2011. Non-Viral Gene Delivery to Mesenchymal Stem Cells: Methods, Strategies and Application in Bone Tissue Engineering and Regeneration. *Current Gene Therapy,* 11**,** 46-57.

SATO, H. & FELIX, J. B. 2006. Peptide-membrane interactions and mechanisms of membrane destruction by amphipathic alpha-helical antimicrobial peptides. *Biochimica Et Biophysica Acta-Biomembranes,* 1758**,** 1245-1256.

SCHAMHART, D. H. J. & KURTH, K. H. 1997. Role of proteoglycans in cell adhesion of prostate cancer cells: From review to experiment. *Urological Research,* 25**,** S89-S96.

SCHNOLZER, M., ALEWOOD, P., JONES, A., ALEWOOD, D. & KENT, S. B. H. 1992. INSITU NEUTRALIZATION IN BOC-CHEMISTRY SOLID-PHASE PEPTIDE-SYNTHESIS - RAPID, HIGH-YIELD ASSEMBLY OF DIFFICULT SEQUENCES. *International Journal of Peptide and Protein Research,* 40**,** 180-193.

SCHOONBROODT, S., STEUKERS, M., VISWANATHAN, M., FRANS, N., TIMMERMANS, M., WEHNERT, A., NGUYEN, M., LADNER, R. C. & HOET, R. M. 2008. Engineering Antibody Heavy Chain CDR3 to Create a Phage Display Fab Library Rich in Antibodies That Bind Charged Carbohydrates. *Journal of Immunology,* 181**,** 6213-6221.

SCHUSTER, B. S., ENSIGN, L. M., ALLAN, D. B., SUK, J. S. & HANES, J. 2015. Particle tracking in drug and gene delivery research: State-of-the-art applications and methods. *Advanced Drug Delivery Reviews,* 91**,** 70-91.

SCHUSTER, B. S., KIM, A. J., KAYS, J. C., KANZAWA, M. M., GUGGINO, W. B., BOYLE, M. P., ROWE, S. M., MUZYCZKA, N., SUK, J. S. & HANES, J. 2014. Overcoming the Cystic Fibrosis Sputum Barrier to Leading Adeno-associated Virus Gene Therapy Vectors. *Molecular Therapy,* 22**,** 1484-1493.

SCHWARZE, S. R., HO, A., VOCERO-AKBANI, A. & DOWDY, S. F. 1999. In vivo protein transduction: Delivery of a biologically active protein into the mouse. *Science,* 285**,** 1569-1572.

SEO, S. J., KIM, T. H., CHOI, S. J., PARK, J. H., WALL, I. B. & KIM, H. W. 2013. Gene delivery techniques for adult stem cell-based regenerative therapy. *Nanomedicine,* 8**,** 1875-1891.

SHEN, B. Q., XU, K. Y., LIU, L. N., RAAB, H., BHAKTA, S., KENRICK, M., PARSONS-REPONTE, K. L., TIEN, J., YU, S. F., MAI, E., LI, D. W., TIBBITTS, J., BAUDYS, J., SAADI, O. M., SCALES, S. J., MCDONALD, P. J., HASS, P. E., EIGENBROT, C., NGUYEN, T., SOLIS, W. A., FUJI, R. N., FLAGELLA, K. M., PATEL, D., SPENCER, S. D., KHAWLIL, L. A., EBENS, A., WONG, W. L., VANDLEN, R., KAUR, S., SLIWKOWSKI, M. X., SCHELLER, R. H., POLAKIS, P. & JUNUTULA, J. R. 2012. Conjugation site modulates the in vivo stability and therapeutic activity of antibody-drug conjugates. *Nature Biotechnology,* 30**,** 184-189.

SHERIDAN, C. 2011. Gene therapy finds its niche. *Nature Biotechnology,* 29**,** 121-128.

SHIRAISHI, T. & NIELSEN, P. E. 2006. Enhanced delivery of cell-penetrating peptide-peptide nucleic acid conjugates by endosomal disruption. *Nature Protocols,* 1**,** 633-636.

SIMOES, S., SLEPUSHKIN, V., GASPAR, R., DE LIMA, M. C. P. & DUZGUNES, N. 1998. Gene delivery by negatively charged ternary complexes of DNA, cationic liposomes and transferrin or fusigenic peptides. *Gene Therapy,* 5**,** 955-964.

SIMOES, S., SLEPUSHKIN, V., PIRES, P., GASPAR, R., DE LIMA, M. C. P. & DUZGUNES, N. 1999a. Mechanisms of gene transfer mediated by lipoplexes associated with targeting ligands or pH-sensitive peptides. *Gene Therapy,* 6**,** 1798-1807.

SIMOES, S., SLEPUSHKIN, V., PRETZER, E., DAZIN, P., GASPAR, R., DE LIMA, M. C. P. & DUZGUNES, N. 1999b. Transfection of human macrophages by lipoplexes via the combined use of transferrin and pH-sensitive peptides. *Journal of Leukocyte Biology,* 65**,** 270-279.

SORKIN, A. & VON ZASTROW, M. 2002. Signal transduction and endocytosis: Close encounters of many kinds. *Nature Reviews Molecular Cell Biology,* 3**,** 600-614.

STRINGER, S. E., FORSTER, M. J., MULLOY, B., BISHOP, C. R., GRAHAM, G. J. & GALLAGHER, J. T. 2002. Characterization of the binding site on heparan sulfate for macrophage inflammatory protein 1 alpha. *Blood,* 100**,** 1543-1550.

SUK, J. S., LAI, S. K., WANG, Y. Y., ENSIGN, L. M., ZEITLIN, P. L., BOYLE, M. P. & HANES, J. 2009. The penetration of fresh undiluted sputum expectorated by cystic fibrosis patients by non-adhesive polymer nanoparticles. *Biomaterials,* 30**,** 2591-2597.

SUK, J. S., XU, Q. G., KIM, N., HANES, J. & ENSIGN, L. M. 2016. PEGylation as a strategy for improving nanoparticle-based drug and gene delivery. *Advanced Drug Delivery Reviews,* 99**,** 28-51.

SUZUKI, R., YAMADA, Y. & HARASHIMA, H. 2007. Efficient cytoplasmic protein delivery by means of a multifunctional envelope-type nano device. *Biological & Pharmaceutical Bulletin,* 30**,** 758-762.

SWIECICKI, J. M., DI PISA, M., LIPPI, F., CHWETZOFF, S., MANSUY, C., TRUGNAN, G., CHASSAING, G., LAVIELLE, S. & BURLINA, F. 2015. Unsaturated acyl chains dramatically enhanced cellular uptake by direct translocation of a minimalist oligo-arginine lipopeptide. *Chemical Communications,* 51**,** 14656-14659.

SZWERAS, M., LIU, D. M., PARTRIDGE, E. A., PAWLING, J., SUKHU, B., CLOKIE, C., JAHNEN-DECHENT, W., TENENBAUM, H. C., SWALLOW, C. J., GRYNPAS, M. D. & DENNIS, J. W. 2002. alpha 2-HS glycoprotein/fetuin, a transforming growth factor-beta/bone morphogenetic protein antagonist, regulates postnatal bone growth and remodeling. *Journal of Biological Chemistry,* 277**,** 19991-19997.

TAKAHASHI, K. & YAMANAKA, S. 2006. Induction of pluripotent stem cells from mouse embryonic and adult fibroblast cultures by defined factors. *Cell,* 126**,** 663-676.

TERAN, M. & NUGENT, M. A. 2015. Synergistic Binding of Vascular Endothelial Growth Factor-A and Its Receptors to Heparin Selectively Modulates Complex Affinity. *Journal of Biological Chemistry,* 290**,** 16451-16462.

TJELLE, T. E., BRECH, A., JUVET, L. K., GRIFFITHS, G. & BERG, T. 1996. Isolation and characterization of early endosomes, late endosomes and terminal lysosomes: Their role in protein degradation. *Journal of Cell Science,* 109**,** 2905-2914.

TUNNEMANN, G., MARTIN, R. M., HAUPT, S., PATSCH, C., EDENHOFER, F. & CARDOSO, M. C. 2006. Cargo-dependent mode of uptake and bioavailability of TAT-containing proteins and peptides in living cells. *Faseb Journal,* 20**,** 1775-1784.

UNIEWICZ, K. A., ORI, A., XU, R. Y., AHMED, Y., WILKINSON, M. C., FERNIG, D. G. & YATES, E. A. 2010. Differential Scanning Fluorimetry Measurement of Protein Stability Changes upon Binding to Glycosaminoglycans: A Screening Test for Binding Specificity. *Analytical Chemistry,* 82**,** 3796-3802.

VAN KUPPEVELT, T. H., DENNISSEN, M., VAN VENROOIJ, W. J., HOET, R. M. A. & VEERKAMP, J. H. 1998. Generation and application of type-specific anti-heparan sulfate antibodies using phage display technology - Further evidence for heparan sulfate heterogeneity in the kidney. *Journal of Biological Chemistry,* 273**,** 12960-12966.

VEIMAN, K. L., KUNNAPUU, K., LEHTO, T., KIISHOLTS, K., PARN, K., LANGEL, U. & KURRIKOFF, K. 2015. PEG shielded MMP sensitive CPPs for efficient and tumor specific gene delivery in vivo. *Journal of Controlled Release,* 209**,** 238-247.

VERCAUTEREN, D., VANDENBROUCKE, R. E., JONES, A. T., REJMAN, J., DEMEESTER, J., DE SMEDT, S. C., SANDERS, N. N. & BRAECKMANS, K. 2010. The Use of Inhibitors to Study Endocytic Pathways of Gene Carriers: Optimization and Pitfalls. *Molecular Therapy,* 18**,** 561-569.

VERDURMEN, W. P. R., BOVEE-GEURTS, P. H., WADHWANI, P., ULRICH, A. S., HALLBRINK, M., VAN KUPPEVELT, T. H. & BROCK, R. 2011. Preferential Uptake of L- versus D-Amino Acid Cell-Penetrating Peptides in a Cell Type-Dependent Manner. *Chemistry & Biology,* 18**,** 1000-1010.

VERKMAN, A. S., LUKACS, G. L. & GALIETTA, L. J. V. 2006. CFTR chloride channel drug discovery - Inhibitors as antidiarrheals and activators for therapy of cystic fibrosis. *Current Pharmaceutical Design,* 12**,** 2235-2247.

VERONESE, F. M. & PASUT, G. 2005. PEGylation, successful approach to drug delivery. *Drug Discovery Today,* 10**,** 1451-1458.

VIVES, E., BRODIN, P. & LEBLEU, B. 1997. A truncated HIV-1 Tat protein basic domain rapidly translocates through the plasma membrane and accumulates in the cell nucleus. *Journal of Biological Chemistry,* 272**,** 16010-16017.

WADIA, J. S., STAN, R. V. & DOWDY, S. F. 2004. Transducible TAT-HA fusogenic peptide enhances escape of TAT-fusion proteins after lipid raft macropinocytosis. *Nature Medicine,* 10**,** 310-315.

WANG, H. Y., CHEN, J. X., SUN, Y. X., DENG, J. Z., LI, C., ZHANG, X. Z. & ZHUO, R. X. 2011. Construction of cell penetrating peptide vectors with N-terminal stearylated nuclear localization signal for targeted delivery of DNA into the cell nuclei. *Journal of Controlled Release,* 155**,** 26-33.

WILKINSPORT, C. E. & MCKEOWNLONGO, P. J. 1996. Heparan sulfate proteoglycans function in the binding and degradation of vitronectin by fibroblast monolayers. *Biochemistry and Cell Biology-Biochimie Et Biologie Cellulaire,* 74**,** 887-897.

WONG, F. K., HAFFNER, C., HUTTNER, W. B. & TAVERNA, E. 2014. Microinjection of membrane-impermeable molecules into single neural stem cells in brain tissue. *Nature Protocols,* 9**,** 1170-1182.

WU, H. M., PAN, S. R., CHEN, M. W., WU, Y., WANG, C., WEN, Y. T., ZENG, X. & WU, C. B. 2011. A serum-resistant polyamidoamine-based polypeptide dendrimer for gene transfection. *Biomaterials,* 32**,** 1619-1634.

WU, Z. L. L., ZHANG, L. J., YABE, T., KUBERAN, B., BEELER, D. L., LOVE, A. & ROSENBERG, R. D. 2003. The involvement of heparan sulfate (HS) in FGF1/HS/FGFR1 signaling complex. *Journal of Biological Chemistry,* 278**,** 17121-17129.

WYMAN, T. B., NICOL, F., ZELPHATI, O., SCARIA, P. V., PLANK, C. & SZOKA, F. C. 1997. Design, synthesis, and characterization of a cationic peptide that binds to nucleic acids and permeabilizes bilayers. *Biochemistry,* 36**,** 3008-3017.

XIAO, K., LI, Y. P., LUO, J. T., LEE, J. S., XIAO, W. W., GONIK, A. M., AGARWAL, R. G. & LAM, K. S. 2011. The effect of surface charge on in vivo biodistribution of PEG-oligocholic acid based micellar nanoparticles. *Biomaterials,* 32**,** 3435-3446.

XIE, Z. L., SHAO, S. L., LV, J. W., WANG, C. H., YUAN, C. Z., ZHANG, W. W. & XU, X. J. 2011. Co-transfection and tandem transfection of HEK293A cells for overexpression and Riled experiments. *Cell Biology International,* 35**,** 187-192.

YAMADA, Y., AKITA, H. & HARASHIMA, H. 2012. MULTIFUNCTIONAL ENVELOPE-TYPE NANO DEVICE (MEND) FOR ORGANELLE TARGETING VIA A STEPWISE MEMBRANE FUSION PROCESS. *In:* DUZGUNES, N. (ed.) *Nanomedicine: Infectious Diseases, Immunotherapy, Diagnostics, Antifibrotics, Toxicology and Gene Medicine.* San Diego: Elsevier Academic Press Inc.

YAMAMOTO, S., NAKASE, H., MATSUURA, M., HONZAWA, Y., MATSUMURA, K., UZA, N., YAMAGUCHI, Y., MIZOGUCHI, E. & CHIBA, T. 2013. Heparan sulfate on intestinal epithelial cells plays a critical role in intestinal crypt homeostasis via Wnt/beta-catenin signaling. *American Journal of Physiology-Gastrointestinal and Liver Physiology,* 305**,** G241-G249.

YARMUSH, M. L., GOLBERG, A., SERSA, G., KOTNIK, T. & MIKLAVCIC, D. 2014. Electroporation-Based Technologies for Medicine: Principles, Applications, and Challenges. *In:* YARMUSH, M. L. (ed.) *Annual Review of Biomedical Engineering, Vol 16.* Palo Alto: Annual Reviews.

YIN, H., KANASTY, R. L., ELTOUKHY, A. A., VEGAS, A. J., DORKIN, J. R. & ANDERSON, D. G. 2014. Non-viral vectors for gene-based therapy. *Nature Reviews Genetics,* 15**,** 541-555.

ZHANG, G. D., YANG, Z., LU, W., ZHANG, R., HUANG, Q., TIAN, M., LI, L., LIANG, D. & LI, C. 2009. Influence of anchoring ligands and particle size on the colloidal stability and in vivo biodistribution of polyethylene

glycol-coated gold nanoparticles in tumor-xenografted mice. *Biomaterials,* 30**,** 1928-1936.

ZHANG, X., PAN, S. R., HU, H. M., WU, G. F., FENG, M., ZHANG, W. & LU, X. 2008. Poly(ethylene glycol)-block-polyethylenimine copolymers as carriers for gene delivery: Effects of PEG molecular weight and PEGylation degree. *Journal of Biomedical Materials Research Part A,* 84A**,** 795-804.

ABRAMSSON, A., KURUP, S., BUSSE, M., YAMADA, S., LINDBLOM, P., SCHALLMEINER, E., STENZEL, D., SAUVAGET, D., LEDIN, J., RINGVALL, M., LANDEGREN, U., KJELLEN, L., BONDJERS, G., LI, J. P., LINDAHL, U., SPILLMANN, D., BETSHOLTZ, C. & GERHARDT, H. 2007. Defective N-sulfation of heparan sulfate proteoglycans limits PDGF-BB binding and pericyte recruitment in vascular development. *Genes & Development,* 21**,** 316-331.

ALLEN, T. M. & CULLIS, P. R. 2013. Liposomal drug delivery systems: From concept to clinical applications. *Advanced Drug Delivery Reviews,* 65**,** 36-48.

ALTON, E., ARMSTRONG, D. K., ASHBY, D., BAYFIELD, K. J., BILTON, D., BLOOMFIELD, E. V., BOYD, A. C., BRAND, J., BUCHAN, R., CALCEDO, R., CARVELLI, P., CHAN, M., CHENG, S. H., COLLIE, D. D. S., CUNNINGHAM, S., DAVIDSON, H. E., DAVIES, G., DAVIES, J. C., DAVIES, L. A., DEWAR, M. H., DOHERTY, A., DONOVAN, J., DWYER, N. S., ELGMATI, H. I., FEATHERSTONE, R. F., GAVINO, J., GEA-SORLI, S., GEDDES, D. M., GIBSON, J. S. R., GILL, D. R., GREENING, A. P., GRIESENBACH, U., HANSELL, D. M., HARMAN, K., HIGGINS, T. E., HODGES, S. L., HYDE, S. C., HYNDMAN, L., INNES, J. A., JACOB, J., JONES, N., KEOGH, B. F., LIMBERIS, M. P., LLOYD-EVANS, P., MACLEAN, A. W., MANVELL, M. C., MCCORMICK, D., MCGOVERN, M., MCLACHLAN, G., MENG, C. X., MONTERO, M. A., MILLIGAN, H., MOYCE, L. J., MURRAY, G. D., NICHOLSON, A. G., OSADOLOR, T., PARRA-LEITON, J., PORTEOUS, D. J., PRINGLE, I. A., PUNCH, E. K., PYTEL, K. M., QUITTNER, A. L., RIVELLINI, G., SAUNDERS, C. J., SCHEULE, R. K., SHEARD, S., SIMMONDS, N. J., SMITH, K., SMITH, S. N., SOUSSI, N., SOUSSI, S., SPEARING, E. J., STEVENSON, B. J., SUMNER-JONES, S. G., TURKKILA, M., URETA, R. P., WALLER, M. D., WASOWICZ, M. Y., WILSON, J. M., WOLSTENHOLME-HOGG, P. & CO, U. K. C. F. G. T. 2015. Repeated nebulisation of non-viral CFTR gene therapy in patients with cystic fibrosis: a randomised, double-blind, placebo-controlled, phase 2b trial. *Lancet Respiratory Medicine,* 3**,** 684-691.

ANDALOUSSI, S. E. L., LEHTO, T., MAGER, I., ROSENTHAL-AIZMAN, K., OPREA, II, SIMONSON, O. E., SORK, H., EZZAT, K., COPOLOVICI, D. M., KURRIKOFF, K., VIOLA, J. R., ZAGHLOUL, E. M., SILLARD, R., JOHANSSON, H. J., HASSANE, F. S., GUTERSTAM, P., SUHORUTSENKO, J., MORENO, P. M. D., OSKOLKOV, N., HALLDIN, J., TEDEBARK, U., METSPALU, A., LEBLEU, B., LEHTIO, J., SMITH, C. I. E. & LANGEL, U. 2011. Design of a peptide-based vector, PepFect6, for efficient delivery of

siRNA in cell culture and systemically in vivo. *Nucleic Acids Research,* 39**,** 3972-3987.

ARAP, M. A. 2005. Phage display technology - Applications and innovations. *Genetics and Molecular Biology,* 28**,** 1-9.

ASHIKARI, S., HABUCHI, H. & KIMATA, K. 1995. CHARACTERIZATION OF HEPARAN-SULFATE OLIGOSACCHARIDES THAT BIND TO HEPATOCYTE GROWTH-FACTOR. *Journal of Biological Chemistry,* 270**,** 29586-29593.

BALDWIN, R. J., TEN DAM, G. B., VAN KUPPEVELT, T. H., LACAUD, G., GALLAGHER, J. T., KOUSKOFF, V. & MERRY, C. L. R. 2008. A Developmentally Regulated Heparan Sulfate Epitope Defines a Subpopulation with Increased Blood Potential During Mesodermal Differentiation. *Stem Cells,* 26**,** 3108-3118.

BAREFORD, L. A. & SWAAN, P. W. 2007. Endocytic mechanisms for targeted drug delivery. *Advanced Drug Delivery Reviews,* 59**,** 748-758.

BECATTINI, G., MATTOS, L. S. & CALDWELL, D. G. 2014. A Fully Automated System for Adherent Cells Microinjection. *Ieee Journal of Biomedical and Health Informatics,* 18**,** 83-93.

BELAYET, H. M., KANAYAMA, N., KHATUN, S., SUMIMOTO, K., KOBAYASHI, T. & TERAO, T. 1999. Binding of interleukin-8 to heparan sulphate enhances cervical maturation in rabbits. *Molecular Human Reproduction,* 5**,** 261-269.

BREUNIG, M., LUNGWITZ, U., LIEBL, R. & GOEPFERICH, A. 2007. Breaking up the correlation between efficacy and toxicity for nonviral gene delivery. *Proceedings of the National Academy of Sciences of the United States of America,* 104**,** 14454-14459.

BRICKMAN, Y. G., FORD, M. D., GALLAGHER, J. T., NURCOMBE, V., BARTLETT, P. F. & TURNBULL, J. E. 1998. Structural modification of fibroblast growth factor-binding heparan sulfate at a determinative stage of neural development. *Journal of Biological Chemistry,* 273**,** 4350-4359.

CARPENTIER, M., DENYS, A., ALLAIN, F. & VERGOTEN, G. 2014. Molecular docking of heparin oligosaccharides with Hep-II heparin-binding domain of fibronectin reveals an interplay between the different positions of sulfate groups. *Glycoconjugate Journal,* 31**,** 161-169.

CARTER, N. M., ALI, S. & KIRBY, J. A. 2003. Endothelial inflammation: the role of differential expression of N-deacetylase/N-sulphotransferase enzymes in alteration of the immunological properties of heparan sulphate. *Journal of Cell Science,* 116**,** 3591-3600.

CHIAPPINI, C., DE ROSA, E., MARTINEZ, J. O., LIU, X., STEELE, J., STEVENS, M. M. & TASCIOTTI, E. 2015. Biodegradable silicon nanoneedles delivering nucleic acids intracellularly induce localized in vivo neovascularization. *Nature Materials,* 14**,** 532-539.

CHOI, S. I., MAENG, Y. S., KIM, T. I., LEE, Y., KIM, Y. S. & KIM, E. K. 2015. Lysosomal Trafficking of TGFBIp via Caveolae-Mediated Endocytosis. *Plos One,* 10.

CIFTCI, K. & LEVY, R. J. 2001. Enhanced plasmid DNA transfection with lysosomotropic agents in cultured fibroblasts. *International Journal of Pharmaceutics,* 218**,** 81-92.

COHEN, H., LEVY, R. J., GAO, J., FISHBEIN, I., KOUSAEV, V., SOSNOWSKI, S., SLOMKOWSKI, S. & GOLOMB, G. 2000. Sustained delivery and expression of DNA encapsulated in polymeric nanoparticles. *Gene Therapy,* 7**,** 1896-1905.

COOMBE, D. R. 2008. Biological implications of glycosaminoglycan interactions with haemopoietic cytokines. *Immunology and Cell Biology,* 86**,** 598-607.

COPOLOVICI, D. M., LANGEL, K., ERISTE, E. & LANGEL, U. 2014. Cell-Penetrating Peptides: Design, Synthesis, and Applications. *Acs Nano,* 8**,** 1972-1994.

CROMBEZ, L., MORRIS, M. C., DESHAYES, S., HEITZ, F. & DIVITA, G. 2008. Peptide-Based Nanoparticle for Ex Vivo and In Vivo Dug Delivery. *Current Pharmaceutical Design,* 14**,** 3656-3665.

DE FIGUEIREDO, I. R., FREIRE, J. M., FLORES, L., VEIGA, A. S. & CASTANHO, M. 2014. Cell-penetrating peptides: A tool for effective delivery in gene-targeted therapies. *Iubmb Life,* 66**,** 182-194.

DEAN, D. A., STRONG, D. D. & ZIMMER, W. E. 2005. Nuclear entry of nonviral vectors. *Gene Therapy,* 12**,** 881-890.

DELEHEDDE, M., DEUDON, E., BOILLY, B. & HONDERMARCK, H. 1997. Proteoglycans in breast cancer. *Pathologie Biologie,* 45**,** 305-311.

DEMETRIOU, M., BINKERT, C., SUKHU, B., TENENBAUM, H. C. & DENNIS, J. W. 1996. Fetuin/alpha 2-HS glycoprotein is a transforming growth factor-beta type II receptor mimic and cytokine antagonist. *Journal of Biological Chemistry,* 271**,** 12755-12761.

DESHAYES, S., KONATE, K., ALDRIAN, G., HEITZ, F. & DIVITA, G. 2011. Interactions of Amphipathic CPPs with Model Membranes. *In:* LANGEL, U. (ed.) *Cell-Penetrating Peptides: Methods and Protocols.* Totowa: Humana Press Inc.

DI PISA, M., CHASSAING, G. & SWIECICKI, J. M. 2015. Translocation Mechanism(s) of Cell-Penetrating Peptides: Biophysical Studies Using Artificial Membrane Bilayers. *Biochemistry,* 54**,** 194-207.

DICK, E., MATSA, E., YOUNG, L. E., DARLING, D. & DENNING, C. 2011. Faster generation of hiPSCs by coupling high-titer lentivirus and column-based positive selection. *Nature Protocols,* 6**,** 701-714.

DIXON, J. E., OSMAN, G., MORRIS, G. E., MARKIDES, H., ROTHERHAM, M., BAYOUSSEF, Z., EL HAJ, A. J., DENNING, C. & SHAKESHEFF, K. M. 2016. Highly efficient delivery of functional cargoes by the synergistic effect of GAG binding motifs and cell-penetrating peptides. *Proceedings of the National Academy of Sciences of the United States of America,* 113**,** E291-E299.

DOHERTY, G. J. & MCMAHON, H. T. 2009. Mechanisms of Endocytosis. *Annual Review of Biochemistry.*

DUCHARDT, F., FOTIN-MLECZEK, M., SCHWARZ, H., FISCHER, R. & BROCK, R. 2007. A comprehensive model for the cellular uptake of cationic cell-penetrating peptides. *Traffic,* 8**,** 848-866.

DURAN, M. C., WILLENBROCK, S., BARCHANSKI, A., MULLER, J. M. V., MAIOLINI, A., SOLLER, J. T., BARCIKOWSKI, S., NOLTE, I., FEIGE, K. & ESCOBAR, H. M. 2011. Comparison of nanoparticle-mediated transfection methods for DNA expression plasmids: efficiency and cytotoxicity. *Journal of Nanobiotechnology,* 9.

EGUCHI, A., MEADE, B. R., CHANG, Y. C., FREDRICKSON, C. T., WILLERT, K., PURI, N. & DOWDY, S. F. 2009. Efficient siRNA delivery into primary cells by a peptide transduction domain-dsRNA binding domain fusion protein. *Nature Biotechnology,* 27**,** 567-U110.

ELMQUIST, A., HANSEN, M. & LANGEL, U. 2006. Structure-activity relationship study of the cell-penetrating peptide pVEC. *Biochimica Et Biophysica Acta-Biomembranes,* 1758**,** 721-729.

ELTAHER, H. M., YANG, J., SHAKESHEFF, K. M. & DIXON, J. E. 2016. Highly efficient intracellular transduction in three-dimensional gradients for programming cell fate. *Acta Biomaterialia,* 41**,** 181-192.

FAHY, J. V. & DICKEY, B. F. 2010. MEDICAL PROGRESS Airway Mucus Function and Dysfunction. *New England Journal of Medicine,* 363**,** 2233-2247.

FEITSMA, K., HAUSSER, H., ROBENEK, H., KRESSE, H. & VISCHER, P. 2000. Interaction of thrombospondin-1 and heparan sulfate from endothelial cells - Structural requirements of heparan sulfate. *Journal of Biological Chemistry,* 275**,** 9396-9402.

FISCHER, R., WAIZENEGGER, T., KOHLER, K. & BROCK, R. 2002. A quantitative validation of fluorophore-labelled cell-permeable peptide conjugates: fluorophore and cargo dependence of import. *Biochimica Et Biophysica Acta-Biomembranes,* 1564**,** 365-374.

FOERG, C. & MERKLE, H. P. 2008. On the biomedical promise of cell penetrating peptides: Limits versus prospects. *Journal of Pharmaceutical Sciences,* 97**,** 144-162.

FONSECA, S. B., PEREIRA, M. P. & KELLEY, S. O. 2009. Recent advances in the use of cell-penetrating peptides for medical and biological applications. *Advanced Drug Delivery Reviews,* 61**,** 953-964.

FRENCH, M. M., SMITH, S. E., AKANBI, K., SANFORD, T., HECHT, J., FARACH-CARSON, M. C. & CARSON, D. D. 1999. Expression of the heparan sulfate proteoglycan, perlecan, during mouse embryogenesis and perlecan chondrogenic activity in vitro. *Journal of Cell Biology,* 145**,** 1103-1115.

FUSTER, M. M. & ESKO, J. D. 2005. The sweet and sour of cancer: Glycans as novel therapeutic targets. *Nature Reviews Cancer,* 5**,** 526-542.

FUTAKI, S., NAKASE, I., TACLOKORO, A., TAKEUCHI, T. & JONES, A. T. 2007. Arginine-rich peptides and their internalization mechanisms. *Biochemical Society Transactions,* 35**,** 784-787.

FUTAKI, S., SUZUKI, T., OHASHI, W., YAGAMI, T., TANAKA, S., UEDA, K. & SUGIURA, Y. 2001. Arginine-rich peptides - An abundant source of membrane-permeable peptides having potential as carriers for intracellular protein delivery. *Journal of Biological Chemistry,* 276**,** 5836-5840.

GAJ, T., GERSBACH, C. A. & BARBAS, C. F. 2013. ZFN, TALEN, and CRISPR/Cas-based methods for genome engineering. *Trends in Biotechnology,* 31**,** 397-405.

GAO, X. X., STANGER, K., KALUARACHCHI, H., MAURER, T., CIEPLA, P., CHALOUNI, C., FRANKE, Y. & HANNOUSH, R. N. 2016. Cellular uptake of a cystine-knot peptide and modulation of its intracellular trafficking. *Scientific Reports,* 6.

GERLZA, T., HECHER, B., JEREMIC, D., FUCHS, T., GSCHWANDTNER, M., FALSONE, A., GESSLBAUER, B. & KUNGL, A. J. 2014. A Combinatorial Approach to Biophysically Characterise Chemokine-Glycan Binding Affinities for Drug Development. *Molecules,* 19**,** 10618-10634.

GINDY, M. E., JI, S. X., HOYE, T. R., PANAGIOTOPOULOS, A. Z. & PRUD'HOMME, R. K. 2008. Preparation of Poly(ethylene glycol) Protected Nanoparticles with Variable Bioconjugate Ligand Density. *Biomacromolecules,* 9**,** 2705-2711.

GIRALDO, A. M. V., APPELQVIST, H., EDERTH, T. & OLLINGER, K. 2014. Lysosomotropic agents: impact on lysosomal membrane permeabilization and cell death. *Biochemical Society Transactions,* 42**,** 1460-1464.

GODBEY, W. T., WU, K. K. & MIKOS, A. G. 1999. Poly(ethylenimine) and its role in gene delivery. *Journal of Controlled Release,* 60**,** 149-160.

GOLLAPUDI, L. & OBLINGER, M. M. 1999. Stable transfection of PC12 cells with estrogen receptor (ER alpha): Protective effects of estrogen on cell survival after serum deprivation. *Journal of Neuroscience Research,* 56**,** 99-108.

GREEN, M. & LOEWENSTEIN, P. M. 1988. AUTONOMOUS FUNCTIONAL DOMAINS OF CHEMICALLY SYNTHESIZED HUMAN IMMUNODEFICIENCY VIRUS TAT TRANS-ACTIVATOR PROTEIN. *Cell,* 55**,** 1179-1188.

GRIESENBACH, U., PYTEL, K. M. & ALTON, E. 2015. Cystic Fibrosis Gene Therapy in the UK and Elsewhere. *Human Gene Therapy,* 26**,** 266-275.

HUANG, Y. W., LEE, H. J., TOLLIVER, L. M. & ARONSTAM, R. S. 2015. Delivery of Nucleic Acids and Nanomaterials by Cell-Penetrating Peptides: Opportunities and Challenges. *Biomed Research International*.

JIAO, C. Y., DELAROCHE, D., BURLINA, F., ALVES, I. D., CHASSAING, G. & SAGAN, S. 2009. Translocation and Endocytosis for Cell-penetrating Peptide Internalization. *Journal of Biological Chemistry,* 284**,** 33957-33965.

JONES, A. M. & HELM, J. M. 2009. Emerging Treatments in Cystic Fibrosis. *Drugs,* 69**,** 1903-1910.

KAPLAN, I. M., WADIA, J. S. & DOWDY, S. F. 2005. Cationic TAT peptide transduction domain enters cells by macropinocytosis. *Journal of Controlled Release,* 102**,** 247-253.

KARMALI, P. P. & CHAUDHURI, A. 2007. Cationic Liposomes as non-viral carriers of gene medicines: Resolved issues, open questions, and future promises. *Medicinal Research Reviews,* 27**,** 696-722.

KHANDARE, J. & MINKO, T. 2006. Polymer-drug conjugates: Progress in polymeric prodrugs. *Progress in Polymer Science,* 31**,** 359-397.

KIM, T. K. & EBERWINE, J. H. 2010. Mammalian cell transfection: the present and the future. *Analytical and Bioanalytical Chemistry,* 397**,** 3173-3178.

KLEEMANN, E., NEU, M., JEKEL, N., FINK, L., SCHMEHL, T., GESSLER, T., SEEGER, W. & KISSEL, T. 2005. Nano-carriers for DNA delivery to the lung based upon a TAT-derived peptide covalently coupled to PEG-PEI. *Journal of Controlled Release,* 109**,** 299-316.

KOGURE, K., AKITA, H., YAMADA, Y. & HARASHIMA, H. 2008. Multifunctional envelope-type nano device (MEND) as a non-viral gene delivery system. *Advanced Drug Delivery Reviews,* 60**,** 559-571.

KOIVUSALO, M., WELCH, C., HAYASHI, H., SCOTT, C. C., KIM, M., ALEXANDER, T., TOURET, N., HAHN, K. M. & GRINSTEIN, S. 2010. Amiloride inhibits macropinocytosis by lowering submembranous pH and preventing Rac1 and Cdc42 signaling. *Journal of Cell Biology,* 188**,** 547-563.

KOTTERMAN, M. A. & SCHAFFER, D. V. 2014. Engineering adeno-associated viruses for clinical gene therapy. *Nature Reviews Genetics,* 15**,** 445-451.

KWOK, K. Y., PARK, Y., YANG, Y. S., MCKENZIE, D. L., LIU, Y. H. & RICE, K. G. 2003. In vivo gene transfer using sulfhydryl cross-linked PEG-peptide/glycopeptide DNA co-condensates. *Journal of Pharmaceutical Sciences,* 92**,** 1174-1185.

LAI, S. K., WANG, Y. Y. & HANES, J. 2009. Mucus-penetrating nanoparticles for drug and gene delivery to mucosal tissues. *Advanced Drug Delivery Reviews,* 61**,** 158-171.

LAM, A. P. & DEAN, D. A. 2010. Progress and prospects: nuclear import of nonviral vectors. *Gene Therapy,* 17**,** 439-447.

LAMBRICHT, L., LOPES, A., KOS, S., SERSA, G., PREAT, V. & VANDERMEULEN, G. 2016. Clinical potential of electroporation for gene therapy and DNA vaccine delivery. *Expert Opinion on Drug Delivery,* 13**,** 295-310.

LAWRENCE, M. S., PHILLIPS, K. J. & LIU, D. R. 2007. Supercharging proteins can impart unusual resilience. *Journal of the American Chemical Society,* 129**,** 10110-+.

LEE, A. V., OESTERREICH, S. & DAVIDSON, N. E. 2015. MCF-7 Cells-Changing the Course of Breast Cancer Research and Care for 45 Years. *Jnci-Journal of the National Cancer Institute,* 107.

LEHTO, T., ABES, R., OSKOLKOV, N., SUHORUTSENKO, J., COPOLOVICI, D. M., MAGER, I., VIOLA, J. R., SIMONSON, O. E., EZZAT, K., GUTERSTAM, P., ERISTE, E., SMITH, C. I. E., LEBLEU, B., EL ANDALOUSSI, S. & LANGEL, U. 2010. Delivery of nucleic acids with a stearylated (RxR)(4) peptide using a non-covalent co-incubation strategy. *Journal of Controlled Release,* 141**,** 42-51.

LEHTO, T., KURRIKOFF, K. & LANGEL, U. 2012. Cell-penetrating peptides for the delivery of nucleic acids. *Expert Opinion on Drug Delivery,* 9**,** 823-836.

LEHTO, T., SIMONSON, O. E., MAGER, I., EZZAT, K., SORK, H., COPOLOVICI, D. M., VIOLA, J. R., ZAGHLOUL, E. M., LUNDIN, P., MORENO, P. M. D., MAE, M., OSKOLKOV, N., SUHORUTSENKO, J., SMITH, C. I. E. & ANDALOUSSI, S. E. L. 2011. A Peptide-based Vector for Efficient Gene Transfer In Vitro and In Vivo. *Molecular Therapy,* 19**,** 1457-1467.

LI, W. J., NICOL, F. & SZOKA, F. C. 2004. GALA: a designed synthetic pH-responsive amphipathic peptide with applications in drug and gene delivery. *Advanced Drug Delivery Reviews,* 56**,** 967-985.

LI, Y., SUN, C. Y., YATES, E. A., JIANG, C., WILKINSON, M. C. & FERNIG, D. G. 2016. Heparin binding preference and structures in the

fibroblast growth factor family parallel their evolutionary diversification. *Open Biology,* 6.

LINHARDT, J. D. E. A. R. J. 2009. Proteins that Bind Sulfated Glycosaminoglycans. *Essentials of Glycobiology. 2nd edition,* 35.

LIPSCOMBE, R. J., NAKHOUL, A. M., SANDERSON, C. J. & COOMBE, D. R. 1998. Interleukin-5 binds to heparin heparan sulfate. A model for an interaction with extracellular matrix. *Journal of Leukocyte Biology,* 63**,** 342-350.

LO, S. L. & WANG, S. 2008. An endosomolytic Tat peptide produced by incorporation of histidine and cysteine residues as a nonviral vector for DNA transfection. *Biomaterials,* 29**,** 2408-2414.

LORTAT-JACOB, H. 2006. Interferon and heparan sulphate. *Biochemical Society Transactions,* 34**,** 461-464.

LU, H., MCDOWELL, L. M., STUDELSKA, D. R. & ZHANG, L. 2010. Glycosaminoglycans in Human and Bovine Serum: Detection of Twenty-Four Heparan Sulfate and Chondroitin Sulfate Motifs Including a Novel Sialic Acid-modified Chondroitin Sulfate Linkage Hexasaccharide. *Glycobiology insights,* 2010**,** 13-28.

LUAN, L., MENG, Q. B., XU, L., MENG, Z., YAN, H. S. & LIU, K. L. 2015. Peptide amphiphiles with multifunctional fragments promoting cellular uptake and endosomal escape as efficient gene vectors. *Journal of Materials Chemistry B,* 3**,** 1068-1078.

LV, H. T., ZHANG, S. B., WANG, B., CUI, S. H. & YAN, J. 2006. Toxicity of cationic lipids and cationic polymers in gene delivery. *Journal of Controlled Release,* 114**,** 100-109.

MA, D. X., SHI, N. Q. & QI, X. R. 2011. Distinct transduction modes of arginine-rich cell-penetrating peptides for cargo delivery into tumor cells. *International Journal of Pharmaceutics,* 419**,** 200-208.

MADANI, F., LINDBERG, S., LANGEL, #220, LO, FUTAKI, S., GR, #228 & SLUND, A. 2011. Mechanisms of Cellular Uptake of Cell-Penetrating Peptides. *Journal of Biophysics,* 2011.

MAHTOUK, K., CREMER, F. W., REME, T., JOURDAN, M., BAUDARD, M., MOREAUX, J., REQUIRAND, G., FIOL, G., DE VOS, J., MOOS, M., QUITTET, P., GOLDSCHMIDT, H., ROSSI, J. F., HOSE, D. & KLEIN, B. 2006. Heparan sulphate proteoglycans are essential for the myeloma cell growth activity of EGF-family ligands in multiple myeloma. *Oncogene,* 25**,** 7180-7191.

MAIOLO, J. R., FERRER, M. & OTTINGER, E. A. 2005. Effects of cargo molecules on the cellular uptake of arginine-rich cell-penetrating epeptides. *Biochimica Et Biophysica Acta-Biomembranes,* 1712**,** 161-172.

MAO, S. R., SUN, W. & KISSEL, T. 2010. Chitosan-based formulations for delivery of DNA and siRNA. *Advanced Drug Delivery Reviews,* 62**,** 12-27.

MARIE, D., VAULOT, D. & PARTENSKY, F. 1996. Application of the novel nucleic acid dyes YOYO-1, YO-PRO-1, and PicoGreen for flow cytometric analysis of marine prokaryotes. *Applied and Environmental Microbiology,* 62**,** 1649-1655.

MARUYAMA, S., CANTU, E., GALILI, U., D'AGATI, V., GODMAN, G., STERN, D. M. & ANDRES, G. 2000. alpha-Galactosyl epitopes on

glycoproteins of porcine renal extracellular matrix. *Kidney International,* 57**,** 655-663.

MASTORAKOS, P., DA SILVA, A. L., CHISHOLM, J., SONG, E., CHOI, W. K., BOYLE, M. P., MORALES, M. M., HANES, J. & SUK, J. S. 2015. Highly compacted biodegradable DNA nanoparticles capable of overcoming the mucus barrier for inhaled lung gene therapy. *Proceedings of the National Academy of Sciences of the United States of America,* 112**,** 8720-8725.

MATSUBARA, Y., CHIBA, T., KASHIMADA, K., MORIO, T., TAKADA, S., MIZUTANI, S. & ASAHARA, H. 2014. Transcription activator-like effector nuclease-mediated transduction of exogenous gene into IL2RG locus. *Scientific Reports,* 4.

MCNAUGHTON, B. R., CRONICAN, J. J., THOMPSON, D. B. & LIU, D. R. 2009. Mammalian cell penetration, siRNA transfection, and DNA transfection by supercharged proteins. *Proceedings of the National Academy of Sciences of the United States of America,* 106**,** 6111-6116.

MEHTA, A. 2010. The how (and why) of disease registers. *Early Human Development,* 86**,** 723-728.

MIDOUX, P., PICHON, C., YAOUANC, J. J. & JAFFRES, P. A. 2009. Chemical vectors for gene delivery: a current review on polymers, peptides and lipids containing histidine or imidazole as nucleic acids carriers. *British Journal of Pharmacology,* 157**,** 166-178.

MONTIER, T., DELEPINE, P., PICHON, C., FEREC, C., PORTEOUS, D. J. & MIDOUX, P. 2004. Non-viral vectors in cystic fibrosis gene therapy: progress and challenges. *Trends in Biotechnology,* 22**,** 586-592.

MORIGUCHI, R., KOGURE, K., AKITA, H., FUTAKI, S., MIYAGISHI, M., TAIRA, K. & HARASHIMA, H. 2005. A multifunctional envelope-type nano device for novel gene delivery of siRNA plasmids. *International Journal of Pharmaceutics,* 301**,** 277-285.

NAIMY, H., LEYMARIE, N., BOWMAN, M. J. & ZAIA, J. 2008. Characterization of heparin oligosaccharides binding specifically to antithrombin III using mass spectrometry. *Biochemistry,* 47**,** 3155-3161.

NAKAMURA, Y., KOGURE, K., YAMADA, Y., FUTAKI, S. & HARASHIMA, H. 2006. Significant and prolonged antisense effect of a multifunctional envelope-type nano device encapsulating antisense oligodeoxynucleotide. *Journal of Pharmacy and Pharmacology,* 58**,** 431-437.

OHTSUKI, T., MIKI, S., KOBAYASHI, S., HARAGUCHI, T., NAKATA, E., HIRAKAWA, K., SUMITA, K., WATANABE, K. & OKAZAKI, S. 2015. The molecular mechanism of photochemical internalization of cell penetrating peptide-cargophoto-sensitizer conjugates. *Scientific Reports,* 5.

OKITA, K. & YAMANAKA, S. 2011. Induced pluripotent stem cells: opportunities and challenges. *Philosophical Transactions of the Royal Society B-Biological Sciences,* 366**,** 2198-2207.

ORAVECZ, T., PALL, M., WANG, J. H., RODERIQUEZ, G., DITTO, M. & NORCROSS, M. A. 1997. Regulation of anti-HIV-1 activity of RANTES by heparan sulfate proteoglycans. *Journal of Immunology,* 159**,** 4587-4592.

ORTMANN, C., PICKHINKE, U., EXNER, S., OHLIG, S., LAWRENCE, R., JBOOR, H., DREIER, R. & GROBE, K. 2015. Sonic hedgehog processing and release are regulated by glypican heparan sulfate proteoglycans. *Journal of Cell Science,* 128**,** 2374-2385.

PALM-APERGI, C., LONN, P. & DOWDY, S. F. 2012. Do Cell-Penetrating Peptides Actually "Penetrate" Cellular Membranes? *Molecular Therapy,* 20**,** 695-697.

PAN, C. P., KUMAR, C., BOHL, S., KLINGMUELLER, U. & MANN, M. 2009. Comparative Proteomic Phenotyping of Cell Lines and Primary Cells to Assess Preservation of Cell Type-specific Functions. *Molecular & Cellular Proteomics,* 8**,** 443-450.

PAN, R., XU, W., DING, Y., LU, S. & CHEN, P. 2016. Uptake Mechanism and Direct Translocation of a New CPP for siRNA Delivery. *Molecular Pharmaceutics,* 13**,** 1366-1374.

PARK, T. G., JEONG, J. H. & KIM, S. W. 2006. Current status of polymeric gene delivery systems. *Advanced Drug Delivery Reviews,* 58**,** 467-486.

PARN, K., VIRU, L., LEHTO, T., OSKOLKOV, N., LANGEL, U. & MERITS, A. 2013. Transfection of Infectious RNA and DNA/RNA Layered Vectors of Semliki Forest Virus by the Cell-Penetrating Peptide Based Reagent PepFect6. *Plos One,* 8.

PETTY, J. T., BORDELON, J. A. & ROBERTSON, M. E. 2000. Thermodynamic characterization of the association of cyanine dyes with DNA. *Journal of Physical Chemistry B,* 104**,** 7221-7227.

POOGA, M., SOOMETS, U., HALLBRINK, M., VALKNA, A., SAAR, K., REZAEI, K., KAHL, U., HAO, J. X., XU, X. J., WIESENFELD-HALLIN, Z., HOKFELT, T., BARTFAI, T. & LANGEL, U. 1998. Cell penetrating PNA constructs regulate galanin receptor levels and modify pain transmission in vivo. *Nature Biotechnology,* 16**,** 857-861.

PRESTA, M., LEALI, D., STABILE, H., RONCA, R., CAMOZZI, M., COCO, L., MORONI, E., LIEKENS, S. & RUSNATI, M. 2003. Heparin derivatives as angiogenesis inhibitors. *Current Pharmaceutical Design,* 9**,** 553-566.

PUJALS, S., SABIDO, E., TARRAGO, T. & GIRALT, E. 2007. all-D proline-rich cell-penetrating peptides: a preliminary in vivo internalization study. *Biochemical Society Transactions,* 35**,** 794-796.

RAUCHER, D. & RYU, J. S. 2015. Cell-penetrating peptides: strategies for anticancer treatment. *Trends in Molecular Medicine,* 21**,** 560-570.

RICHARD, J. P., MELIKOV, K., VIVES, E., RAMOS, C., VERBEURE, B., GAIT, M. J., CHERNOMORDIK, L. V. & LEBLEU, B. 2003. Cell-penetrating peptides - A reevaluation of the mechanism of cellular uptake. *Journal of Biological Chemistry,* 278**,** 585-590.

RICHARDSON, T. P., TRINKAUS-RANDALL, V. & NUGENT, M. A. 2001. Regulation of heparan sulfate proteoglycan nuclear localization by fibronectin. *Journal of Cell Science,* 114**,** 1613-1623.

RIDER, C. C. & MULLOY, B. 2010. Bone morphogenetic protein and growth differentiation factor cytokine families and their protein antagonists. *Biochemical Journal,* 429**,** 1-12.

ROBINSON, M., EBERL, S., TOMLINSON, C., DAVISKAS, E., REGNIS, J. A., BAILEY, D. L., TORZILLO, P. J., MENACHE, M. & BYE, P. T. 2000. Regional mucociliary clearance in patients with cystic fibrosis.

Journal of Aerosol Medicine-Deposition Clearance and Effects in the Lung, 13**,** 73-86.

ROWE, S. M., MILLER, S. & SORSCHER, E. J. 2005. Mechanisms of disease: Cystic fibrosis. *New England Journal of Medicine,* 352**,** 1992-2001.

SALEH, A. F., AOJULA, H., ARTHANARI, Y., OFFERMAN, S., ALKOTAJI, M. & PLUEN, A. 2010. Improved Tat-mediated plasmid DNA transfer by fusion to LK15 peptide. *Journal of Controlled Release,* 143**,** 233-242.

SANDERS, N. N., DE SMEDT, S. C., VAN ROMPAEY, E., SIMOENS, P., DE BAETS, F. & DEMEESTER, J. 2000. Cystic fibrosis sputum - A barrier to the transport of nanospheres. *American Journal of Respiratory and Critical Care Medicine,* 162**,** 1905-1911.

SANTOS, J. L., PANDITA, D., RODRIGUES, J., PEGO, A. P., GRANJA, P. L. & TOMAS, H. 2011. Non-Viral Gene Delivery to Mesenchymal Stem Cells: Methods, Strategies and Application in Bone Tissue Engineering and Regeneration. *Current Gene Therapy,* 11**,** 46-57.

SATO, H. & FELIX, J. B. 2006. Peptide-membrane interactions and mechanisms of membrane destruction by amphipathic alpha-helical antimicrobial peptides. *Biochimica Et Biophysica Acta-Biomembranes,* 1758**,** 1245-1256.

SCHAMHART, D. H. J. & KURTH, K. H. 1997. Role of proteoglycans in cell adhesion of prostate cancer cells: From review to experiment. *Urological Research,* 25**,** S89-S96.

SCHNOLZER, M., ALEWOOD, P., JONES, A., ALEWOOD, D. & KENT, S. B. H. 1992. INSITU NEUTRALIZATION IN BOC-CHEMISTRY SOLID-PHASE PEPTIDE-SYNTHESIS - RAPID, HIGH-YIELD ASSEMBLY OF DIFFICULT SEQUENCES. *International Journal of Peptide and Protein Research,* 40**,** 180-193.

SCHOONBROODT, S., STEUKERS, M., VISWANATHAN, M., FRANS, N., TIMMERMANS, M., WEHNERT, A., NGUYEN, M., LADNER, R. C. & HOET, R. M. 2008. Engineering Antibody Heavy Chain CDR3 to Create a Phage Display Fab Library Rich in Antibodies That Bind Charged Carbohydrates. *Journal of Immunology,* 181**,** 6213-6221.

SCHUSTER, B. S., ENSIGN, L. M., ALLAN, D. B., SUK, J. S. & HANES, J. 2015. Particle tracking in drug and gene delivery research: State-of-the-art applications and methods. *Advanced Drug Delivery Reviews,* 91**,** 70-91.

SCHUSTER, B. S., KIM, A. J., KAYS, J. C., KANZAWA, M. M., GUGGINO, W. B., BOYLE, M. P., ROWE, S. M., MUZYCZKA, N., SUK, J. S. & HANES, J. 2014. Overcoming the Cystic Fibrosis Sputum Barrier to Leading Adeno-associated Virus Gene Therapy Vectors. *Molecular Therapy,* 22**,** 1484-1493.

SCHWARZE, S. R., HO, A., VOCERO-AKBANI, A. & DOWDY, S. F. 1999. In vivo protein transduction: Delivery of a biologically active protein into the mouse. *Science,* 285**,** 1569-1572.

SEO, S. J., KIM, T. H., CHOI, S. J., PARK, J. H., WALL, I. B. & KIM, H. W. 2013. Gene delivery techniques for adult stem cell-based regenerative therapy. *Nanomedicine,* 8**,** 1875-1891.

SHEN, B. Q., XU, K. Y., LIU, L. N., RAAB, H., BHAKTA, S., KENRICK, M., PARSONS-REPONTE, K. L., TIEN, J., YU, S. F., MAI, E., LI, D. W., TIBBITTS, J., BAUDYS, J., SAADI, O. M., SCALES, S. J.,

MCDONALD, P. J., HASS, P. E., EIGENBROT, C., NGUYEN, T., SOLIS, W. A., FUJI, R. N., FLAGELLA, K. M., PATEL, D., SPENCER, S. D., KHAWLIL, L. A., EBENS, A., WONG, W. L., VANDLEN, R., KAUR, S., SLIWKOWSKI, M. X., SCHELLER, R. H., POLAKIS, P. & JUNUTULA, J. R. 2012. Conjugation site modulates the in vivo stability and therapeutic activity of antibody-drug conjugates. *Nature Biotechnology,* 30**,** 184-189.

SHERIDAN, C. 2011. Gene therapy finds its niche. *Nature Biotechnology,* 29**,** 121-128.

SHIRAISHI, T. & NIELSEN, P. E. 2006. Enhanced delivery of cell-penetrating peptide-peptide nucleic acid conjugates by endosomal disruption. *Nature Protocols,* 1**,** 633-636.

SIMOES, S., SLEPUSHKIN, V., GASPAR, R., DE LIMA, M. C. P. & DUZGUNES, N. 1998. Gene delivery by negatively charged ternary complexes of DNA, cationic liposomes and transferrin or fusigenic peptides. *Gene Therapy,* 5**,** 955-964.

SIMOES, S., SLEPUSHKIN, V., PIRES, P., GASPAR, R., DE LIMA, M. C. P. & DUZGUNES, N. 1999a. Mechanisms of gene transfer mediated by lipoplexes associated with targeting ligands or pH-sensitive peptides. *Gene Therapy,* 6**,** 1798-1807.

SIMOES, S., SLEPUSHKIN, V., PRETZER, E., DAZIN, P., GASPAR, R., DE LIMA, M. C. P. & DUZGUNES, N. 1999b. Transfection of human macrophages by lipoplexes via the combined use of transferrin and pH-sensitive peptides. *Journal of Leukocyte Biology,* 65**,** 270-279.

SORKIN, A. & VON ZASTROW, M. 2002. Signal transduction and endocytosis: Close encounters of many kinds. *Nature Reviews Molecular Cell Biology,* 3**,** 600-614.

STRINGER, S. E., FORSTER, M. J., MULLOY, B., BISHOP, C. R., GRAHAM, G. J. & GALLAGHER, J. T. 2002. Characterization of the binding site on heparan sulfate for macrophage inflammatory protein 1 alpha. *Blood,* 100**,** 1543-1550.

SUK, J. S., LAI, S. K., WANG, Y. Y., ENSIGN, L. M., ZEITLIN, P. L., BOYLE, M. P. & HANES, J. 2009. The penetration of fresh undiluted sputum expectorated by cystic fibrosis patients by non-adhesive polymer nanoparticles. *Biomaterials,* 30**,** 2591-2597.

SUK, J. S., XU, Q. G., KIM, N., HANES, J. & ENSIGN, L. M. 2016. PEGylation as a strategy for improving nanoparticle-based drug and gene delivery. *Advanced Drug Delivery Reviews,* 99**,** 28-51.

SUZUKI, R., YAMADA, Y. & HARASHIMA, H. 2007. Efficient cytoplasmic protein delivery by means of a multifunctional envelope-type nano device. *Biological & Pharmaceutical Bulletin,* 30**,** 758-762.

SWIECICKI, J. M., DI PISA, M., LIPPI, F., CHWETZOFF, S., MANSUY, C., TRUGNAN, G., CHASSAING, G., LAVIELLE, S. & BURLINA, F. 2015. Unsaturated acyl chains dramatically enhanced cellular uptake by direct translocation of a minimalist oligo-arginine lipopeptide. *Chemical Communications,* 51**,** 14656-14659.

SZWERAS, M., LIU, D. M., PARTRIDGE, E. A., PAWLING, J., SUKHU, B., CLOKIE, C., JAHNEN-DECHENT, W., TENENBAUM, H. C., SWALLOW, C. J., GRYNPAS, M. D. & DENNIS, J. W. 2002. alpha 2-HS glycoprotein/fetuin, a transforming growth factor-beta/bone

morphogenetic protein antagonist, regulates postnatal bone growth and remodeling. *Journal of Biological Chemistry,* 277**,** 19991-19997.

TAKAHASHI, K. & YAMANAKA, S. 2006. Induction of pluripotent stem cells from mouse embryonic and adult fibroblast cultures by defined factors. *Cell,* 126**,** 663-676.

TERAN, M. & NUGENT, M. A. 2015. Synergistic Binding of Vascular Endothelial Growth Factor-A and Its Receptors to Heparin Selectively Modulates Complex Affinity. *Journal of Biological Chemistry,* 290**,** 16451-16462.

TJELLE, T. E., BRECH, A., JUVET, L. K., GRIFFITHS, G. & BERG, T. 1996. Isolation and characterization of early endosomes, late endosomes and terminal lysosomes: Their role in protein degradation. *Journal of Cell Science,* 109**,** 2905-2914.

TUNNEMANN, G., MARTIN, R. M., HAUPT, S., PATSCH, C., EDENHOFER, F. & CARDOSO, M. C. 2006. Cargo-dependent mode of uptake and bioavailability of TAT-containing proteins and peptides in living cells. *Faseb Journal,* 20**,** 1775-1784.

UNIEWICZ, K. A., ORI, A., XU, R. Y., AHMED, Y., WILKINSON, M. C., FERNIG, D. G. & YATES, E. A. 2010. Differential Scanning Fluorimetry Measurement of Protein Stability Changes upon Binding to Glycosaminoglycans: A Screening Test for Binding Specificity. *Analytical Chemistry,* 82**,** 3796-3802.

VAN KUPPEVELT, T. H., DENNISSEN, M., VAN VENROOIJ, W. J., HOET, R. M. A. & VEERKAMP, J. H. 1998. Generation and application of type-specific anti-heparan sulfate antibodies using phage display technology - Further evidence for heparan sulfate heterogeneity in the kidney. *Journal of Biological Chemistry,* 273**,** 12960-12966.

VEIMAN, K. L., KUNNAPUU, K., LEHTO, T., KIISHOLTS, K., PARN, K., LANGEL, U. & KURRIKOFF, K. 2015. PEG shielded MMP sensitive CPPs for efficient and tumor specific gene delivery in vivo. *Journal of Controlled Release,* 209**,** 238-247.

VERCAUTEREN, D., VANDENBROUCKE, R. E., JONES, A. T., REJMAN, J., DEMEESTER, J., DE SMEDT, S. C., SANDERS, N. N. & BRAECKMANS, K. 2010. The Use of Inhibitors to Study Endocytic Pathways of Gene Carriers: Optimization and Pitfalls. *Molecular Therapy,* 18**,** 561-569.

VERDURMEN, W. P. R., BOVEE-GEURTS, P. H., WADHWANI, P., ULRICH, A. S., HALLBRINK, M., VAN KUPPEVELT, T. H. & BROCK, R. 2011. Preferential Uptake of L- versus D-Amino Acid Cell-Penetrating Peptides in a Cell Type-Dependent Manner. *Chemistry & Biology,* 18**,** 1000-1010.

VERKMAN, A. S., LUKACS, G. L. & GALIETTA, L. J. V. 2006. CFTR chloride channel drug discovery - Inhibitors as antidiarrheals and activators for therapy of cystic fibrosis. *Current Pharmaceutical Design,* 12**,** 2235-2247.

VERONESE, F. M. & PASUT, G. 2005. PEGylation, successful approach to drug delivery. *Drug Discovery Today,* 10**,** 1451-1458.

VIVES, E., BRODIN, P. & LEBLEU, B. 1997. A truncated HIV-1 Tat protein basic domain rapidly translocates through the plasma membrane and

accumulates in the cell nucleus. *Journal of Biological Chemistry,* 272**,** 16010-16017.

WADIA, J. S., STAN, R. V. & DOWDY, S. F. 2004. Transducible TAT-HA fusogenic peptide enhances escape of TAT-fusion proteins after lipid raft macropinocytosis. *Nature Medicine,* 10**,** 310-315.

WALTER, E. & MERKLE, H. P. 2002. Microparticle-mediated transfection of non-phagocytic cells in vitro. *Journal of Drug Targeting,* 10**,** 11-21.

WANG, H. Y., CHEN, J. X., SUN, Y. X., DENG, J. Z., LI, C., ZHANG, X. Z. & ZHUO, R. X. 2011. Construction of cell penetrating peptide vectors with N-terminal stearylated nuclear localization signal for targeted delivery of DNA into the cell nuclei. *Journal of Controlled Release,* 155**,** 26-33.

WILKINSPORT, C. E. & MCKEOWNLONGO, P. J. 1996. Heparan sulfate proteoglycans function in the binding and degradation of vitronectin by fibroblast monolayers. *Biochemistry and Cell Biology-Biochimie Et Biologie Cellulaire,* 74**,** 887-897.

WONG, F. K., HAFFNER, C., HUTTNER, W. B. & TAVERNA, E. 2014. Microinjection of membrane-impermeable molecules into single neural stem cells in brain tissue. *Nature Protocols,* 9**,** 1170-1182.

WU, H. M., PAN, S. R., CHEN, M. W., WU, Y., WANG, C., WEN, Y. T., ZENG, X. & WU, C. B. 2011. A serum-resistant polyamidoamine-based polypeptide dendrimer for gene transfection. *Biomaterials,* 32**,** 1619-1634.

WU, Z. L. L., ZHANG, L. J., YABE, T., KUBERAN, B., BEELER, D. L., LOVE, A. & ROSENBERG, R. D. 2003. The involvement of heparan sulfate (HS) in FGF1/HS/FGFR1 signaling complex. *Journal of Biological Chemistry,* 278**,** 17121-17129.

WYMAN, T. B., NICOL, F., ZELPHATI, O., SCARIA, P. V., PLANK, C. & SZOKA, F. C. 1997. Design, synthesis, and characterization of a cationic peptide that binds to nucleic acids and permeabilizes bilayers. *Biochemistry,* 36**,** 3008-3017.

XIAO, K., LI, Y. P., LUO, J. T., LEE, J. S., XIAO, W. W., GONIK, A. M., AGARWAL, R. G. & LAM, K. S. 2011. The effect of surface charge on in vivo biodistribution of PEG-oligocholic acid based micellar nanoparticles. *Biomaterials,* 32**,** 3435-3446.

XIE, Z. L., SHAO, S. L., LV, J. W., WANG, C. H., YUAN, C. Z., ZHANG, W. W. & XU, X. J. 2011. Co-transfection and tandem transfection of HEK293A cells for overexpression and Riled experiments. *Cell Biology International,* 35**,** 187-192.

YAMADA, Y., AKITA, H. & HARASHIMA, H. 2012. MULTIFUNCTIONAL ENVELOPE-TYPE NANO DEVICE (MEND) FOR ORGANELLE TARGETING VIA A STEPWISE MEMBRANE FUSION PROCESS. *In:* DUZGUNES, N. (ed.) *Nanomedicine: Infectious Diseases, Immunotherapy, Diagnostics, Antifibrotics, Toxicology and Gene Medicine.* San Diego: Elsevier Academic Press Inc.

YAMAMOTO, S., NAKASE, H., MATSUURA, M., HONZAWA, Y., MATSUMURA, K., UZA, N., YAMAGUCHI, Y., MIZOGUCHI, E. & CHIBA, T. 2013. Heparan sulfate on intestinal epithelial cells plays a critical role in intestinal crypt homeostasis via Wnt/beta-catenin

signaling. *American Journal of Physiology-Gastrointestinal and Liver Physiology,* 305**,** G241-G249.

YARMUSH, M. L., GOLBERG, A., SERSA, G., KOTNIK, T. & MIKLAVCIC, D. 2014. Electroporation-Based Technologies for Medicine: Principles, Applications, and Challenges. *In:* YARMUSH, M. L. (ed.) *Annual Review of Biomedical Engineering, Vol 16.* Palo Alto: Annual Reviews.

YIN, H., KANASTY, R. L., ELTOUKHY, A. A., VEGAS, A. J., DORKIN, J. R. & ANDERSON, D. G. 2014. Non-viral vectors for gene-based therapy. *Nature Reviews Genetics,* 15**,** 541-555.

ZHANG, G. D., YANG, Z., LU, W., ZHANG, R., HUANG, Q., TIAN, M., LI, L., LIANG, D. & LI, C. 2009. Influence of anchoring ligands and particle size on the colloidal stability and in vivo biodistribution of polyethylene glycol-coated gold nanoparticles in tumor-xenografted mice. *Biomaterials,* 30**,** 1928-1936.

ZHANG, X., PAN, S. R., HU, H. M., WU, G. F., FENG, M., ZHANG, W. & LU, X. 2008. Poly(ethylene glycol)-block-polyethylenimine copolymers as carriers for gene delivery: Effects of PEG molecular weight and PEGylation degree. *Journal of Biomedical Materials Research Part A,* 84A**,** 795-804.